# Southeastern Geology: Volume 37, No. 4 May 1998

Editor in Chief: S. Duncan Heron, Jr.

**Abstract**

Academic journal published quarterly by the Department of Geology, Duke University.

# SOUTHEASTERN GEOLOGY

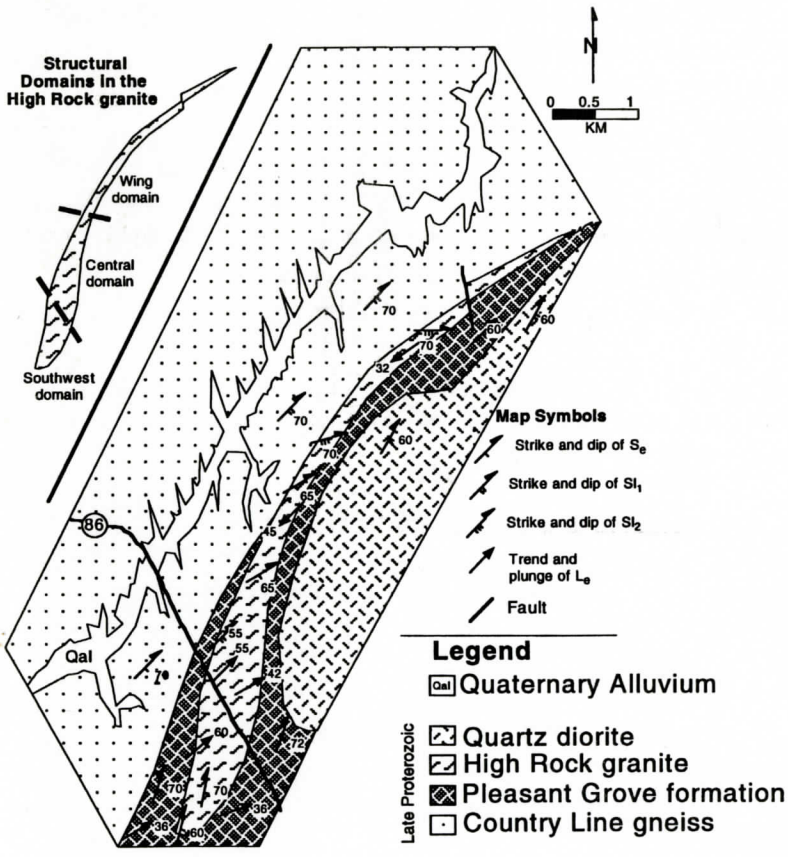


VOL. 37, NO. 4 MAY 1998

# SOUTHEASTERN GEOLOGY

PUBLISHED

at

DUKE UNIVERSITY

Editor in Chief:

Duncan Heron


This journal publishes the results of original research on all phases of geology, geophysics, geochemistry and environmental geology as related to the Southeast. Send manuscripts to **DUNCAN HERON, DUKE UNIVERSITY, BOX 90233, DURHAM, NORTH CAROLINA 27708-0233**. Phone: 919-684-5321, Fax: 919-684-5833, Email: heron@geo.duke.edu Please observe the following:

1) Type the manuscript with double space lines and submit in duplicate.
2) Cite references and prepare bibliographic lists in accordance with the method found within the pages of this journal.
3) Submit line drawings and complex tables reduced to final publication size (no bigger than 8 x 5 3/8 inches).
4) Make certain that all photographs are sharp, clear, and of good contrast.
5) Stratigraphic terminology should abide by the North American Stratigraphic Code (American Association Petroleum Geologists Bulletin, v. 67, p. 841-875).


Subscriptions to *Southeastern Geology* for volume 37 are: individuals - $18.00 (paid by personal check); corporations and libraries - $23.00; foreign $27. Inquires should be sent to: **SOUTHEASTERN GEOLOGY, DUKE UNIVERSITY, BOX 90233, DURHAM, NORTH CAROLINA 27708-0233**. Make checks payable to: *Southeastern Geology.*

Information about SOUTHEASTERN GEOLOGY is on the World Wide Web including a seachable author-title index 1958-1996. The URL for the Web site is:

http://www.geo.duke.edu/seglgy.htm

SOUTHEASTERN GEOLOGY is a peer review journal.

ISSN 0038-3678

# SOUTHEASTERN GEOLOGY

## Table of Contents

Volume 37, No. 4

May 1998

SOUTHEASTERN GEOLOGY
V. 37, No. 4, May 1998, p. 163-176

# STRUCTURAL GEOLOGY OF THE HIGH ROCK GRANITE: IMPLICATIONS FOR DISPLACEMENT ALONG THE HYCO SHEAR ZONE, NORTH CAROLINA

JOHN A. VINES[1], JAMES P. HIBBARD, AND GLENN S. SHELL

*Department of Marine, Earth and Atmospheric Sciences, Box 8208*
*North Carolina State University*
*Raleigh, NC 27695-8208*

## ABSTRACT

**The High Rock granite is an elongate stock that has been deformed by the Mississippian Hyco shear zone. Detailed mesoscale mapping of fabrics within the granite and microstructural analysis indicate that the body contains pervasive low to moderate temperature solid-state fabrics. The High Rock granite is divided into three structural domains on the basis of foliation development. In the southwestern and central domains, two foliations, $S_e$ and $Sl_1$, are common, whereas in the wing domain, a third foliation, $Sl_2$, is prominent. $S_e$ is the oldest foliation and is weakly developed. Toward the wing domain the foliations become more intense and $Sl_1$ and $Sl_2$ are mylonitic. Stretching lineations in the southwestern and central domains consistently plunge to the northeast, whereas in the wing domain stretching lineations plunge to the southwest. The pervasive solid-state fabrics indicate that the High Rock granite is pretectonic with respect to the Hyco shear zone. Foliation development in the pluton is consistent with thrusting of the body along a flat and subsequently up a frontal ramp in the Hyco shear zone, with the wing domain overprinted by deformation along a lateral ramp in the zone. From this structural model, we estimate a minimum displacement of 35 km along the Hyco shear zone.**

## INTRODUCTION

The High Rock pluton is an equigranular granite stock that is situated in the hanging wall of the Mississippian Hyco shear zone near Yanceyville, North Carolina (Figure 1) (Hibbard and others, in press). The stock is located along the southern margin of the shear zone where it is roughly concordant with the locally arcuate surface trace of the zone. In map view, it displays an elongate wing that extends eastward from the main body (Shell, 1996; Hibbard and others, in press). This geometry has led to questions regarding both timing of emplacement and deformation history of the granite.

Shell (1996) first mapped the elongate wing of the granite as extending, at a low angle, across the strain gradient at the margin of the Hyco shear zone. On the basis of the extreme aspect ratio of the wing, he suggested that the pluton may have been emplaced syntectonically into the shear zone. This interpretation was also predicated on the presence of Mississippian syntectonic granitoids elsewhere in the shear zone (Shell, 1996; Hibbard and others, in press; Wortman and others, in press). Alternatively, the wing of the granite could be considered to have formed by solid state processes, in which case, the High Rock pluton could be pretectonic with respect to the shear zone. This interpretation is also consistent with the local geology, as Neoproterozoic granitoids, ranging in age from approximately 616 to 545 Ma are common in the hanging wall of the shear zone (Wortman and others, 1996).

The focus of this study is to resolve the question of the timing of emplacement of the High Rock pluton relative to motion along the Hyco shear zone. Specifically, we studied the fabrics

1. Present address: *Dept. of Geological Sciences, Virginia Polytechnic Institute and State University, Blacksburg, VA 24061-0420*

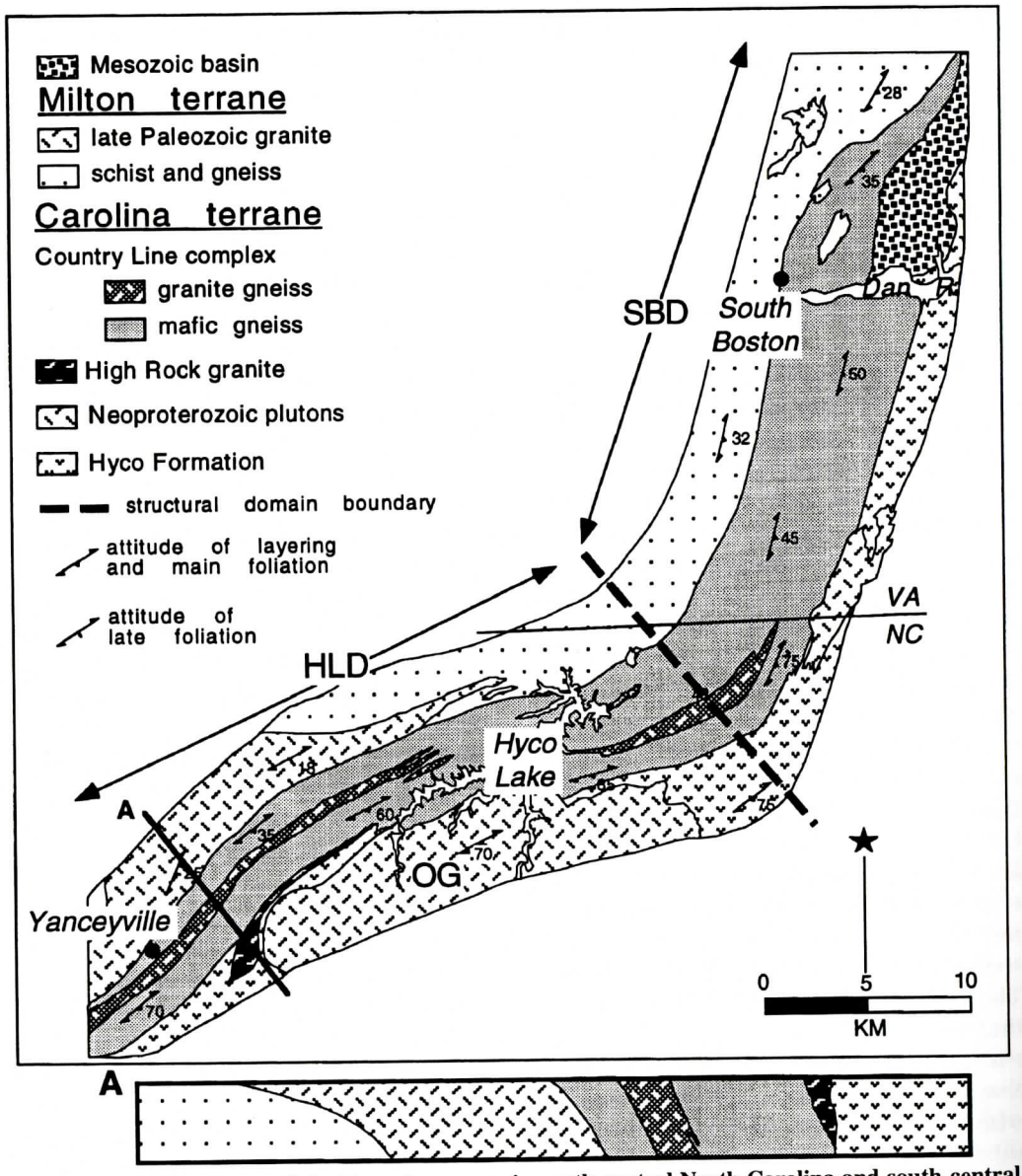


**Figure 1. General geology of the Hyco shear zone in north-central North Carolina and south-central Virginia. See Figure 2 for regional location. OG = Osmond granite phase of Neoproterozoic plutonic suite; HLD = Hyco Lake structural domain; SBD = South Boston structural domain.**

in the pluton to determine the crustal conditions of deformation and to determine whether or not the fabrics were formed by magmatic or solid-state processes (Hutton, 1988; Paterson and others, 1989; Morand, 1992; Karlstrom and others, 1993). Based on our results, we present a new model for the deformation history of the stock; this model also enables us to estimate minimum displacement along the Hyco shear zone.

## FABRIC CRITERIA FOR TIMING OF GRANITOID EMPLACEMENT

In recent years, structural geologists have gained insight into determining the emplace-

ment age of granites relative to regional deformation. In general, pre-, syn-, and post-tectonic plutons are recognized on the basis of the geometry and origin of fabrics found within the plutons and at the pluton-wallrock interface. In particular, distinguishing magmatic from solid-state fabrics and establishing their interrelationship are critical in determining relative emplacement age of a pluton (e.g, Vernon and others, 1983; Gapais and Barbarin, 1986; Hutton, 1988; Blumenfeld and Bouchez, 1988; Paterson and others, 1989; Morand, 1992; Karlstrom and others, 1993). Prior to describing the High Rock granite, it is useful to briefly summarize how these fabrics can be used as indicators for determining the relative timing of emplacement of the granite within the Hyco shear zone.

Magmatic fabrics are caused by flow during pluton ascent and emplacement in the crust. The best evidence for magmatic flow is the preferred alignment of undeformed primary igneous minerals (Berger and Pitcher, 1970; Johnson and Pollard, 1973; Vernon and others, 1988; Paterson and others, 1989). The alignment of euhedral feldspar best demonstrates magmatic flow because feldspars tend not to grow as euhedral crystals in metamorphic rocks (Vernon, 1983). In addition, the twin planes (albite twinning) should be concordant with the long axes of the feldspars for an igneous origin to be inferred for a given foliation (Paterson and others, 1989).

Just as feldspar is a key mineral in identifying magmatic fabrics, quartz is an important mineral for interpreting the extent of solid-state deformation. Under most conditions quartz is the first mineral in a granite to undergo crystal-plastic deformation (Vauchez, 1980; Marre, 1986). Microscopic evidence for crystal-plastic deformation in quartz ranges from undulatory extinction to recrystallization textures like grain boundary migration. However, other minerals and deformational fabrics within a granite can provide evidence for crystal-plastic deformation. Orthoclase commonly inverts to microcline during solid-state deformation (Eggleton and Buseck, 1980). Strong minerals such as feldspars and amphiboles can fracture and experience boudinage, with recrystallized quartz and mica aggregates between the fractures and in boudin necks (Vernon and others, 1983; Simpson, 1985). Penetrative fabrics such as mylonitic foliations provide good mesoscopic evidence for solid-state deformation within granites.

The magmatic and solid-state fabrics discussed above are end-member guides to determining how and when foliations within granites may develop. However, fabrics in plutons such as the High Rock may result from both magmatic flow and solid state processes. Therefore, it is important to understand the relationship between the magmatic and solid-state fabrics in the granite and how they correspond to fabrics in the country rock. For example, if the High Rock granite was emplaced before regional tectonism, we might expect magmatic fabrics to either be absent or overprinted by a solid-state fabric associated with regional deformation (Paterson and others, 1989). If it is syntectonic, we would expect to see a continuum between magmatic and high temperature (650°-700°C) solid state fabrics concordant with the regional tectonic fabric (Paterson and others, 1989). The geometry of the High Rock granite clearly indicates that it was deformed by the Hyco shear zone (Shell, 1996), thus negating post-tectonic emplacement.

## GEOLOGIC SETTING

The High Rock granite lies at the base of the hanging wall of the Hyco shear zone. The shear zone is a first-order tectonic boundary in the southern Appalachians, separating rocks of the Carolina terrane that are clearly exotic with respect to North America, from those of the Milton terrane, with unknown crustal affinity (Figure 2). The two terranes have contrasting rock types, structural styles, and Nd-isotopic signatures (Wortman and others, 1996; Hibbard and others, in press). The shear zone trends east-northeast in northern North Carolina, changing to a north-northeast trend in southern Virginia (Figure 1) (Hibbard and others, in press). The age of the Hyco shear zone is tightly constrained by precise U-Pb zircon ages to the

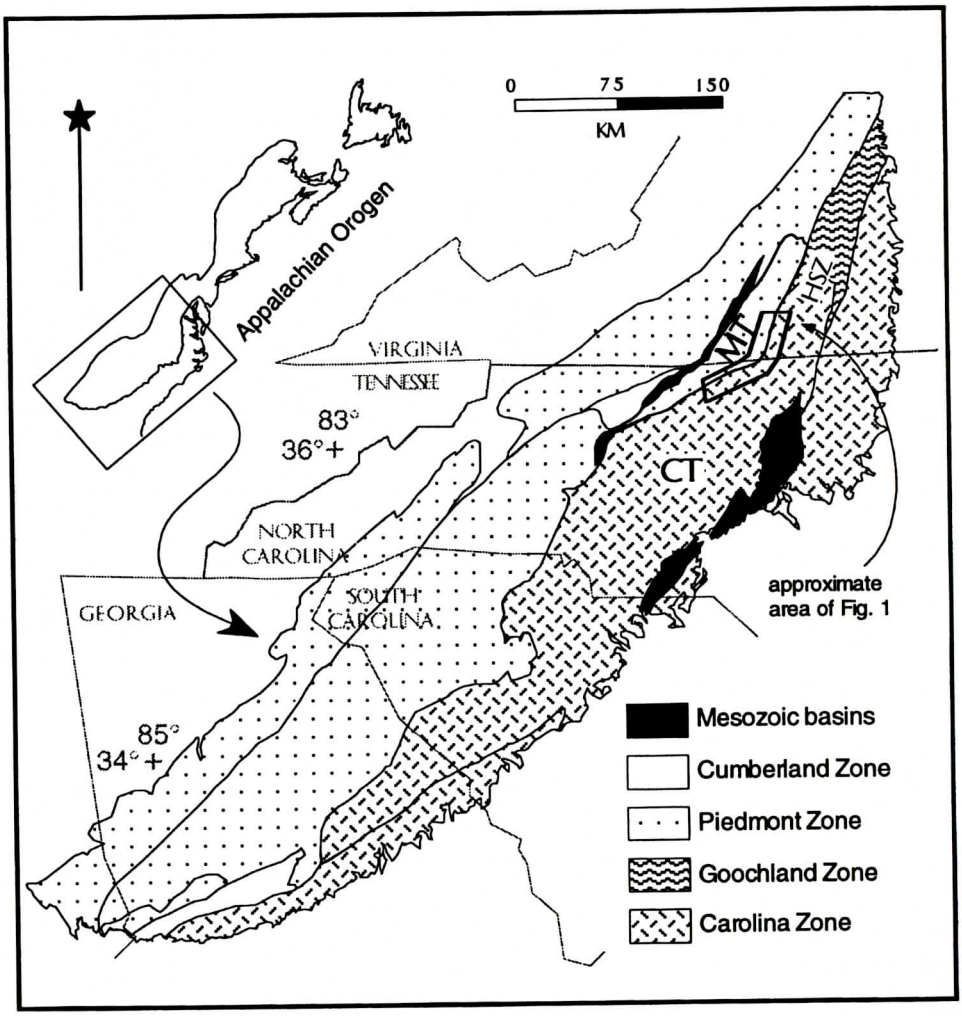


**Figure 2. Regional setting of the Hyco shear zone in the southern Appalachians (CT = Carolina terrane; HSZ = Hyco shear zone; MT = Milton terrane)**

Mississippian (approximately 335-320 Ma) (Wortman and others, in press).

To the northwest, in the footwall of the zone, the Milton terrane consists of upper amphibolite facies biotite schist and gneiss, with minor pelitic schist, marble, pegmatite, and quartzite (Tobisch and Glover, 1971; Tobisch, 1972; Butler and Secor, 1991; Hibbard and others, in press). The protoliths for the Milton terrane probably represent an Ordovician volcanic-plutonic complex associated with clastic sedimentary rocks (Hibbard, 1993; Hund, 1987; Wortman and others, 1996). The structural geometry of the Milton terrane is interpreted to be characterized by recumbent isoclinal fold nappes that affect layering and a strong, generally layer-parallel foliation (Tobisch and Glover, 1971; Henika, 1977). To the southwest, in the hanging wall of the zone, lie greenschist to amphibolite facies metavolcanic and metaplutonic rocks of the Carolina terrane, interpreted as representing remnants of a Precambrian-Cambrian volcanic arc system (Butler and Ragland, 1969; Feiss, 1982; Secor and others, 1983). Structurally, the Carolina terrane is dominated by open upright folds with a steeply dipping axial planar folia-

tion that may be associated with the Neoproterozoic Virgilina orogeny (Glover and Sinha, 1973; Hibbard and Samson, 1995; Dennis, 1995). Two suites of granitoids are recognized in the area; a pretectonic Neoproterozoic suite is confined to the hanging wall and a syntectonic Mississippian suite intrudes the shear zone and adjacent footwall (Hibbard and others, in press).

On the basis of structural trend, the Hyco shear zone consists of two structural domains (Figure 1). The Hyco Lake domain displays moderately to steeply south-southeast-dipping layering and foliation and has structures that give evidence for dextral strike slip (Hibbard and others, in press). In the South Boston domain, the foliations are moderately and shallowly east-dipping, with structures indicating thrusting of the Carolina terrane over the Milton terrane (Bradley, 1996; Hibbard and others, in press). The two domains are continuous with each other, and the change in trend is abrupt. This geometry has been interpreted to reflect an early Mississippian regional scale frontal and lateral ramp system within an overall thrust regime (Hibbard and others, in press).

## HIGH ROCK GRANITE

The High Rock granite is located at the base of the hanging wall of the Hyco shear zone, in the Carolina terrane (Figure 1). It is informally named after the crossroads community of High Rock, at the eastern end of the wing of the stock. The granite intrudes Neoproterozoic mafic schists and gneisses of the Country Line complex and Neoproterozoic felsic volcanics of the Pleasant Grove formation (Shell, 1996; Hibbard and others, in press). Shell (1996) noticed that the stock straddles the strain gradient at the margin of the Hyco shear zone, with the southwestern portion of the stock being relatively undeformed and the northern portion being strongly deformed by the shear zone; he suggested that it is a syntectonic granitoid, similar to other Mississippian granites in the shear zone.

In map view, the High Rock granite is elongate with approximate map dimensions of 4.3 km x 1.1 km (Figure 3) (Shell, 1996). Throughout the stock, exposures commonly are whitish-pink in color and vary from coarse- to fine-grained, and weakly to strongly foliated, with local unfoliated zones. The granite consists of potassium feldspar (orthoclase and microcline), plagioclase, biotite, and quartz with minor amounts of muscovite, garnet, chlorite, sericite, epidote, titanite, and zircon. The feldspars, biotite and quartz along with two of the accessory minerals, titanite and zircon, represent the primary igneous minerals. Muscovite increases in abundance northeastward through the stock, concomitant with an increase in deformation; muscovite, as well as garnet, and chlorite, are considered to be metamorphic in origin. Epidote and sericite form alteration minerals within the feldspars. The mineral assemblage suggests that the granite was subjected to at least greenschist facies metamorphism. Plagioclase ($An_{37}$) displays Carlsbad and albite twinning with local oscillatory zoning; potassium feldspar displays Carlsbad and gridiron twinning with local perthite. In moderately to highly deformed portions of the stock orthoclase is partly inverted to microcline, muscovite is the dominant mica phase, and myrmekite is common along fractures in feldspars.

Amphibolite xenoliths, lithically similar to the bordering rocks of the Country Line complex, are scattered throughout the granite, ranging from 20 cm x 5 cm to 10 m x 4 m. Felsic aplite dikes are commonly observed throughout the granite. The dominant foliation in the mafic xenoliths and felsic dikes is parallel to foliations related to the Hyco shear zone. The contact of the stock with the enclosing country rock is generally concordant and sharp. The granite margin is locally chilled along its northern contact, but no contact aureole was observed within the country rock. These observations suggest that either the country rocks were also hot at the time of granite emplacement or that any aureole associated with the granite was obliterated by subsequent deformation and metamorphism in the shear zone.

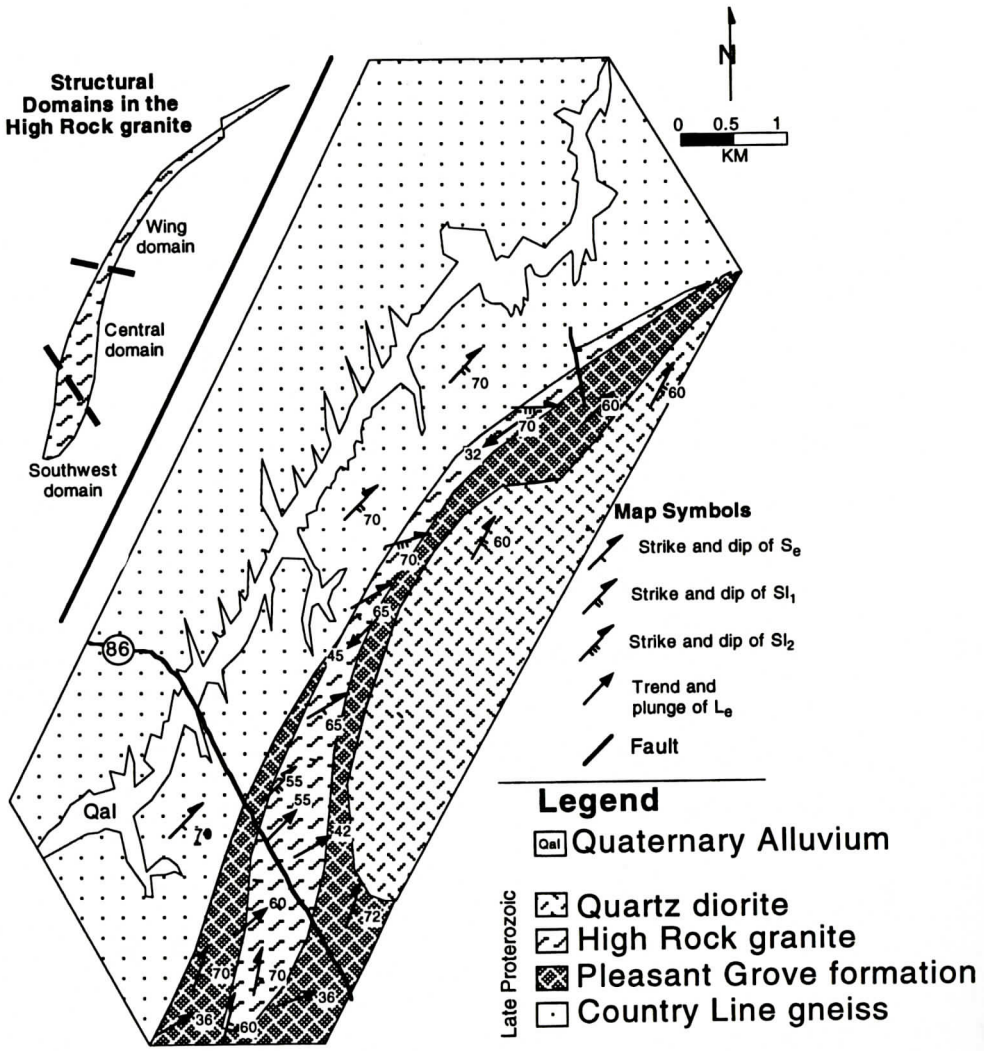


**Figure 3. Detailed geologic map of the High Rock granite; inset map of High Rock pluton shows location of structural domains.**

## STRUCTURE OF THE HIGH ROCK GRANITE

### Mesoscale Structures

Based on differences in foliation development, we divide the High Rock granite into three structural domains, named the southwest, central, and wing domains (Figure 3). The southwest domain is confined to the area southwest of state highway 86 and is characterized by a medium- to coarse-grained, weakly to nonfoliated rock. The central domain is primarily defined by a medium-grained, moderately foliated rock with local mylonitic zones. The wing domain is commonly defined by a fine-grained, strongly foliated mylonitic rock. All foliations observed in the granite are strongest near the north and northwest contacts.

The High Rock granite contains three generations of foliation, including an early foliation, $S_e$, and two later foliations, $Sl_1$ and $Sl_2$ (Figure 3). Their chronology is established by overprinting relationships where the oldest, Se , is overprinted by $Sl_1$, which in turn is overprinted by $Sl_2$. Se and $Sl_1$ are prominent in the south-

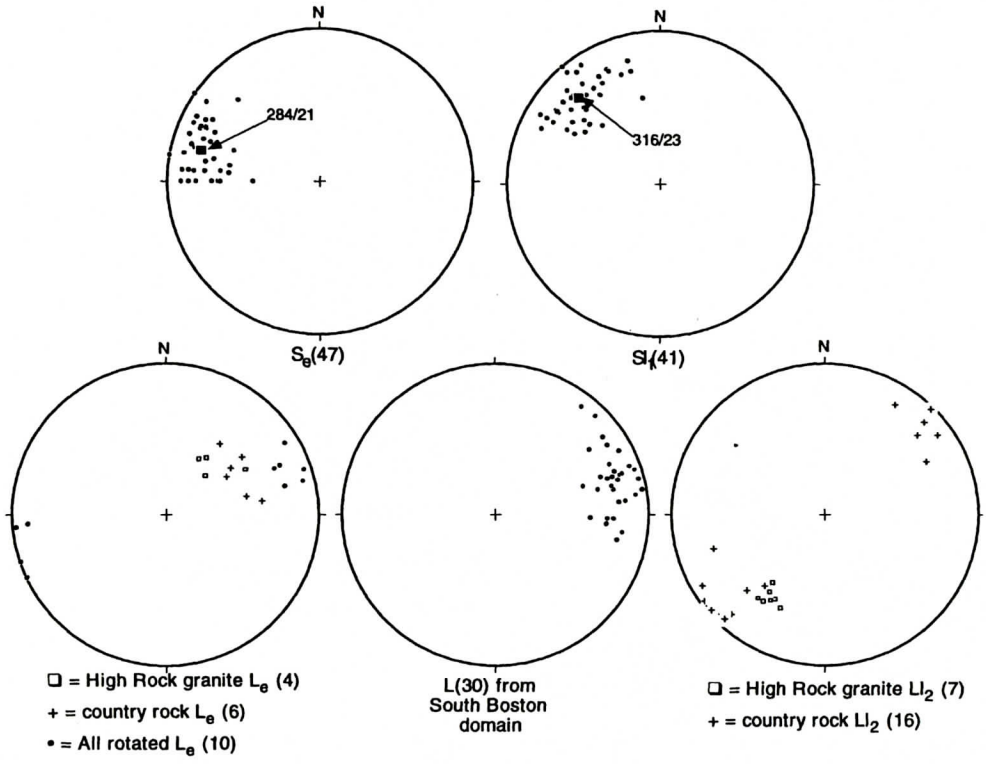


**Figure 4. Equal area lower hemisphere stereoplots of poles to foliation planes, lineations (from High Rock granite and immediately surrounding country rock), and rotation of all $L_e$ to a horizontal thrust flat attitude (see text for explanation). Lineation data for the South Boston domain from Bradley (1996).**

western and central domains. Toward and within the wing domain, Se is rotated into parallelism with $Sl_1$ and both are sheared by $Sl_2$. The country rock is characterized by a strong foliation that is parallel to $Sl_1$; this foliation is locally composite, offsetting an earlier foliation that is possibly equivalent to Se and is also offset by local shear bands that are parallel to $Sl_2$ of the pluton.

Se strikes north-northeast and dips steeply to the east-southeast, whereas $Sl_1$ strikes northeast and dips moderately to steeply to the southeast (Figure 4). $Sl_1$ cross-cuts and offsets Se throughout the central domain forming shear fabrics that indicate a dextral shear sense where seen in map view. Because slip apparently occurred along $Sl_1$, and Se represents a passive foliation that was offset, we interpret the two foliations as representing S-C fabric (Berthé et al., 1979; Vernon and others, 1983), with Se forming the S-plane and $Sl_1$ as the C-plane[2]. $Sl_2$ strikes from east-northeast to east and dips steeply to the south (Figure 3). $Sl_2$ crosscuts and offsets $Sl_1$ producing a shear fabric similar in geometry to a C' fabric. Asymmetric foliations indicate that the sense of shear along $Sl_2$ is dextral where seen in map view.

Two generations of lineations, $L_e$ and $Ll_2$, are associated with the foliations $S_e$ and $Sl_2$. $L_e$ was

2. We use the term "S-C" in a strictly geometric sense, with no genetic implications, for foliations with a configuration like that described by Berthé *et al.* (1979).


B
D
A
C

observed along $S_e$ in the southwestern and central domains, whereas $Ll_2$ was observed along $Sl_2$ in the wing domain. The observed lineations are defined by shape-preferred orientations of quartz, biotite smears, and feldspar grains. The average trend of $L_e$ is ~052° with an average plunge of ~42°, whereas the average trend of $Ll_2$ in the pluton is ~220° with an average plunge of ~30° (Figure 4). Both generations of lineation are found in the country rock around the pluton (Figure 4).

$S_e$ is found in the southwest domain where it is defined by a weak preferred alignment of biotite and muscovite which define the boundaries of coarse quartz and feldspar aggregates. $S_e$ in this part of the granite body is weakly developed to nonexistent and rock exposures here, typically have a coarse-grained, undeformed appearance.

$S_e$ and $Sl_1$ are common throughout the central domain of the granite body. $S_e$ is defined by aligned quartz blebs, quartz ribbons, biotite, muscovite, and feldspar aggregates inclined at an intermediate to high angle to $Sl_1$. $Sl_1$ is defined by micas that anastomose around $S_e$. There is less grain size reduction within this domain relative to the wing domain; grain size reduction is largely confined to local mylonitic zones in the central domain.

$Sl_1$ and $Sl_2$ are prominent in the wing domain of the High Rock granite. $Sl_1$ is defined by quartz ribbons, aligned mica, and feldspar porphyroclasts, inclined at an intermediate to shallow angle to $Sl_2$. $Sl_2$ is defined by aligned micas. The rock in the wing domain is noticeably grain size reduced and locally displays asymmetric mesofolds of $Sl_2$. The consistent downplunge asymmetry of the folds suggests that they formed by dextral shear, consistent with the other shear fabrics.

The sum of these observations indicates heterogeneous deformation of the granite. There was less penetrative deformation in the southwest and central domains of the stock, where the granite displays weakly to moderately developed foliations with coarse textures and local unfoliated zones of granite. The wing domain is interpreted to have experienced the most penetrative deformation, displaying prominent foliations and noticeable grain size reduction.

## Microscale Structures

Like the mesoscale foliation characteristics, the microfabrics in the three structural domains are also heterogeneously developed across the stock. In particular, fabrics in the southwest domain are different from fabrics in the central and wing domains.

### Southwest Domain

In this domain, rocks are predominantly non- to weakly foliated. Where there are no foliations at the hand sample scale, in thin section the micas are randomly distributed with no preferred orientation. Biotite is the dominant mica and displays sharp extinction with little or no deformation. Where there is a weak foliation, biotite is still the dominant mica phase and shows an incipient preferred orientation parallel to $S_e$ with its grain boundaries truncating quartz and feldspar aggregates.

Quartz has commonly undergone dynamic recrystallization, displaying progressive subgrain rotation accompanied by grain boundary migration recrystallization suggesting that deformation occurred at low to moderate temperatures by dislocation creep (Figure 5A) (Regimes 2 and 3 of Hirth and Tullis, 1992).

Feldspars tend to retain their euhedral shape and interlocking igneous textures lacking any planar alignment. The grains predominantly show no preferred orientation, but in two rocks the feldspars are slightly aligned with their long axes and twin planes in the same direction. The

**Figure 5. (A) Quartz displaying grain boundary migration recrystallization in an unfoliated rock from the southwestern domain. Field of view = 1.7 mm, crossed polars. (B) Muscovite fish indicating dextral motion. Note myrmekite in the extinct feldspar above the muscovite Field of view = 1.7 mm. (C) Type 2a quartz ribbon (Boullier and Bouchez, 1978) displaying grain shape-preferred orientation fabric in quartz. Field of view = 1.7 mm. (D) Fractured feldspar with recrystallized quartz infilling. Field of view = 0.72 mm.**

**Figure 6. Sigma-type porphyroclast indicating dextral sense of motion. Note epidote and sericite throughout the feldspar grain. Field of view = 3.55 mm.**

preferred orientation of feldspars in two undeformed rocks could be interpreted either as relict magmatic flow textures or coincidental alignment. The latter interpretation is more likely, because almost all of the undeformed rocks do not contain feldspars with preferred orientations.

## Central and Wing Domains

In the central and wing domains of the granite, both muscovite and biotite define $Sl_1$ and $Sl_2$. Muscovite is the dominant mica in the wing domain. Muscovite and biotite have a preferred orientation and display solid-state fabrics such as undulatory extinction, mica fish, and grain size reduction (neocrystallization and dynamic recrystallization) (Figure 5B).

Quartz grains have been deformed into ribbons, ranging from stretched and flattened monocrystalline quartz, to type 1-, type 2-, and type 4-ribbons (Boullier and Bouchez, 1978) (Figure 5C) (Regime 2 to Regime 3 of Hirth and Tullis, 1992). Other microstructures within quartz include undulatory extinction, deformation bands, and a grain shape-preferred orientation fabric (Figure 5C). These microstructures suggest that the rocks within these portions of the granite were subjected to low to moderate temperatures (450°-500°C) (Regime 2 and Regime 3 of Hirth and Tullis, 1992) (Fitz Gerald and Stunitz, 1993).

The feldspars in the more deformed rocks tend to be rounded with their long axes lying slightly oblique to concordant with $Sl_1$. This latter observation suggests that the feldspars define $S_e$ and with increasing deformation their long axes rotated towards $Sl_1$. Common textures observed in more deformed feldspars include deformation bands and patchy undulatory extinction. The latter feature may be the result of microfractures that were caused by cataclasis (Tullis and others, 1980). Also some feldspars are visibly fractured or cracked and filled with very fine recrystallized quartz and feldspar grains (Figure 5D). Other deformation features observed in the feldspars were core and mantle textures, sigma-type porphyroclasts (Figure 6), grain size reduction, myrmekite, mechanical twinning, and boudinage. These observations indicate that the feldspars experienced some ductile deformation and are consistent with a low to moderate temperature (450°-500° C) deformational regime (Tullis, 1983; Fitz Gerald et al., 1983).

Thin sections taken parallel to $L_e$ and $Ll_2$ commonly display boudinage of strong minerals such as feldspar. This observation suggests that $L_e$ and $Ll_2$ are stretching lineations and

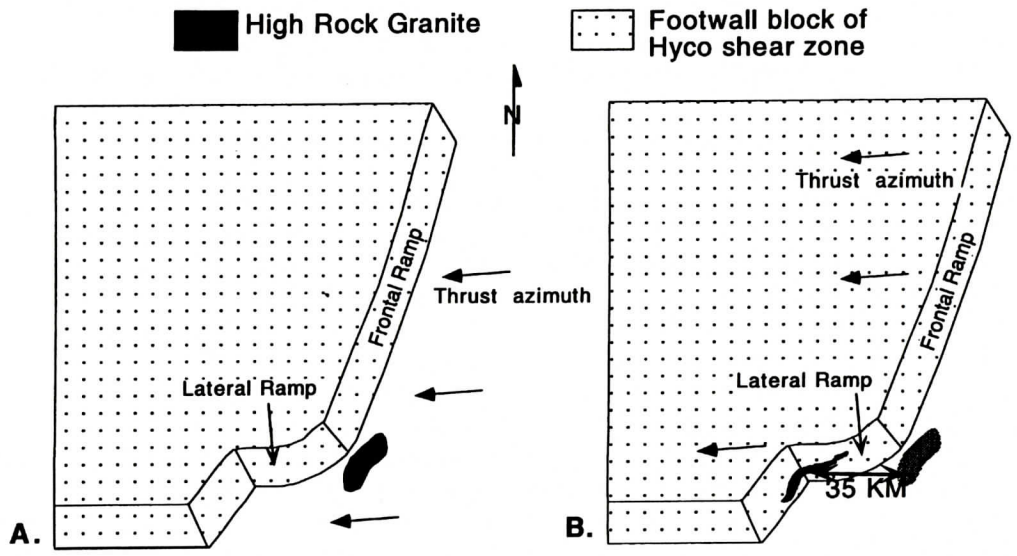


**Figure 7. Emplacement model for the High Rock granite based on retrodeformation of our kinematic interpretation: A. Generation of $S_e$ along a thrust flat in the Hyco shear zone, B. Generation of $Sl_1$ and $Sl_2$ along a lateral ramp in the Hyco shear zone Minimum displacement estimate of 35 km denoted by double ended arrow.**

hence, reflect the transport direction (Figs. 3 and 4). This observation is supported by observations elsewhere in the shear zone (Hibbard and others, in press).

In summary, fabric development in the High Rock granite is characteristically disparate in different portions of the stock. It is least deformed in the southwest domain. Toward the wing domain, foliations become more intense and the grain size is noticeably reduced. The northern contact of the High Rock granite displays penetrative fabrics, whereas the southern contact displays less developed fabrics. However, an important observation in the High Rock granite is that quartz has been deformed by solid-state processes throughout all portions of the stock. This observation combined with the lack of evidence for magmatic fabrics, the presence of low to moderate temperature (450°-500° C) solid state fabrics and the presence of xenoliths with foliations parallel to the regional fabric all indicate that the High Rock granite is pretectonic with respect to the Hyco shear zone. The low to moderate temperature foliations, in particular, are inconsistent with a syntectonic origin for the stock, in which case we would expect to develop high temperature (650°-700° C) fabrics.

## DISCUSSION AND CONCLUSION

Considered in conjunction with other observations, our interpretation that the High Rock granite is pretectonic with respect to the Hyco shear zone has age implications for the stock. The High Rock granite strongly resembles the nearby Osmond granite (Figure 1). Zircon from the Osmond granite has yielded a preliminary U-Pb age of approximately 616 Ma (Wortman et al., 1995). Petrographically, the two granites are very similar to one another and both contain plagioclase with a composition of roughly $An_{35}$. In addition, solid state fabrics within the Osmond granite are indistinguishable from those in the High Rock and appear to have formed at low to medium temperatures (J. Vines, unpublished notes). Thus we conclude from the data at hand that the High Rock pluton is most likely related to the Neoproterozoic granite suite that is found in the hanging wall of the shear zone.

Our structural study of the High Rock granite can also yield insights into the kinematics of the

Hyco shear zone. The lineations, $L_e$ and $Ll_2$, are represented in separate portions of the stock. $L_e$ is only observed in the southwestern and central domains, whereas $Ll_2$ is only seen in the wing domain of the granite. We rotated $S_e$ and the associated $L_e$ around the strike of $S_e$ to a subhorizontal thrust flat attitude (Figure 4). The rotated northeast-plunging lineations show a strikingly similar orientation to northeast-plunging lineations observed in the South Boston domain of the Hyco shear zone (Figure 4) (Bradley, 1996; Hibbard and others, in press). Thus, kinematically, $S_e$ rotated to the horizontal is compatible with thrust flat motion along the Hyco shear zone. The southwest-plunging $Ll_2$ in the wing domain of the granite is directly correlative with southwest-plunging lineations typical of the Hyco Lake domain lateral ramp of the Hyco shear zone (Shell, 1996; Hibbard and others, in press).

The foliation development within the granite is progressively more intense from the southwest domain to the wing domain. In the structurally lowest portions of the southwest and central domains, $S_e$ and $Sl_1$ are prominent, whereas in the wing domain $Sl_2$ is dominant. $S_e$, $Sl_1$, and $Sl_2$ are defined by the same minerals and there is no evidence of alteration, such as chlorite along these foliations. In addition, on the basis of associated microstructures, all of the foliations appear to have formed at low to medium temperatures (450°-500° C). These observations suggest that all of the foliations formed under the same crustal conditions and likely during the same event. In addition, a similar sequence of foliations in the adjacent Country Line complex has been related to progressive deformation during a single shearing event in the Hyco shear zone (Shell, 1996; Hibbard and others, 1998).

Based on these observations, we present a model for the structural history of the High Rock granite (Figure 7); the granite is interpreted to be a pretectonic granite at the base of the hanging wall of the Hyco shear zone. $L_e$, when rotated to horizontal, is compatible with the kinematics of the South Boston domain of the Hyco shear zone; thus, we suggest that $S_e$ and $L_e$ formed along a thrust flat in the shear zone as the Carolina terrane was thrust over the Milton terrane. The progressive weakening of $S_e$ away from the structural base of the stock in the northwest, is compatible with this interpretation as deformation of the hanging wall, including the structural base of the pluton, would be expected to be localized immediately adjacent to a shear zone flat. The present orientation of $S_e$ suggests that the High Rock granite was thrust up a local frontal ramp similar to the South Boston domain of the Hyco shear zone. The local change in the trend of the shear zone near Yanceyville, North Carolina supports this interpretation (Shell, 1996). $Sl_1$ and $Sl_2$ are parallel to the structural trend of the Hyco Lake domain lateral ramp of the Hyco shear zone and are confined to the portion of the pluton adjacent to that ramp. The intense overprint of the later foliations, $Sl_1$ and $Sl_2$ is consistent with intense deformation of that section of the hanging wall, and in particular, that part of the stock, "sideswiped" by an obstructing lateral ramp. The orientations of $Ll_2$ and associated shear sense indicators are compatible with those found elsewhere in the Hyco Lake domain lateral ramp (Hibbard and others, in press). Consequently, we interpret all three foliations and associated microstructures as having formed during the progressive interaction of the hanging wall of the Hyco shear zone with a thrust flat and subsequently a lateral ramp at upper-mid crustal conditions.

Our kinematic interpretation of the High Rock pluton allows us to estimate the minimum displacement along the Hyco shear zone. Retrodeforming displacement of $Sl_1$ and $Sl_2$ along the Hyco Lake domain lateral ramp by moving the stock east-northeast along $Ll_2$, the nearest thrust flat that could be responsible for the development of $S_e$ and $L_e$ would be at the corner of the ramp system at the junction of the Hyco Lake and South Boston domains (Figure 7). The distance from the present position of the stock to the ramp corner is approximately 35 km. The development of $S_e$ must have required further motion along the shear zone flat, so we consider this 35 km displacement along the lateral ramp to represent a minimum displacement along the Mississippian Hyco shear zone.

Our estimate is the only available constraint on displacement along the Hyco shear zone at present. Considering that the shear zone is interpreted to be the northern segment of the central Piedmont shear zone, a ductile thrust that extends the length of the southern Appalachians (Hibbard and others, in press; Wortman and others, in press), we suspect that there was substantially more displacement along this structure than our minimum estimate.

## ACKNOWLEDGMENTS

This study constitutes a senior research project by JV. It was partially supported by the National Science Foundation (Grant EAR-9219979 to JH); additional finances were provided by the North Carolina Geological Survey (GSS), and the Geological Society of America (GSS). We thank Rick Law and Skip Stoddard for constructive comments on the manuscript and Allen Dennis and Robert Hatcher Jr. for journal reviews; all of their comments helped to substantially improve the manuscript.

## REFERENCES

Berger, A.R. and Pitcher, W.S., 1970, Structures in granite rocks: a commentary and critique on granite tectonics: Proceedings of the Geological Association, v. 81, p. 441-461.

Berthé, D., Choukroune, P., and Gapais, D., 1979, Orthogneiss, mylonite and non-coaxial deformation of granites: the example of the South Armorican shear zone: Journal of Structural Geology, v. 1, p. 31-42.

Blumenfeld, P. and Bouchez, J.L., 1988, Shear criteria and migmatite deformed in the magmatic and solid states: Journal of Structural Geology, v. 10, p. 361-372.

Boullier, A.M. and Bouchez, J.L., 1978, Le quartz en rubans dans les mylonites: Bulletin de la Société Geologique de France, v. 7, p. 253-262.

Bradley, P. J., 1996, The structural relationship between the Hyco shear zone and the Milton terrane in the South Boston, Virginia area: M.Sc. Thesis, North Carolina State University, Raleigh, North Carolina, 86p.

Butler, J.R. and Ragland, P., 1969, Petrology and chemistry of meta-igneous rocks in the Albemarle area, North Carolina slate belt: American Journal Science, v. 267, p. 700-726.

Butler, J.R. and Secor, D.T., Jr., 1991, The central Piedmont: in Horton, J.W. and Zullo, J., editors, Geology of the Carolinas, Carolina Geological Society 50th Anniversary Volume, University of Tennessee Press, Knoxville, Tennessee, p. 59-78.

Dennis, A., 1995, The Carolina terrain in northwestern South Carolina: Relative timing of events and recent tectonic models: in Hibbard, J., van Staal, C., and Cawood, P., editors, Current Perspectives in the Appalachian-Caledonian Orogen, Geological Association of Canada Special Paper 41, p. 173-189.

Eggleton, R.A. and Buseck, P.R., 1980, The orthoclase-microcline inversion: a high-resolution transmission electron microscope study and strain analysis: Contributions to Mineralogy and Petrology, v. 74, p. 123-133.

Feiss, G., 1982, Geochemistry and tectonic setting of the volcanics of the Carolina slate belt: Economic Geology, v. 77, p. 273-293.

Fitz Gerald, J., Etheridge, M., and Vernon, R., 1983, Dynamic recrystallization in a naturally deformed albite: Textures and Microstructures, v. 5, p. 219-229.

Fitz Gerald, J. and Stunitz, H., 1993, Deformation of granitoids at low metamorphic grade. I: Reactions and grain size reduction: Tectonophysics, v. 221, p. 269-297.

Gapais, D. and Barbarin, B., 1986, Quartz fabric transition in a cooling syntectonic granite (Hermitage Massif, France): Tectonophysics, v. 125, p. 357-370.

Glover, L. III and Sinha, A., 1973, The Virgilina deformation, a late Precambrian to Early Cambrian orogenic event in the central Piedmont of Virginia and North Carolina: American Journal of Science, v. 273-A, p. 234-251.

Henika, W., 1977, Geology of the Blairs, Mount Hermon, Danville, and Ringgold quadrangles, Virginia: Virginia Division of Mineral Resources Publication 2, 45 p.

Hibbard, J., 1993, The Milton belt-Carolina slate belt boundary; The northern extension of the Central Piedmont Suture?: in Hatcher, R. and Davis, T., editors, Studies of Inner Piedmont Geology: 1993 Carolina Geological Society Guidebook, p. 85-89.

Hibbard, J. and Samson, S., 1995, Orogenesis exotic to the Iapetan cycle in the southern Appalachians: in Hibbard, J.P., van Staal, C.R., and Cawood, P.A., editors, Current Perspectives in the Appalachian-Caledonian Orogen, Geological Association of Canada Special Paper 41, p. 191-205.

Hibbard, J., Shell, G., Bradley, P., Samson, S., and Wortman, S., in press, The Hyco shear zone in North Carolina and southern Virginia: Implications for the Piedmont Zone - Carolina Zone boundary in the southern Appalachians: American Journal of Science, v. 298.

Hirth, G. and Tullis, J., 1992, Dislocation creep regimes in quartz aggregates: Journal of Structural Geology, v. 14, p. 145-159.

Hund, E., ms, 1987, U-Pb dating of granites from the Charlotte Belt of the Southern Appalachians: M.Sc. thesis, Virginia Polytechnical Institute, Blacksburg, Virginia, 73 p.

Hutton, D.H.W., 1988, Granite emplacement mechanisms and tectonic controls: Inferences from deformation studies: Transactions of the Royal Society of Edinburgh, Earth Sciences, v. 79, p. 245-255.

Karlstrom, K.E., Miller, C.F., Kingsbury, J.A. and Wooden,

J.L., 1993, Pluton emplacement along an active ductile thrust zone, Piute Mountains, southeastern California: Interaction between deformational and solidification processes: Geological Society of America Bulletin, v. 105, p. 213-230.

Marre, J., 1986, The Structural Analysis of Granitic Rocks: Elsevier, Amsterdam, 123 p.

Morand, V.J., 1992, Pluton emplacement in a strike-slip fault zone: The Doctors Flat Pluton, Victoria, Australia: Journal of Structural Geology, v. 14, p. 205-213.

Paterson, S.R., Vernon, R.H, and Tobisch, O.T., 1989, A review of criteria for the identification of magmatic and tectonic foliations in granitoids: Journal of Structural Geology, v. 11, p. 349-363.

Secor, D., Samson, S., Snoke, A. and Palmer, A., 1983, Confirmation of the Carolina slate belt as an exotic terrane: Science, v. 221, p. 649-651.

Shell, G.S., 1996, Nature of the Carolina slate-Milton belt boundary near Yanceyville, North Carolina: M.Sc. Thesis, North Carolina State University, Raleigh, North Carolina, 96 p.

Simpson, C., 1985, Deformation of granitic rocks across the brittle-ductile transition: Journal of Structural Geology, v. 7, p. 69-79.

Tobisch, O., 1972, Geologic Map of the Milton Quadrangle, Virginia-North Carolina and adjacent areas of Virginia, scale 1:62,500: United States Geological Survey Miscellaneous Geological Investigations, Map 1-683.

Tobisch, O. and Glover, L. III, 1971, Nappe formation in part of the southern Appalachian Piedmont: Geological Society of America Bulletin, v. 82, p. 2209-2230.

Tullis, J., 1983, Deformation of feldspars: in Ribbe, P. (ed.), Feldspar Mineralogy, Reviews in Mineralogy, v. 2, Mineralogical Society of America, Washington DC, p. 297-323.

Tullis, J., Dell'Angelo, L., and Yund, R.A., 1980, Ductile shear zones from brittle precursors in feldspathic rocks: the role of dynamic recrystallization: in Hobbs, B.E., Heard, H.C., editors, Mineral and rock deformation: laboratory studies, American Geophysical Union, Geophysical Monograph 56, p. 67-87.

Vauchez, A., 1980, Ribbon texture and deformation mechanisms in quartz in a mylonitized granite of Great Kabylia (Algeria): Tectonophysics, v. 67, p. 1-2.

Vernon, R.H., 1983, Restite, xenoliths, and microgranitoid enclaves in granites: Journal of the Royal Society of New South Wales, v. 116, p. 77-103.

Vernon, R.H., Williams, V.A., D'arcy, W.F., 1983, Grain size reduction and foliation development in a deformed granitoid batholith: Tectonophysics, v. 92, p. 123-145.

Vernon, R.H., Etheridge, M.A., and Wall, V.J., 1988, Shape and microstructure of microgranitoid enclaves: indicators of magma mingling and flow: Lithos, v. 22, p. 1-12.

Wortman, G., Samson, S., and Hibbard, J., 1995, U-Pb zircon geochronology of the Milton and Carolina slate belts, southern Appalachians: Geological Society of America Abstracts with Program, v. 27, no. 2, p. 98.

Wortman, G., Samson, S., and Hibbard, J., 1996, Discrimination of the Milton belt and Carolina terrane in the southern Appalachians: a Nd isotopic approach: Journal of Geology, v. 104, p. 239-247.

Wortman, G., Samson, S., and Hibbard, J., in press, Precise timing constraints on the kinematic development of the Hyco shear zone: Implications for the central Piedmont shear zone, southern Appalachian orogen: American Journal of Science, v. 298.

SOUTHEASTERN GEOLOGY
V. 37, No. 4, May 1998, p. 177-188

# THE LATE NEOPROTEROZOIC POND MOUNTAIN VOLCANIC COMPLEX, BLUE RIDGE PROVINCE SOUTHERN APPALACHIANS

**CHRISTOPHER M. BAILEY**

*Department of Geology*
*College of William & Mary*
*Williamsburg, VA 23187*
*cmbail@facstaff.wm.edu*

**KELLY K. ROSE**

*Department of Geological Sciences*
*Virginia Tech*
*Blacksburg, VA 24061*
*kerose@vt.edu*

## ABSTRACT

**Weakly metamorphosed late Neoproterozoic felsic igneous rocks of the Pond Mountain volcanic center crop out between the Stone Mountain and Catface thrusts in northwestern North Carolina. Porphyritic rhyolites are interlayered with volcaniclastic sedimentary rocks and comprise a two kilometer thick sequence. The small (< 2 km²) Whindling Ridge alkali feldspar granite intrudes the Pond Mountain volcanics and Mesoproterozoic basement rocks. Petrographic and chemical analysis suggests that the Whindling Ridge pluton is the intrusive equivalent of the Pond Mountain volcanics. Both intrusive and extrusive rocks are characterized by high $SiO_2$, $Al_2O_3$, $K_2O$ and low $Na_2O$, CaO, $Fe_2O_3$. Volcanics are overlain by a locally extensive arkosic conglomerate and fine-grained volcaniclastic rocks. Younger non-volcanogenic metagraywackes and quartz-rich schists stratigraphically overlie the Pond Mountain complex. Stratigraphic evidence suggests that the Pond Mountain volcanic center is older than the 758 ± 12 Ma Mount Rogers volcanic complex.**

## INTRODUCTION

Late Neoproterozoic rocks in the central and southern Appalachian Blue Ridge record an extended episode of rifting in eastern Laurentia that culminated in the opening of the Iapetus Ocean. Magmatic activity occurred during both the early (750-700 Ma) and late stages (590-550 Ma) of rifting, but was neither temporally nor spatially continuous (Rankin, 1975; Su and others, 1994; Aleinikoff and others, 1995; Fetter and Goldberg, 1995). This late Neoproterozoic magmatic suite includes a diverse array of both intrusive and extrusive rocks. Early stage volcanic activity occurred in the Grandfather Mountain area (765-740 Ma) in northwestern North Carolina, the Mount Rogers area (760 Ma) in southwestern Virginia, and in the northern Virginia Blue Ridge (700 Ma) (Aleinikoff and others, 1995; Fetter and Goldberg, 1995, Tollo and Aleinikoff, 1996). The 570 Ma Catoctin Formation in northern Virginia, Maryland, and southern Pennsylvania and basalts associated with the lower Unicoi Formation in southwestern Virginia formed during the later stages of rifting (Badger and Sinha, 1988; Aleinikoff and others, 1995).

The Mount Rogers Formation in southwestern Virginia, northwestern North Carolina, and northeastern Tennessee is the most extensive package of late Neoproterozoic felsic volcanic rocks exposed in the central and southern Appalachians (Figure 1) (Rankin and others, 1989). The Mount Rogers Formation is a thick, heterogeneous package of rhyolitic lavas, tuffs, associated volcaniclastic sedimentary rocks, and minor mafic igneous rocks. Rankin (1993) recognized three different volcanic centers (or

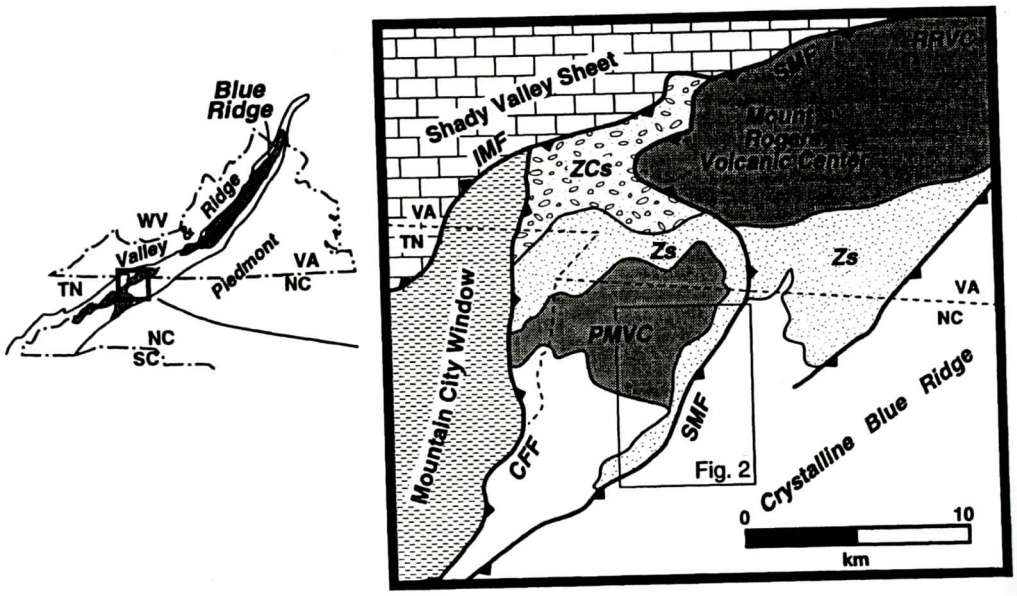


**Figure 1. Geologic overview map of northwestern North Carolina, southwestern Virginia, and northeastern Tennessee. Modified from King and Ferguson (1960), Rankin and others (1972), and Rankin (1993). CFF- Catface fault, IMF- Iron Mountain fault, PMVC- Pond Mountain volcanic center, RRVC- Razor Ridge volcanic center, SMF- Stone Mountain fault, Zcs- Konnarock and Unicoi Formations in Catface thrust sheet, Zs- sedimentary rocks associated with the Mount Rogers and Pond Mountain volcanic centers.**

complexes) in the Mount Rogers Formation based on characteristic lithologies, stratigraphic position, and structural level. From east to west these include the Razor Ridge, Mount Rogers, and Pond Mountain centers (Figure 1). The Mount Rogers volcanic center is the most extensively studied, containing basal volcanic and sedimentary rocks overlain by three distinct rhyolitic units (Buzzard Rock Member, Whitetop Rhyolite Member, and Wilburn Ridge Rhyolite Member) (Rankin, 1993). Zircons from the Whitetop Rhyolite Member yield a 758 ±12 Ma U-Pb age (Aleinikoff and others, 1995). Unconformably overlying the Mount Rogers Formation are the non-volcanogenic sedimentary rocks of the late Neoproterozoic Konnarock Formation (Rankin, 1993).

The Pond Mountain volcanic complex crops out to the west-southwest of the Mount Rogers volcanic center in the Catface thrust sheet (Figures 1 and 2). Rocks of the Mount Rogers center structurally overlie the Pond Mountain complex in the Stone Mountain thrust sheet (Figures 1 and 3). Rankin (1993) noted that rhyolites in the Pond Mountain complex are similar to rhyolites of the Mount Rogers center, but are coarsely porphyritic (possibly indicative of hypabyssal magmatism). The stratigraphy of the Pond Mountain volcanic complex has never been studied in detailed, and the relationship between the Mount Rogers and Pond Mountain centers is not clear. This study describes the volcanic stratigraphy of the Pond Mountain complex, recognizes a shallow-level granitic pluton associated with volcanic rocks of that complex, and proposes a model for the evolution of late Neoproterozoic volcanism in the region.

## GEOLOGIC SETTING

The Blue Ridge province in the southern Appalachian orogen is a composite crystalline thrust complex that experienced northwest-directed transport during the Paleozoic (Hatcher, 1989). Mesoproterozoic crystalline rocks, late Neoproterozoic Iapetan rift-related units, and lower Cambrian clastic units crop out in a series of thrust sheets along the northwestern edge of

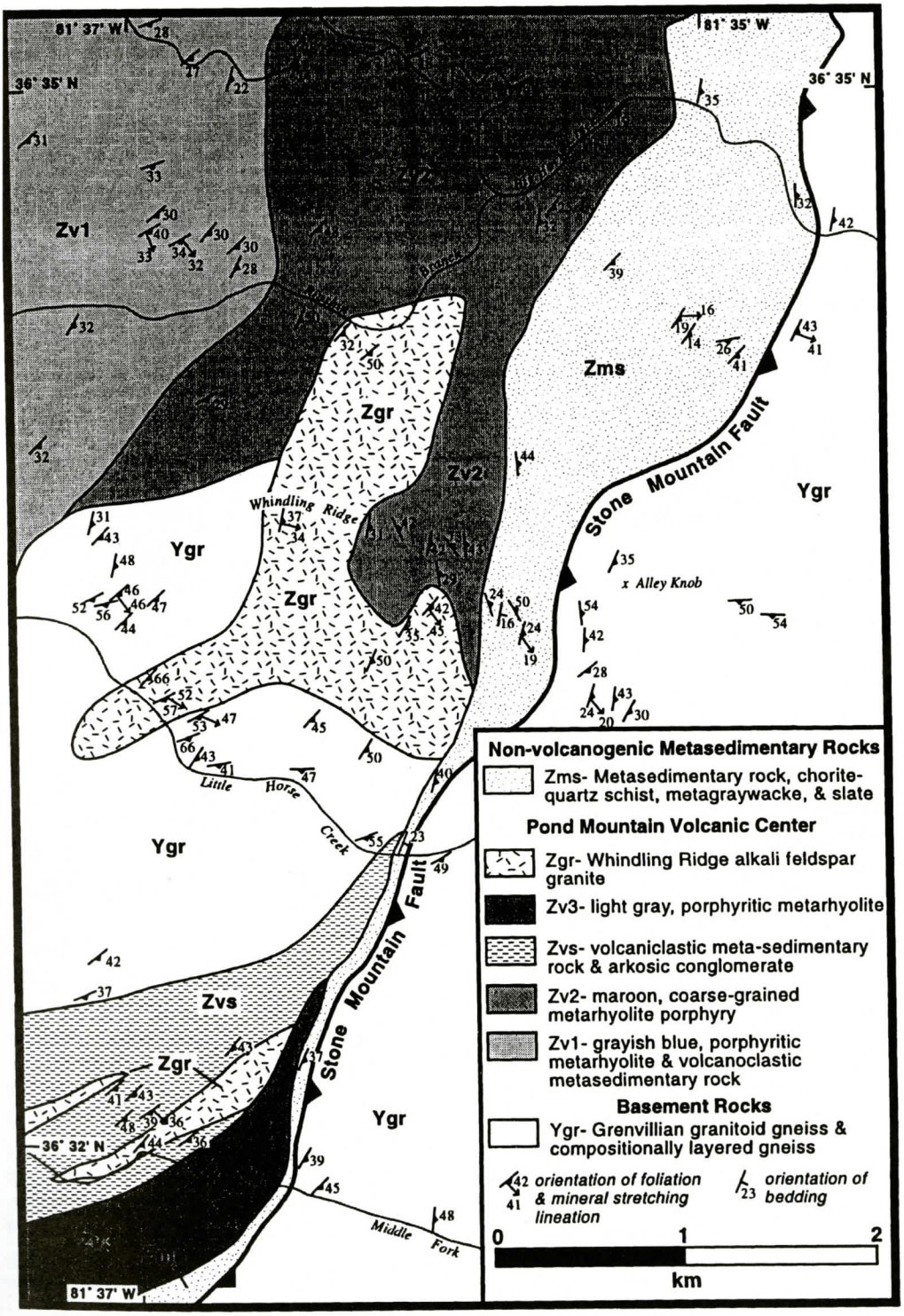


**Figure 2. Detailed geologic map of the eastern portion of the Pond Mountain complex, Ashe County, North Carolina. Park 7.5' quadrangle.**

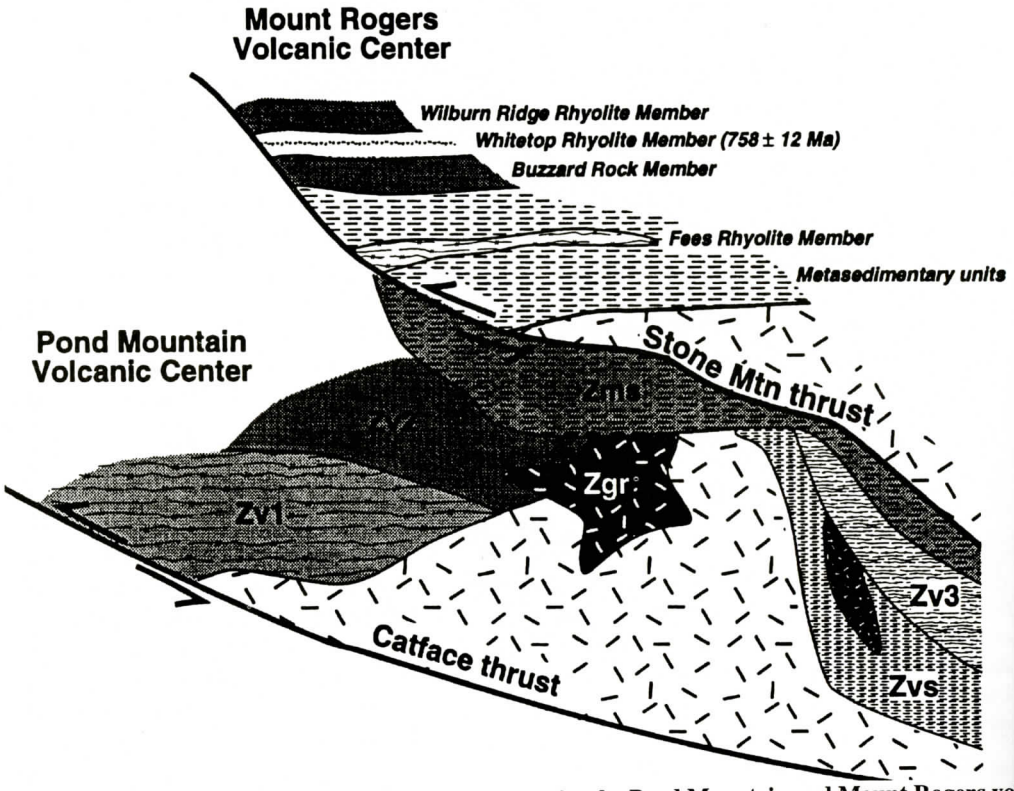


**Figure 3. Generalized structural/stratigraphic column for the Pond Mountain and Mount Rogers volcanic centers. Abbreviations are the same as Figure 2.**

the Blue Ridge (Figure 1). Thrust sheets in the Blue Ridge were deformed and folded by movement on underlying thrusts, and subsequent erosion has produced present-day structures such as the Mountain City window (Figure 1) (Rankin and others, 1991; Boyer, 1992).

The western Blue Ridge underwent greenschist facies metamorphism during the Paleozoic, however metamorphic gradients increase to the southeast and southwest (Butler, 1991). In western North Carolina the Blue Ridge thrust complex experienced at least three Paleozoic tectonothermal events, and records metamorphic crystallization and cooling ages that range from approximately 450 to 300 Ma (Goldberg and Dallmeyer, 1997; Adams and Trupe, 1997). Mylonitic fault rocks in the Blue Ridge basement record ages between 330 and 300 Ma in northwestern North Carolina (Schedl and others, 1992; Adams and Su, 1996; Goldberg and Dallmeyer, 1997).

## STRATIGRAPHY

Our mapping in northwestern Ashe County, North Carolina (structurally above the Mountain City window and below the Gossan Lead fault/Fries fault) indicates that three distinct lithologic packages occur in this portion of the Blue Ridge: 1) Mesoproterozoic gneissic and granitoid basement rocks, 2) late Neoproterozoic metavolcanic, metaplutonic, and associated volcanogenic metasedimentary rocks of the Pond Mountain complex, and 3) late Neoproterozoic (?) non-volcanogenic metasedimentary rocks (Figures 2 and 3). Rocks in northwestern Ashe County experienced Paleozoic greenschist facies metamorphism. For the sake of brevity the prefix "meta" is omitted from the remainder of the text, but should be assumed for these rocks.

## Basement Rocks

Gneissic and granitoid Grenvillian basement rocks crop out in the hanging wall of the Stone Mountain fault east of the Pond Mountain complex, and in the footwall of the Stone Mountain fault to the south of the Pond Mountain volcanics (Figures 1 and 2). Basement rocks are compositionally diverse and distinctive lithologies are mappable at 1:24,000 scale.

The oldest basement unit is a compositionally layered gneiss that crops out in the southeastern portion of the field area. Compositional layering ranges from a few centimeters to several meters in thickness. Felsic layers contain plagioclase, quartz, and alkali feldspar whereas mafic-rich layers are dominated by plagioclase, hornblende, and biotite. The compositionally layered gneiss is intruded by medium-grained granodioritic gneiss and a medium- to coarse-grained granitic unit, both of Mesoproterozoic age. Granitoid basement rocks are composed predominantly of plagioclase and quartz with lesser amounts of alkali feldspar, biotite, and epidote. Modal analysis of the granitoid basement illustrates the compositional differences between the granodioritic and granitic units (Figure 4). Away from ductile fault zones these rocks exhibit only a weak fabric, characterized by aligned phyllosilicates, but near fault zones mylonitic foliation is well developed.

Although, earlier workers (Rankin, 1970; Rankin and others, 1972) recognized a number of distinct rock types, they followed the nomenclature of Keith (1903) and generally mapped the basement complex as Cranberry gneiss. More recent workers have delineated multiple units within the basement (Bartholomew, 1983; Bartholomew and Lewis, 1984). Although no isotopic age dates have been determined for basement rocks in northwestern Ashe County, these units are very similar to Grenvillian rocks dated between 1200 and 1000 Ma in the region (Fullagar and Odom, 1973; Fullagar and Bartholomew, 1983).

## Pond Mountain Volcanic Center

Rocks of the Pond Mountain volcanic center crop out in the hanging wall of the Catface fault and form a sequence of extrusive, intrusive and volcaniclastic sedimentary rocks, at least 2 km in thickness (Figures 1, 2, and 3). The most common rock types are porphyritic rhyolites that are penetratively foliated and contain between 10-50% phenocrysts of quartz and alkali feldspar in a fine-grained matrix.

Three rhyolite units were recognized based on stratigraphic position, phenocryst content, and overall grain size. The western portion of the Pond Mountain complex is composed predominantly of grayish-blue to maroon porphyritic rhyolites (Zv1) that contain between 10 and 25% phenocrysts and are interlayered with medium- to fine-grained schistose volcaniclastic rocks (Figures 2 and 3). A coarse-grained maroon rhyolite porhyry (Zv2) crops out along the northeastern margin of the complex (Figures 2, 3). Phenocrysts of white to greenish alkali feldspar (up to 1 cm), and reddish gray quartz compose between 30 to 50% of this rock (Figure 5a). To the southwest, a gray fine-grained porphryitic rhyolite (Zv3), with 10 to 20% phenocrysts overlies volcaniclastic sedimentary rocks (Figures 2 and 3). Although volcanic units contain a penetrative foliation defined by fine-grained sericite, quartz, and chlorite, many primary volcanic features are preserved. These include embayed quartz phenocrysts (Figure 6a), dipyramidal quartz phenocrysts, euhedral alkali feldspar phenocrysts, and elongate fiamme. Angular, shard-like phenocrysts of both quartz and alkali feldspar are common (Figure 5a). Alkali feldspar and quartz comprise between 95% and 100% of the phenocrysts. Magnetitie and ilmenite phenocrysts occur as accessory phases in all samples and plagioclase phenocrysts are very rare. Modal data for the phenocryst assemblage plot in the alkali feldspar granite field on a QAP ternary diagram (Figure 4). Rhyolites are characterized by high silica (≈75% $SiO_2$), aluminum (≈12% $Al_2O_3$), and potassium (≈ 5.5% $K_2O$); low sodium (≈1% NaO) and iron (≈3% $Fe_2O_3$); and very low calcium (≈0.15% CaO) (Table 1).

A small pluton, here named the Whindling Ridge alkali feldspar granite, intrudes Pond Mountain rhyolites and basement rocks. The

**Table 1. Chemical compositions of granitoid basement rocks, metarhyolites, and Whindling Ridge alkali feldspar granite. X-ray fluorescence analysis done by XRAL Laboratories, Don Mills, Ontario. Weight percent for major elements, parts per million for minor elements. S. D.- Standard Deviation. LOI- Loss on Ignition.**

| | Basement (n = 5) | | Rhyolite (n = 4) | | Whindling Ridge alkali feldspar granite (n = 4) | |
|---|---|---|---|---|---|---|
| | Mean | S. D. | Mean | S. D. | Mean | S. D. |
| $SiO_2$ | 70.9 | 2.0 | 74.9 | 2.0 | 75.0 | 1.9 |
| $Al_2O_3$ | 13.9 | 0.5 | 12.2 | 1.0 | 13.6 | 1.1 |
| CaO | 1.24 | 0.76 | 0.12 | 0.12 | 0.07 | 0.02 |
| MgO | 0.54 | 0.31 | 0.20 | 0.07 | 0.49 | 0.04 |
| $Na_2O$ | 3.75 | 0.55 | 1.21 | 0.77 | 0.14 | 0.02 |
| $K_2O$ | 4.22 | 1.78 | 5.48 | 1.08 | 5.15 | 0.63 |
| $Fe_2O_3$ | 2.50 | 0.79 | 3.04 | 0.95 | 2.40 | 0.32 |
| MnO | 0.02 | 0.02 | 0.02 | 0.01 | 0.01 | 0.01 |
| $TiO_2$ | 0.28 | 0.08 | 0.85 | 1.19 | 0.31 | 0.11 |
| $P_2O_5$ | 0.10 | 0.05 | 0.04 | 0.01 | 0.06 | 0.01 |
| $Cr_2O_3$ | 0.01 | 0.01 | 0.01 | 0.00 | 0.01 | 0.00 |
| LOI | 1.04 | 0.34 | 1.59 | 0.54 | 1.94 | 0.71 |
| Sum | 98.5 | 0.43 | 99.66 | 0.48 | 99.18 | 0.59 |
| Minor Elements | | | | | | |
| Rb | 80 | 23 | 175 | 28 | 162 | 27 |
| Sr | 224 | 127 | 57 | 22 | 62 | 19 |
| Y | 27 | 11 | 92 | 36 | 48 | 25 |
| Zr | 230 | 84 | 474 | 104 | 326 | 178 |
| Nb | 10.5 | 0.6 | 41 | 17 | 24.2 | 13 |
| Ba | 1100 | 267 | 607 | 83 | 847 | 109 |

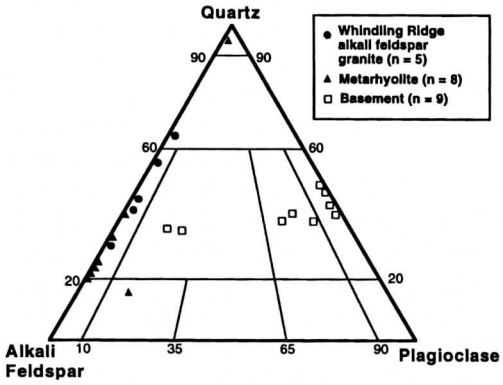


**Figure 4. Ternary diagram of quartz, alkali feldspar, and plagioclase modes in Whindling Ridge alkali feldspar granite, phenocryst assemblage in rhyolites, and basement rocks. Field boundaries after Streckeisen (1973).**

main pluton is an irregularly-shaped body (Figure 2) exposed over <2 km² area. Sill-like bodies of alkali feldspar granite as much as 200 m in thickness also intrude near the top of the volcanic sequence (Figure 2). Dikes of alkali feldspar granite cut rhyolite (Figure 5b), and inclusions of both rhyolite and granitoid basement occur in the alkali feldspar granite. The Whindling Ridge body is composed of both equigranular, medium-grained granite and a fine-grained granite with alkali feldspar and quartz phenocrysts. In thin section the Whindling Ridge intrusion is composed of alkali feldspar, quartz, sericite, and chlorite with accessory magnetite, ilmenite, and zircon (Figure 6b). Feldspar grains have commonly experienced minor to intense amounts of sericitization. Modal data plot in the alkali feldspar granite field on a QAP ternary diagram (Figure 4). Bulk rock geochemical analysis indicates that the Whindling Ridge alkali feldspar granite is similar to the rhyolites, and is characterized by high silica (≈75% $SiO_2$), aluminum (≈13% $Al_2O_3$), and potassium (≈ 5% $K_2O$); low sodium (< 1% NaO) and iron (≈2% $Fe_2O_3$); and very low calcium (≈0.07% CaO) (Table 1).

## Volcanogenic Sedimentary Rocks

In the southern portion of the study area volcaniclastic sedimentary rocks overlie Grenvil-

lian basement (Figures 2 and 3). These rocks are penetratively foliated and bedding was not recognized. The most extensive volcaniclastic sedimentary unit is a greenish-gray schist that contains detrital clasts of volcanics, Whindling Ridge alkali feldspar granite, and basement (Figure 5c). Coarse pebble to granule conglomerate is exposed at a few locations as lenses (up to 30 m in thickness) that pinch out laterally. Conglomerates contain clasts of Grenvillian basement, Whindling Ridge alkali feldspar granite, rhyolite, maroon slate, quartz, and alkali feldspar.

### Non-volcanogenic Sedimentary Rocks

A sequence of non-volcanogenic sedimentary rocks crops out to the east of the Pond Mountain volcanic complex in a belt 100 to 1000 m in width. This sequence contains interbedded dark green graywacke, quartz-muscovite schist, and slate. Bedding is preserved at a few outcrops and consistently is upright dipping shallowly to the east (Figure 5d). A pervasive foliation defined by aligned chlorite, biotite, muscovite, and quartz is common. Relict sand-sized detrital grains include quartz, plagioclase, and Fe/Ti oxides (Figure 6c). This sequence of sedimentary rocks is distinct because it contains no volcanic clasts and plagioclase grains are more abundant than in the volcaniclastics.

## STRUCTURAL GEOMETRY

Rocks throughout the study area are characterized by a northeast-southwest striking foliation that dips to the southeast (Figure 7). The foliation is produced by the alignment of greenschist facies minerals and ranges from weakly-developed to penetrative. Contacts between units are generally concordant with the foliation. To the east of and structurally above the volcanic and sedimentary sequence, mylonitic basement rocks crop out. This belt of mylonitic rocks is heterogeneous and contains zones of higher strain mylonites within lower strain protomylonites. Strongly deformed rocks are most common immediately east of the contact with the non-volcanogenic sedimentary sequence (Figure 2). Mineral stretching lineations, defined by elongate quartz and feldspar grains in the foliation plane, plunge down dip towards the southeast (Figure 7). Kinematic indicators such as asymmetric $\sigma$ and $\delta$ porphyroclasts, imbricated grains, and shear bands consistently indicate top-to-the northwest sense of shear (Figure 6d).

Non-volcanogenic sedimentary rocks are stratigraphically upright and overlie volcanics of the Pond Mountain complex. Highly strained rocks are not localized at the contact between volcanics and sedimentary rocks, but occur further east at the basement-cover contact (Figure 2). Mylonitic basement rocks, with well-developed top-to-the northwest shear sense indicators (Figure 6d), structurally overlie both the Pond Mountain volcanics and the non-volcanogenic sedimentary rocks.

## INTERPRETATIONS

The abundance of phenocrysts, their shard-like geometry, and the presence of relict fiamme throughout the Pond Mountain complex is compatible with an ash flow origin for these rocks. No primary flow fabrics were observed, and the abundance of phenocrysts in these rhyolites is incompatible with a lava flow origin for these rocks. The fine-grained porphryitic nature of the Whindling Ridge alkali feldspar granite is consistent with the emplacement of a shallow level intrusive body. Modal and geochemical data indicate both the extrusive and intrusive rocks of the Pond Mountain volcanic complex are very similar suggesting a genetic relationship between the units. The Whindling Ridge body appears to have intruded at the base of a thick rhyolite pile, and to be derived from the same magma as the overlying extrusive rocks. The interrelationship of volcanic and plutonic rocks of similar composition within the Pond Mountain volcanic complex suggests that the voluminous ash flow units may have experienced partial collapse and foundered into a subvolcanic magma chamber. The composition of the Whindling Ridge alkali feldspar granite is broadly similar to other late Neoproterozoic A-type granitoids in the central and southern Ap-

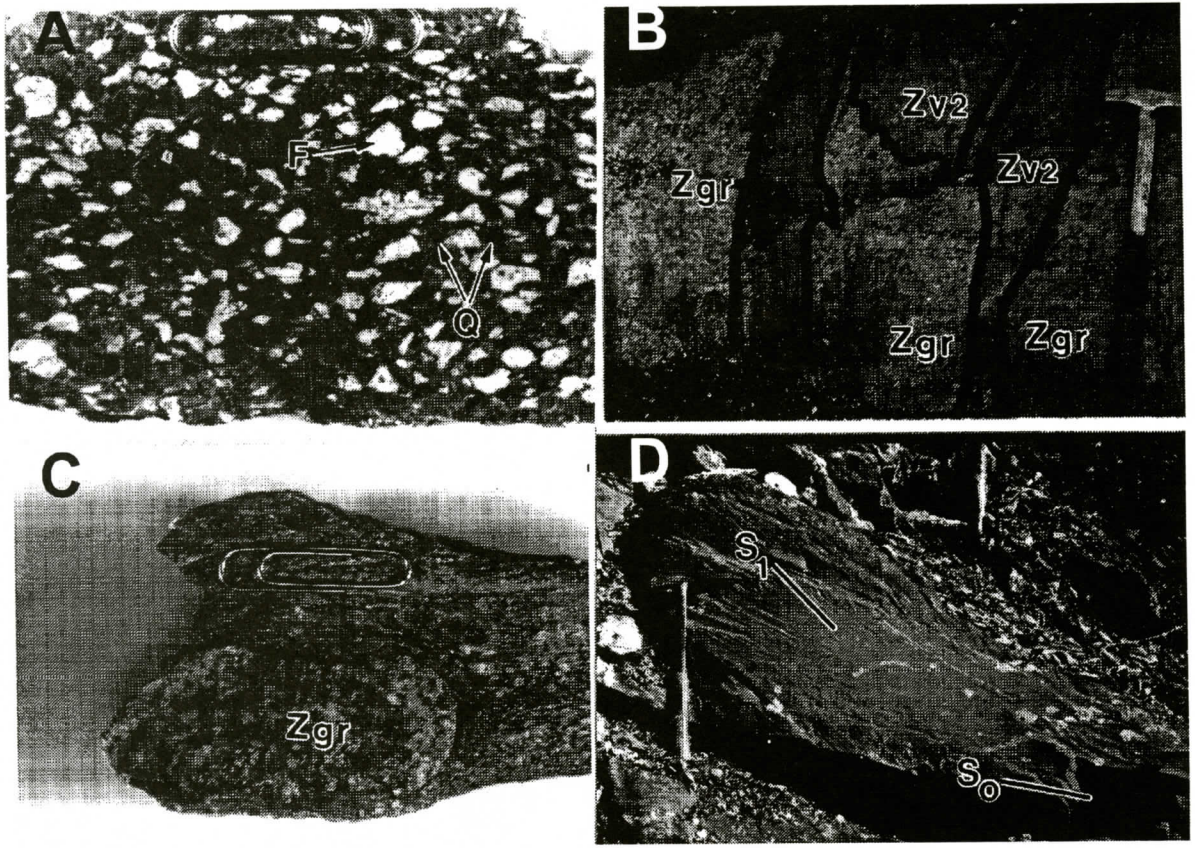


**Figure 5. A. Slab of reddish maroon coarse-grained rhyolite porphyry (Zv2), F- alkali feldspar phenocryst, Q- quartz phenocryst. Paper clip is 2.5 cm in length (from exposure on Ripshin Road, 36° 34' 35" N, 81° 35' 47" W). B. Dikes of Whindling Ridge alkali feldspar granite (Zgr) cutting porphyritic rhyolite (Zv2) (exposure on East Whindling Ridge Road 1.3 miles N of junction with Tucker Road, 36° 33' 37" N, 81° 36' 03" W). C. Clast of Whindling Ridge alkali feldspar granite (Zgr) in finer-grained volcaniclastic schist. Paper clip is 2.5 cm in length (from exposure on John Alley Road. 100 feet W of junction with Coyham Road, 36° 32' 03" N, 81° 37' 03" W). D. Southeast dipping bedding ($S_o$) in graywacke with more steeply dipping penetrative foliation ($S_1$) (exposure on Tucker Road 0.5 miles E of junction with East Whindling Ridge Road,. 36° 32' 51" N, 81° 36' 10" W).**

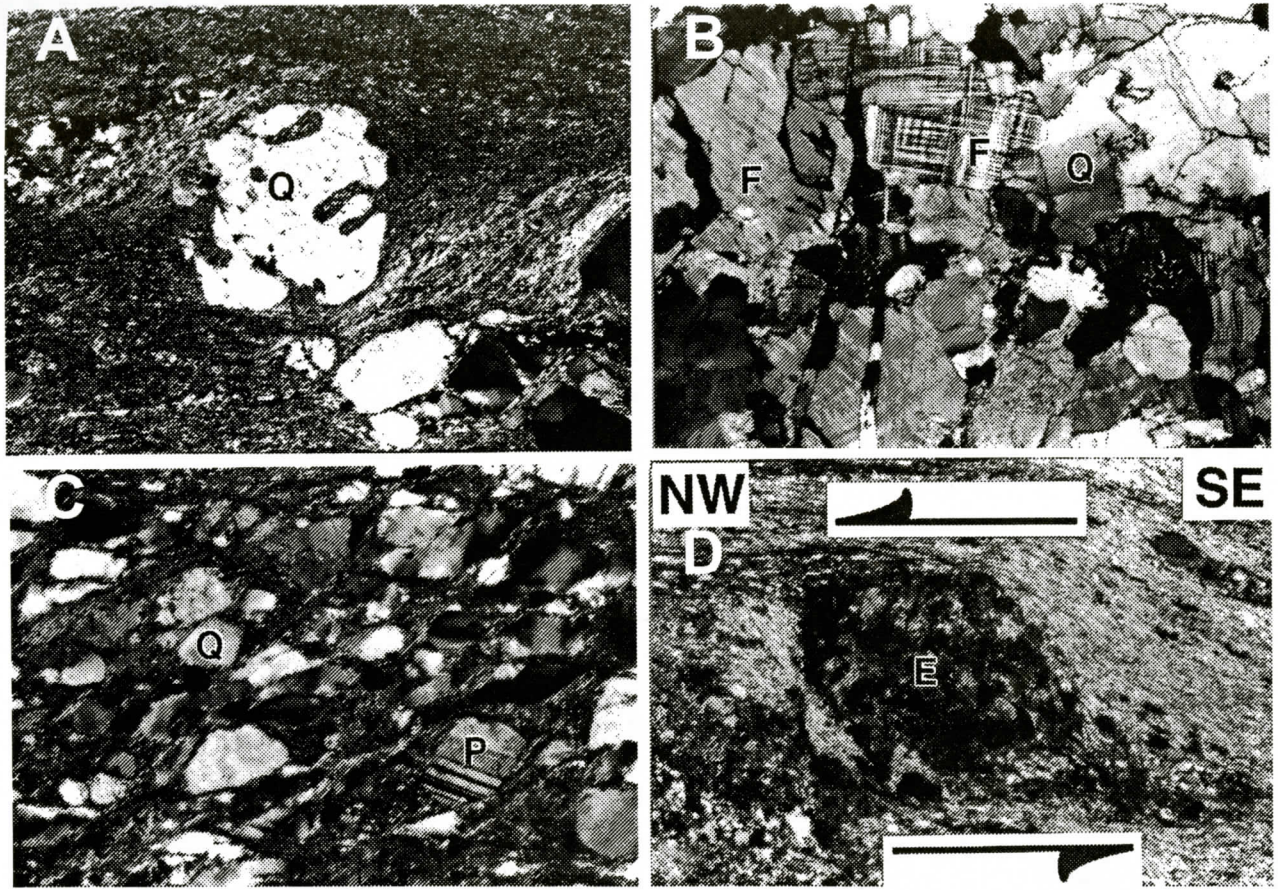


**Figure 6. A. Embayed quartz phenocryst (Q) in porphyritic rhyolite. XPL, Field of View- (FOV) 4.0 x 2.8 mm. B. Whindling Ridge alkali feldspar granite with alkali feldspar (F) and quartz (Q). XPL, FOV 4.0 x 2.8 mm. C. Graywacke with detrital quartz (Q) and plagioclase (P) grains in chlorite-rich matrix. XPL, FOV 4.0 x 2.8 mm. D. Epidote (E) porphyroclast, after garnet, with asymmetric tails indicating top-to-the northwest sense of shear in mylonitic basement rock along the Stone Mountain fault. XPL, FOV 2.0 x 1.4 mm.**

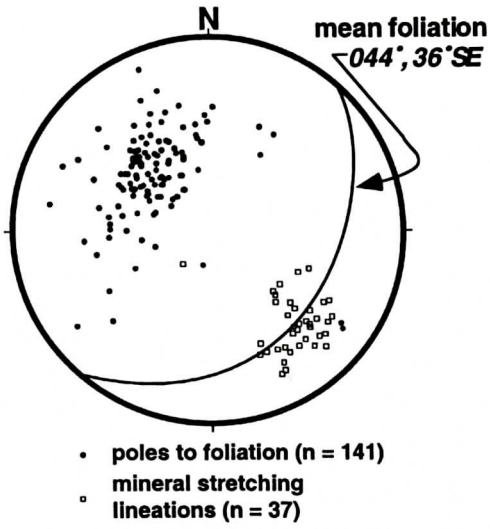


**Figure 7. Stereogram of poles to foliation and mineral stretching lineations in and east of the Pond Mountain volcanic complex. Orientation of mean foliation illustrated as great circle.**

palachians (Rankin, 1970; Su and others, 1994; Tollo and Aleinikoff, 1996).

At a few locations volcanics are overlain by coarse-grained arkosic conglomerates with abundant volcanic clasts suggesting that the region had substantial local relief towards the end of Pond Mountain volcanic activity. However, above the volcanic and volcaniclastic rocks the sedimentary sequence completely lacks volcanic debris and is enriched in plagioclase clasts relative to the volcaniclastic rocks. Feldspars in the Pond Mountain complex are almost exclusively alkali feldspar, and plagioclase is very rare, indicating that the Pond Mountain complex was not the source region for overlying metasedimentary units. Mesoproterozoic plagioclase-rich granodioritic to tonalitic gneisses crop out east of the Pond Mountain complex, and may have served as a source for these deposits. Rapid tectonic subsidence of the Pond Mountain complex may have produced a basin into which basement-derived sediment was transported from the east (present day geography). The fine-grained nature of metagraywackes, schists, and slates is consistent with a subaqueous origin for these deposits.

Rankin (1993) places the Stone Mountain fault between rocks of the Pond Mountain volcanic center and sedimentary rocks to the east (Figure 8). Along this contact non-volcanogenic sedimentary rocks are stratigraphically upright and overlie volcanics, a relationship more consistent with an unconformity than a fault. We interpret the eastern basement/cover contact to be a thrust fault because 1) highly strained rocks are localized at the basement-cover contact not at the contact between volcanics and sedimentary rocks and 2) mylonitic basement rocks, with top-to-the northwest shear sense indicators structurally overlie volcanics and the

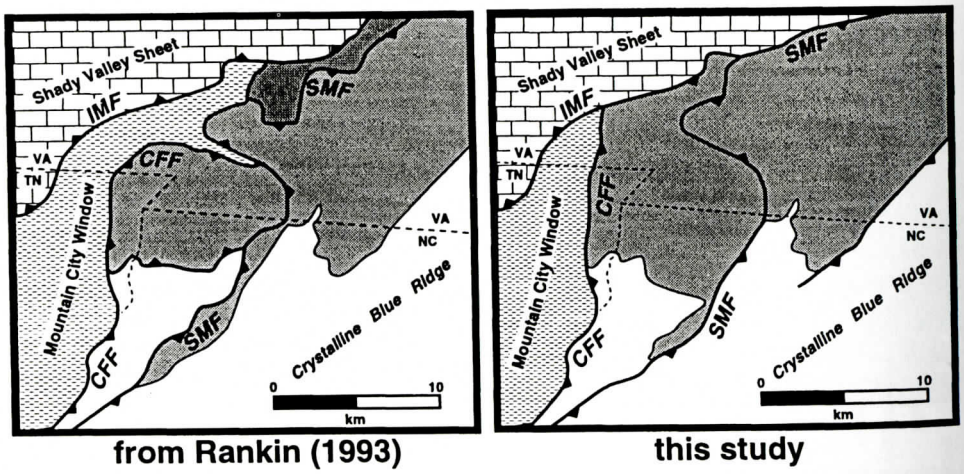


**Figure 8. Simplified structure maps of northwestern North Carolina, southwestern Virginia, and northeastern Tennessee. CFF- Catface fault, IMF- Iron Mountain fault, SMF- Stone Mountain fault.**

non-volcanogenic sedimentary rocks (Figure 8). This fault is presumably the Stone Mountain fault (as defined by King and Ferguson, (1960)), but may also be equivalent to the Fork Ridge fault as mapped by Bartholomew (1983) in the Baldwin Gap quadrangle 15 km to the southwest.

The relationship of the Pond Mountain volcanic complex to the Mount Rogers volcanic complex is not completely understood. The Mount Rogers complex structurally overlies the Pond Mountain complex, but stratigraphic connections are tenuous. Metasedimentary units similar to those exposed near the top of the Pond Mountain sequence crop out to the east and stratigraphically below the Mount Rogers volcanics. This sequence consists of graywacke, siltstone, and conglomerate with minor amounts of rhyolite and greenstone. Rhyolites of the Pond Mountain complex are more silica-rich, and generally coarser-grained than those in the Mount Rogers. Rankin (1993) noted that the Fees Rhyolite Member of the Mount Rogers complex, exposed stratigraphically below the main mass of volcanics (Figure 3), is phenocryst-rich and has a mineral assemblage similar to the Pond Mountain metavolcanics. North of, and stratigraphically above, the Pond Mountain rhyolites, Rankin and others (1972) mapped a phenocryst-poor rhyolite in the Catface thrust sheet that is very similar to the Whitetop Rhyolite Member of the Mount Rogers Formation. The existing data suggest that the Pond Mountain volcanic center may be older than the Mount Rogers volcanic center. The middle member of the Mount Rogers Formation (Whitetop Rhyolite Member) was dated at 758 ± 12 Ma by Aleinikoff and others, (1995), but it is possible that earlier phases of Mount Rogers volcanism were contemporaneous with Pond Mountain magmatism. A better temporal understanding of felsic volcanism in this region must await further geochronologic studies. The original configuration of the volcanic complexes may have been structurally controlled by fault blocks and the volcanic centers may never have been contiguous. Restoration of the Stone Mountain thrust places the Mount Rogers volcanic center to the southeast (present day geography) of the Pond Mountain complex.

## SUMMARY

The late Neoproterozoic Pond Mountain volcanic center is composed of interlayered porphyritic rhyolites and volcaniclastic sedimentary rocks. Rhyolites are intruded by the Whindling Ridge alkali feldspar granite, the intrusive equivalent of the volcanic sequence. Younger non-volcanogenic sedimentary rocks overlie the Pond Mountain complex and probably formed after subsidence of the Pond Mountain complex. The Stone Mountain thrust places Grenvillian basement rock and the Mount Rogers volcanic complex over the Pond Mountain complex. The Pond Mountain volcanic center may be older than the 758 ± 12 Ma Mount Rogers volcanic center.

## ACKNOWLEDGMENTS

We thank the Denison University Research Foundation (CMB) and the Anderson Student Research Scholarship (KKR) for support. We also thank Mark Adams, Brent Owens and Glen Izett for their insightful discussions, and Spencer Brooks and Key Rosebrook for their help in the field. Helpful reviews were provided by Mark Adams, Steve Goldberg, and Jim Hibbard.

## REFERENCES CITED

Adams, M. G., and Su, Q., 1996, The nature and timing of deformation in the Beech Mountain thrust sheet between Grandfather Mountain and Mountain City windows in the Blue Ridge of northwestern North Carolina: Journal of Geology, v. 104, p. 197-213.

Adams, M. G., and Trupe, C. H., 1997, Conditions and timing of metamorphism in the Blue Ridge thrust complex, northwestern North Carolina and eastern Tennessee, *in* Stewart, K. G., Adams, M. G., and Trupe, C. H. eds., Paleozoic structure, metamorphism, and tectonics of the Blue Ridge western North Carolina: Carolina Geological Society Guidebook, p. 33-48.

Aleinikoff, J. N., Zartman R. E, Walter, M., Rankin, D. W., Lyttle, P. T., and Burton, W. C., 1995, U-Pb Ages of Metarhyolites of the Catoctin and Mount Rogers Formations, Central and Southern Appalachians: Evidence for Two Pulses of Iapetan Rifting: American Journal of Science, v. 295, p. 428-454.

Badger, R. L., and Sinha, A. K., 1988, Age and Sr isotopic signature of the Catoctin volcanic province: implications for subcrustal mantle evolution: Geology, v. 16, p. 692-695.

Bartholomew, M. J., 1983, Geologic Map of the Baldwin Gap Quadrangle, North Carolina-Tennessee: North Carolina Geological Survey Section, GM 220-NW.

Bartholomew, M. J., and Lewis, S. E., 1984, Evolution of Grenville Massifs in the Blue Ridge Geologic Province, Southern and Central Appalachians, *in* Bartholomew, M. J., ed., The Grenville Event in the Appalachians and related topics: Geological Society of America Special Paper 194, p. 229-254.

Boyer, S. E., 1992, Sequential development of the southern Blue Ridge province of northwest North Carolina ascertained from the relationships between penetrative deformation and thrusting, *in* Mitra, S. and Fisher, G. W., eds., Structural Geology of Fold and Thrust Belts: Johns Hopkins University, Baltimore, p. 161-188.

Butler, J. R.,1991, Metamorphism, *in* Horton, J. W., Jr., and Zollo, V. A., eds., The Geology of the Carolinas: Carolina Geological Society Fiftieth Anniversary Volume: University of Tennessee, Knoxville, p. 127-141.

Fetter, A. H., and Goldberg, S. A., 1995, Age and geochemical characteristics of bimodal magmatism in the Neoproterozoic Grandfather Mountain rift basin: Journal of Geology, v. 103, p.313-326.

Fullagar, P. D., and Odom, A. L., 1973, Geochronology of Precambrian gneisses in the Blue Ridge province of northwestern North Carolina and adjacent parts of Virginia and Tennessee: Geological Society of America Bulletin, v. 84, p. 3065-3080.

Fullagar, P.D., and Bartholomew, M. J., 1983, Rubidium-Strontium Ages of the Watauga River, Cranberry, and Crossing Knob Gneisses, Northwestern North Carolina; Geological Investigations in the Blue Ridge of Northwestern North Carolina: Guidebook for the Carolina Geological Society, North Carolina Division of Land Resources, Article II, 29 p.

Goldberg, S. A., and Dallmeyer, R. D., 1997, Chronology of Paleozoic metamorphism and deformation in the Blue Ridge thrust complex, North Carolina and Tennessee: American Journal of Science, v. 297, p. 488-526.

Hatcher, R. D., 1989, Tectonic synthesis of the U. S. Appalachians, *in* Hatcher, R. D., Thomas, W. A., and Viele, G. W., eds., The Appalachian-Ouachita orogen in the United States: Geological Society of America, The Geology of North America, v. F-2, p. 511-535.

Keith, A., 1903, Description of the Cranberry quadrangle, North Carolina-Tennessee: U. S. Geological Survey Atlas, Folio 90.

King, P.B., and Ferguson, H. W., 1960, Geology of Northeasternmost Tennessee: U. S. Geological Survey Professional Paper 311, 136 p.

Rankin, D. W., 1970, Stratigraphy and structure of Precambrian rocks in northwestern North Carolina, *in* Fisher, G. W., Pettijohn, F. J., Reed, J. C., Jr., and Weaver, K. N., eds., Appalachian Geology: Central and Southern: Interscience Publishers, New York, p. 227-245.

Rankin, D. W.,1975, The continental margin of eastern North America in the southern Appalachians: The opening and the closing of the proto-Atlantic Ocean: American Journal of Science, v. 275-a, p. 298-336.

Rankin, D. W., 1993, The Volcanogenic Mount Rogers Formation and the Overlying Glaciogenic Konnarock Formation - Two Late Proterozoic Units in Southwestern Virginia: U. S. Geological Survey Bulletin 2029. 26 p.

Rankin, D. W., Dillon, W. P., Black, D. F. B., Boyer, S. E., Danield, D. L., Goldsmith, R., Grow, J. A., Horton, J. W., Jr., Hutchinson, D. R., Klitgord, K. D., McKowell, R. C., Miltop, D. J., Owens, J. P., and Phillips, J. D., 1991, Centennial Continent/Ocean Transect #16, E-4, Central Kentucky to the Carolina Trough: Geological Society of America, 41 p.

Rankin, D. W., Espenshade, G. H., and Newman, R. B., 1972, Geologic map of the western half of the Winston-Salem quadrangle, North Carolina, Virginia, and Tennessee: U. S. Geological Survey, Miscellaneous Investigations, Map I-709-A.

Rankin, D. W., Hall, L. M., Drake, A. A., Jr., Goldsmith, R., Ratcliffe, N. M., and Stanley, R. S., 1989, Proterozoic evolution of the rifted margin of Laurentia *in* Hatcher, R. D., Thomas, W. A., and Viele, G. W., eds., The Appalachian-Ouachita orogen in the United States, Geological Society of America, The Geology of North America, v. F-2, p. 10-42.

Schedl, A., McCabe, C., Montanez, I. Fullagar, P. D., and Valley, J., 1992, Alleghanian regional diagenesis: a response to the migration of modified metamorphic fluids derived from beneath the Blue Ridge-Piedmont thrust sheet: Journal of Geology, v. 100, p. 339-352.

Streckeisen, A. L., 1973, Plutonic rocks: Classification and nomenclature recommended by the IUGS Subcommission on the Systematics of Igneous Rocks: Geology, v. 18, p. 26-30.

Su, Q., Goldberg S. A., and Fullagar, P. D., 1994, Precise U-Pb Zircon Ages of Neoproterozoic plutons in the Southern Appalachian Blue Ridge and their implications for the initial rifting of Laurentia: Precambrian Research, v. 68, p. 81-95.

Tollo, R. P., and Aleinikoff, J. N., 1996, Petrology and U-Pb Geochronology of the Robertson River Igneous Suite, Blue Ridge Province, Virginia - Evidence for Multistage Magmatism Associated with an Early Episode of Laurentian Rifting: American Journal of Science, v. 296, p. 1045-1090.

SOUTHEASTERN GEOLOGY
V. 37, No. 4, May 1998, p. 189-204

# LATE MISSISSIPPIAN TO EARLY PENNSYLVANIAN PALEOKARST IN EAST-CENTRAL TENNESSEE: FIELD, PETROGRAPHIC, AND STABLE ISOTOPE EVIDENCE

STEVEN G. DRIESE, MICHAEL R. CAUDILL[1], AND KRISHNAN SRINIVASAN[2]

*Department of Geological Sciences*
*University of Tennessee-Knoxville*
*Knoxville, TN 37996-1410*

## ABSTRACT

**Field, petrographic, and stable isotope data indicate that the upper limestone deposits of the Pennington Formation (latest Chesterian, Mississippian) in east-central Tennessee were subaerially exposed and subject to dissolution prior to deposition of Lower Pennsylvanian siliciclastic deposits. Evidence for paleokarst includes prominent paleotopographic relief, manifested as paleosinkholes up to 5 m deep and flat-floored low-relief dissolutional surfaces (kamenitzas), both of which are mantled by limestone collapse breccias and red claystone paleosols. Limestone near the exposure surface is commonly reddened, crosscut by vertical dissolution fissures, and exhibits biomoldic and intergranular pores lined with clear, equant, nonferroan meteoric calcite. Stable isotope analyses of micrite (whole-rock) and single echinoderm grains show $\delta^{13}C$ and $\delta^{18}O$ values expected for marine carbonate modified by subaerial exposure and meteoric diagenesis. Echinoderm grain values (mean $\delta^{13}C$ = -0.5 ‰ PDB, mean $\delta^{18}O$ = -5.9 ‰ PDB) suggest stabilization by meteoric water with a $\delta^{18}O$ composition of -4 ‰ SMOW at 25 °C; both echinoderm and whole-rock samples become progressively depleted in $^{13}C$ and $^{18}O$ by about 1-3 ‰ approaching the paleokarst surface and margins of paleosinkholes, thus providing additional evidence for subaerial exposure and karst processes.**

**Documentation of Late Mississippian to Early Pennsylvanian paleokarst at the top of the Pennington Formation reconciles some previous stratigraphic correlation problems, and supports previous contentions of some authors that variable basal Pennsylvanian units reflect deposition on a surface with paleotopographic relief.**

## INTRODUCTION

In this paper we address the following primary question: Are field, petrographic and diagenetic features observed in upper Pennington Formation limestone strata compatible with a subaerial exposure/paleokarst interpretation? Our approach is to first demonstrate that the Raccoon Mountain Formation (or Warren Point Sandstone, in the absence of any older basal Pennsylvanian rocks) disconformably overlies *subaerially weathered and dissolved* Pennington Formation marine limestones regionally along the Cumberland Plateau from Oneida, Tennessee, southward through Monterey to McMinnville, Tennessee. Secondly, we interpret pedogenic and meteoric diagenetic processes that affected the upper 5-6 meters of Pennington Formation limestones during subaerial exposure, based on field, petrographic and geochemical evidence. Lastly, we relate these findings to recent work on basal Pennsylvanian stratigraphy and paleoenvironments (Churnet, 1996; Hurd and Stapor, 1997).

Our identification of the top of the Pennington Formation as a paleokarst surface with vari-

1. Present address: *Department of Geology, University of Akron, Akron, OH 44325-4101*
2. Present address: *Exxon Exploration Company, 233 Benmark Drive, Houston, TX 77060*

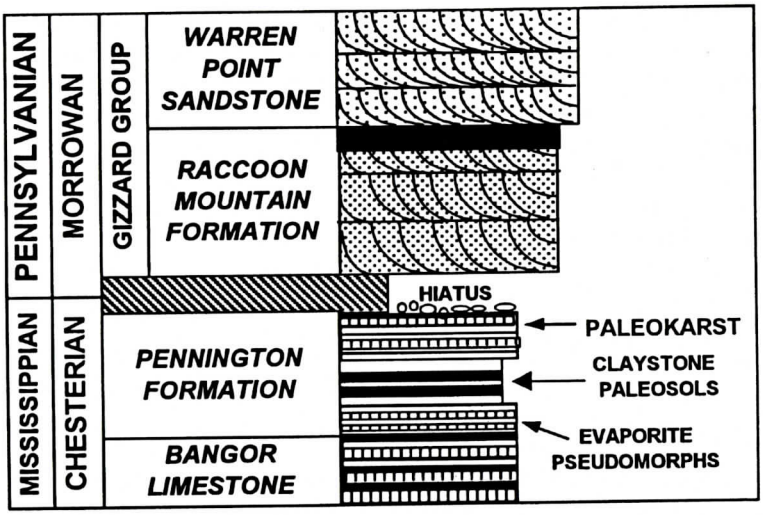


**Figure 1. Generalized stratigraphic column for Upper Mississippian and Lower Pennsylvanian rocks of east-central Tennessee. Variable erosional relief on top of Pennington Formation results in variable stratigraphic placement of Pennsylvanian rocks.**

able paleotopographic relief reconciles a vexing stratigraphic problem for Pennsylvanian stratigraphic, namely, the highly variable stratigraphic thicknesses and concomitant difficulties of lithostratigraphic correlation for basal Pennsylvanian siliciclastic strata in the Cumberland Plateau region. Bergenback (1994) and Churnet (1996) most recently interpreted these stratigraphic variations as due to deposition of basal Pennsylvanian strata within a series of localized, tectonically active "mini-basins" that were undergoing extension. However, we demonstrate that deposition of basal Pennsylvanian strata on a Late Mississippian to Early Pennsylvanian paleokarst surface that had variable relief, as well as collapse of buried paleocaves coeval with deposition of Lower Pennsylvanian strata, are viable alternative explanations for basal Pennsylvanian stratigraphic variations. In addition, our interpretation of subaerial exposure and paleokarst for the upper Pennington Formation more easily explains the sharp juxtaposition (with apparent disconformity) of coal-bearing, fluvio-deltaic Pennsylvanian siliciclastic strata on top of subtidal, open-marine Pennington limestone strata; the paleokarst surface can either be interpreted as a 3rd-order sequence boundary (Vail and others, 1977) formed during a sea-level lowstand, or as due to Early Pennsylvanian exposure accompanying widespread regional uplift (peripheral bulge uplift and migration) related to the inception of the Alleghenian orogeny (Ettensohn and Chestnut, 1989; Ettensohn, 1994).

## LITHOSTRATIGRAPHY

The Pennington Formation is latest Chesterian in age (Crawford, 1985; Patchen and others, 1985), and ranges from 30 to 150 m thickness in Tennessee (Milici and others, 1979). It is a mixed siliciclastic-carbonate sequence comprised of dolostone, limestone, variegated (red, green or gray) shale/claystone (largely paleosols), and fine-grained to pebbly sandstone (Milici, 1974; Milici and others, 1979; Caudill and others, 1992, 1996; Driese and Harding, in revision). The Pennington thins from east to west, and the terrigenous clastic-to-carbonate ratio also decreases westward, reflecting the demise of a late Mississippian carbonate shelf due to influx of terrigenous clastics from the east. Within the study area along the western edge of the Cumberland Plateau, the Pennington gradationally overlies the Bangor limestone (Algeo and Rich, 1992), and in turn is disconformably over-

lain by basal Pennsylvanian deposits of the Gizzard Group, chiefly the Raccoon Mountain Formation (Figure 1). An array of depositional environments have been interpreted for the Pennington Formation, including a variety of peritidal and coastal mudflat/sabkha environments, punctuated by periods of subaerial exposure and pedogenesis (Bergenback and others, 1972, 1980; Milici and others, 1979; Caudill and others, 1992, 1996; Driese and Harding, in revision), barrier beach and marsh environments (Milici, 1974), carbonate tidal island-barrier island complexes and low-energy, terrigenous offshore environments (Ferm and others, 1972; Ferm, 1974), and tidally influenced terrigenous clastic environments (Sedimentation Seminar, 1981).

## PREVIOUS WORK

The unconformable nature of the Mississippian-Pennsylvanian systemic boundary has long been recognized in the southern Appalachians and adjacent Cumberland plateau (Thomas, 1979; Thomas and Cramer, 1979; Milici and others, 1979; England and others, 1985). Ettensohn (1981, 1985, 1986) reported abundant evidence for paleokarst and unconformity at the top of the Pennington Formation in eastern Kentucky, which shows progressively deeper erosional truncation from east to west. However, to our knowledge there are no references to the occurrence of paleokarst at the boundary in east-central Tennessee, except for brief descriptions in Caudill and others (1992) and Driese and others (1994a, b). This is surprising in view of the widespread occurrences of latest Mississippian paleokarst reported elsewhere in North America (see summary of post-Kaskaskia paleokarst by Palmer and Palmer (1989), and related papers published in the Choquette and James (1988) volume). Recent work by Webb (1993, 1994) confirms a paleokarst origin for rocks straddling the Mississippian-Pennsylvanian systemic boundary in northwestern Arkansas. Recent work by Beuthin (1994, 1997) demonstrated a subaerial unconformity, paleovalley, and paleosol complex developed at the Mississippian-Pennsylvanian boundary in southern West Virginia. In general, latest Mississippian paleokarst features are better expressed in the western U.S. and are less easily recognized in the eastern U.S. due to the increasing terrigenous clastic content of the rocks deposited adjacent to the Alleghanian and Ouachita orogens (Palmer and Palmer 1989), as well as the less extensive outcrop exposures in the eastern region. A late Mississippian sea-lev-

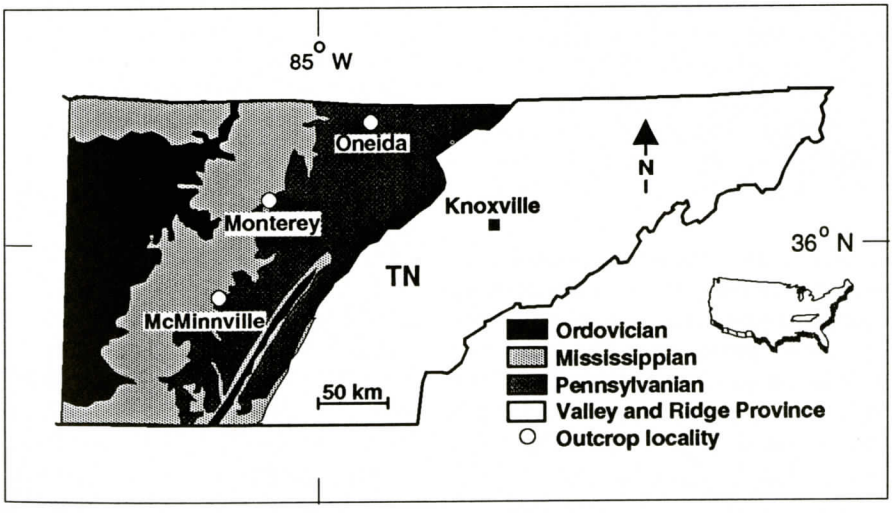


**Figure 2. Simplified geologic map showing locations of three outcrop sections in east-central Tennessee examined for this study. Outcrop sections occur mainly along eastern edge of Cumberland escarpment.**

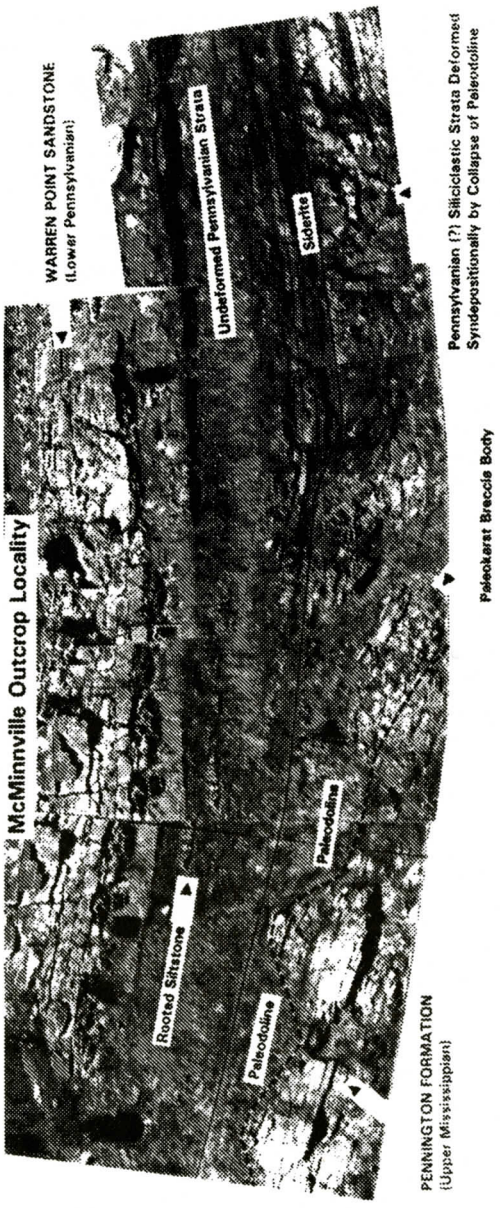


**Figure 3. Outcrop photograph composite for McMinnville locality (Figure 2) showing paleodolines, small karst highs, and paleokarst limestone breccia body developed in upper Pennington Formation limestone strata. Note basal Pennsylvanian siliciclastic strata (Raccoon Mountain Formation?), which were deformed syndepositionally by collapse of paleocaverns in underlying Pennington strata. Siderite pebble conglomate separates deformed and undeformed Pennsylvanian rocks. Man is 2 m tall for scale.**

el lowstand accompanied by a 1 to 2-Ma hiatus is inferred by Vail and others (1977) and Patchen and others (1985) as responsible for the Mississippian-Pennsylvanian boundary paleokarst reported here in east-central Tennessee. This lowstand has been interpreted as glacio-eustatic (Saunders and Ramsbottom, 1986; Veevers and Powell, 1987). Alternatively, the paleokarst could be due to Early Pennsylvanian subaerial exposure accompanying widespread regional uplift (peripheral bulge uplift and migration) related to the inception of the Alleghenian orogeny (Ettensohn and Chestnut, 1989; Ettensohn, 1994).

## METHODS AND STUDY AREA

Three principal outcrop sections of the Pennington-Pennsylvanian stratigraphic contact were examined in the field area, which ranged from the Kentucky-Tennessee border region (Oneida - Leatherwood Ford Locality), southward through middle Tennessee (Monterey and McMinnville Localities) (Figure 2). Photomosaics were constructed to help interpret lateral relationships between rock units and to serve as base maps for sampling for petrographic and geochemical analysis. Thin-sections were treated with a dual stain of Alizarin Red S and potassium ferricyanide (Dickson, 1965, 1966) to identify carbonate mineral phases. Standard thin-section petrography was supplemented with cathodoluminescence (CL) petrography on a Technosyn luminoscope, using an accelerating potential of 10-12 KeV and beam current of 150-200 μA. Carbonate constituents were micro-sampled for stable isotope analysis using a dental drill; average sample size was 3 mg. Oxygen and carbon isotope compositions were determined from $CO_2$ produced by reaction of powdered samples with 100% ortho-phosphoric acid after McCrea (1950). Isotopic ratios were determined using the VG 903 MM gas-source mass spectrometer at the University of Tennessee. Results are reported for 13 single-constituent (echinoderm grain) samples and for 35 whole-rock (micrite) samples in standard δ-permil (‰) notation relative to PDB with a reproducibility of ± 0.05 ‰.

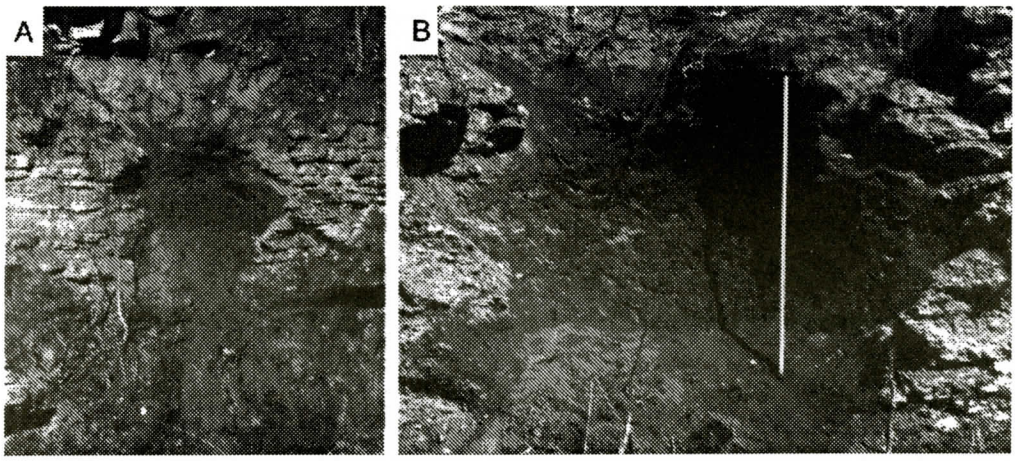


**Figure 4. Examples of macro-scale paleokarst features occurring in the upper Pennington Formation at the Monterey locality. (A) Paleosinkholes are 4 to 6-m deep and 3 to 4-m wide, and occur at east end of outcrop section in upper Pennington limestone and dolostone strata. (B) Red claystone with vertic paleosol features (pedogenic slickensides) and carbonate breccia clasts filling paleosinkhole. Jacob's staff at base of (A) is 1.6-m long.**

## DESCRIPTION OF SUBAERIAL EXPOSURE AND KARST FEATURES

### Macroscale Features

The contact between the Pennington Formation and basal Pennsylvanian siliciclastic strata is sharp and is interpreted to be disconformable across the entire western margin of the Cumberland Plateau of east-central Tennessee (Figures 1 and 2) (Driese and others, 1994a; b). The unnamed upper limestone member of the Pennington Formation generally ranges from 4 to 6-m thick, but is highly variable, as noted previously by Hurd and Stapor (1997). It consists of lithologies ranging from whole-fossil (brachiopod-gastropod) wackestones and packstones, to bioclastic (echinoderm-bryozoan) and peloidal packstones and grainstones. Paleorelief along the disconformity surface at a single outcrop locality may be up to 3 to 4 m, with the majority of the relief developed in the limestones (Figures 3 and 4). Carbonate conglomerate and breccia bodies are up to 1-m thick and mantle the paleorelief features. These deposits contain individual clasts up to 50 cm in diameter, and are locally abundant at both the Oneida-Leatherwood Ford and the McMinnville localities (Figures 3 and 5A). Greenish-gray claystone, and chert and carbonate lithic-dominated sand occurs in the interstices between breccia clasts. Where basal Pennsylvanian sandstone strata overlie paleorelief features at both the Oneida-Leatherwood Ford and the McMinnville localities they are deformed to steep fold-like features (Figures 3 and 5B). Reddish claystone mantles and partially fills paleorelief developed on the limestones at both the Oneida-Leatherwood Ford and Monterey localities (Figures 4 and 5C). The claystone has floating breccia clasts of limestone, rare bowl-shaped slickensided planes, an angular-blocky weathering fabric, gray-green mottles, and rare, fine root traces.

### Mesoscale Features

General reddening of the upper surface of limestones beneath paleorelief features is common at the Oneida-Leatherwood Ford locality, extending downward at least 2-3 cm. Iron oxides partially replace, as well as coat, allochem grain surfaces, and additionally serve as an intergranular cement. Moldic pores of larger allochems, including brachiopods, gastropods, and echinoderm grains, are visible in outcrop and in thin section at all three outcrop sections,

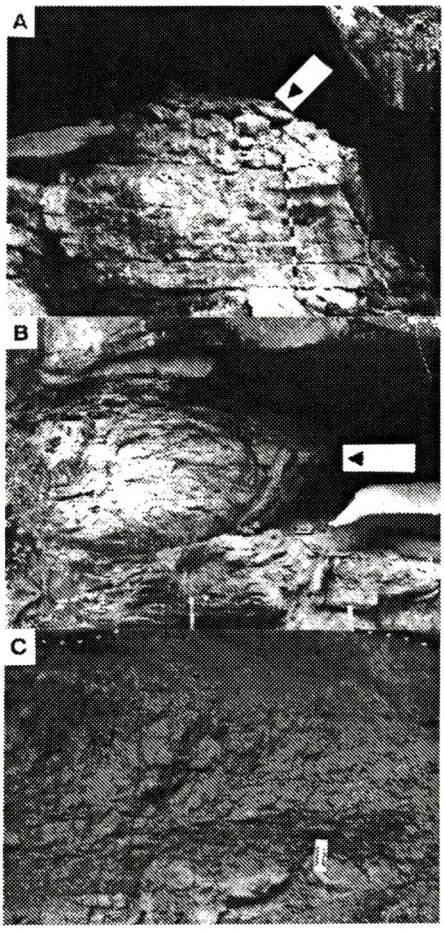


**Figure 5. Examples of macro-scale paleokarst features in upper Pennington Formation limestone strata. (A) Paleokarst limestone breccia resting on subaerially exposed upper Pennington Formation limestone strata and sharply overlain by Warren Point Formation sandstone strata at Oneida-Leatherwood Ford locality. Jacob's staff is 1.5-m long. (B) Basal Pennsylvanian siliciclastic strata (arrow: Raccoon Mountain Formation?) deformed sydepositionally by collapse of paleocavern in underlying Pennington Formation limestone strata at Oneida-Leatherwood Ford locality. 30 cm of top of Jacob's staff for scale. (C) Red vertic claystone paleosol containing limestone breccia clasts and mantling paleotopographic low area underlain by partially weathered (saprolitized) reddened limestone at Oneida-Leatherwood Ford locality. Dashed line in upper photo marks basal Pennsylvanian sandstone strata containing thin coal deposits. Scale card is 15-cm long.**

**Figure 6. Micritized echinoderm-bryozoan grainstone with prominent non-fabric-selective, vertical dissolutional fissure occluded with calcite spar cement, at McMinnville locality. Scale bar increments are 1 cm. Depth is 1 m below paleokarst surface.**

generally occluded with calcite spar cement. Oversize intergranular pores filled with calcite spar cement are also common. Downward-tapering vertical fissures occur in the limestones at both the Oneida-Leatherwood Ford and the McMinnville localities. The fissures are up to 1-cm wide and 30 to 50-cm long (Figure 6), and are generally filled with calcite cement, clays, and iron oxides

## Microscale Features

There is a distinct paragenetic sequence for the limestone strata, which is recognizable at all three outcrop sections.The earliest cement phase, commonly nucleated on echinoderm grain surfaces, is a dully luminescent, nonferroan calcite cement (DNF cement, Figure 7). This cement is water clear to slightly turbid, and exhibits sharp crystal terminations where grown

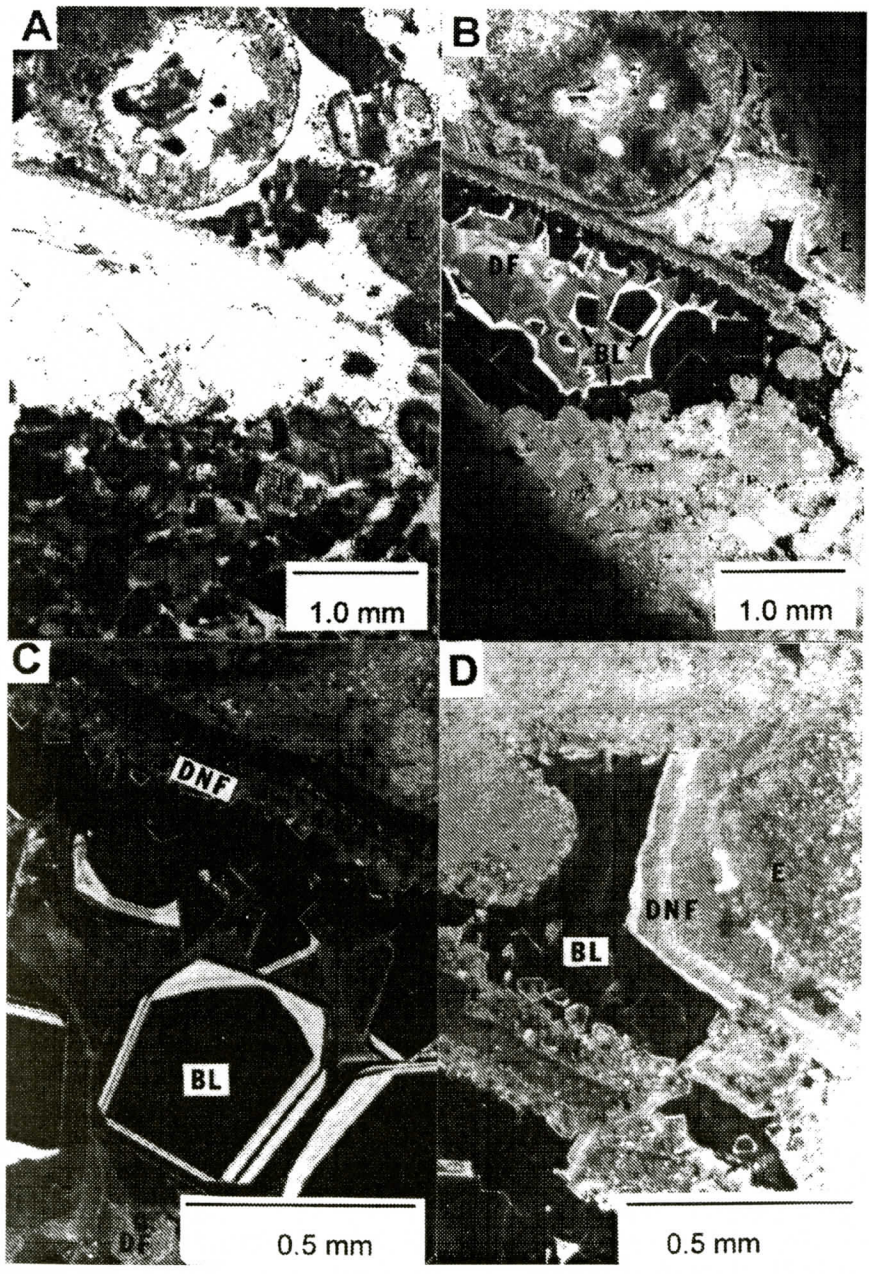


**Figure 7. Photomicrographs of diagenetic features from McMinnville locality. (A) Large calcite spar cement-filled shelter and intergranular pores in echinoderm-bioclast grainstone (plane light). (B) Same field of view as in (A), but under cathodoluminescence (CL) conditions. Note echinoderm grain (E), dully luminescent, nonferroan calcite cement (DNF) grown syntaxially on echinoderm grain (arrow), banded bright-dark luminescent, non-ferroan calcite spar cement (BL), and final pore-occluding, dull luminescent, ferroan calcite spar cement (DF). (C) Subset of field of view in (B), under CL conditions. Note presence of dull luminescent, non-ferroan calcite spar cement (DNF) grown syntaxially on echinoderm host grain (E). (D) Subset of field of view in (B), under CL conditions. Note very small amount of bladed DNF cement nucleated on pore wall, followed by complexly zoned BL cement, and final pore-occluding DF cement.**

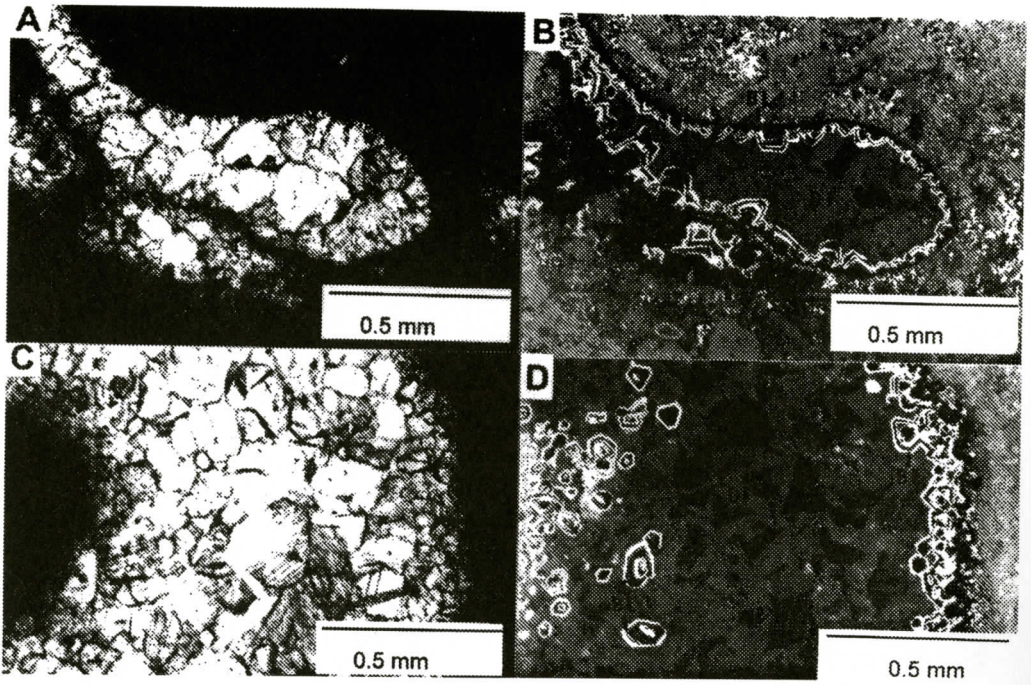


**Figure 8. Photomicrographs of diagenetic features from Oneida-Leatherwood Ford locality. Note similarity of cement sequences between Figures 7 and 8. (A) Mollusk moldic pore filled with calcite spar cement (plane light). (B) Same field of view as in (A), under CL conditions. Note complex concentric banding in early BL cement, followed by sector-zoned DF cement. (C) Echinoderm moldic pore filled with calcite spar cement (plane light). (D) Same field of view as in (A), under CL conditions. Note early BL cement lining pore wall and filling axial pore, followed by DF cement with sector zoning.**

into open pores. Following sequentially in time are nonferroan calcite cements characterized by a strongly banded, bright-dark luminescence, with generally 3-7 microbands (BL cement, Figures 7 and 8). These cements are water clear, and fill both inter- and intragranular pore spaces. Where porosity is not occluded by DNF and BL cements, and in vertical dissolution fissures, a third cement phase consisting of dully luminescent, ferroan calcite occludes the remaining porosity (DF cement, Figures 7 and 8). This cement exhibits a distinct sector-style zoning.

## Stable Isotopes

Stable carbon and oxygen isotope analyses included both whole-rock (micrite-only) samples, as well as samples of individual depositional and diagenetic components. Whole-rock samples from the Oneida-Leatherwood Ford Locality (Locality 1 in Figure 2) were collected normal to the paleokarst surface along three different sample traverses; each exhibits distinctive patterns of lighter $\delta^{13}C$ compositions towards the top of the paleokarst surface, with about a 2 to 3 ‰ shift to more negative values, from less altered to more pedogenically altered marine limestone (Figure 9). The same whole-rock samples also display distinctive patterns showing lighter $\delta^{18}O$ compositions near the top of the paleokarst surface, with about a 2 to 3 ‰ shift to more negative values, from less altered to more pedogenically altered marine limestone (Figure 9). The isotopic compositions of calcitized echinoderm grains ($\delta^{13}C$ = -1.6 to 0.7 ‰ PDB, mean = -0.5; $\delta^{18}O$ = -6.6 to -5.2 ‰ PDB, mean = -5.9) show systematic changes with respect to distance beneath the paleokarst surface, which parallel the patterns suggested by the whole-rock data; echinoderm grains sampled

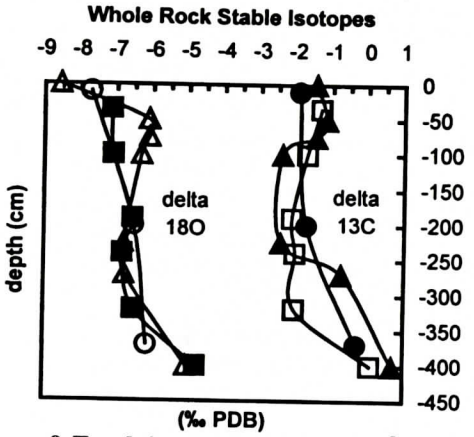


**Figure 9. Trends in whole-rock (micrite) $\delta^{13}C$ and $\delta^{18}O$ values as a function of vertical distance below the Mississippian-Pennsylvania boundary paleokarst surface at the Oneida-Leatherwood Ford section. Samples taken from the paleokarst surface have $\delta^{13}C$ compositions that are about 2-3 ‰ more negative and $\delta^{18}O$ values that are about 2-4 ‰ more negative, relative to samples from 4 m below the surface.**

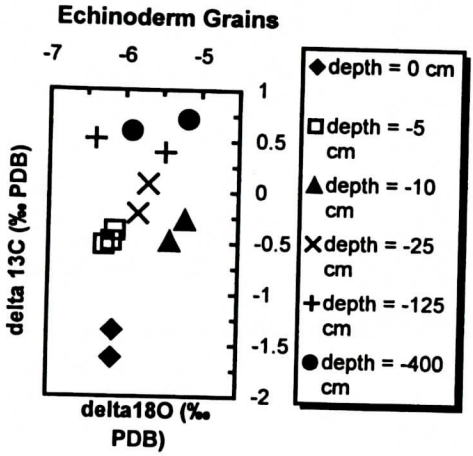


**Figure 10. Single-constituent (echinoderm grain) $\delta^{13}C$ and $\delta^{18}O$ values as a function of vertical distance below the Mississippian-Pennsylvania boundary paleokarst surface at the McMinnville section. Samples taken from the paleokarst surface (depth = 0 cm) have $\delta^{13}C$ values that are about 3 ‰ more negative and $\delta^{18}O$ values that are about 1.5 ‰ more negative, relative to samples from 4 m below the surface (depth = 400 cm).**

nearest the paleokarst surface generally have the lightest $\delta^{13}C$ and $\delta^{18}O$ compositions, with variations of about 3 ‰ for carbon and 1.5 ‰ for oxygen (Figure 10).

## INTERPRETATION OF SUBAERIAL EXPOSURE AND KARST FEATURES

### Macroscale Features

Table 1 summarizes features observed in the upper Pennington Formation limestones in east-central Tennessee that support a subaerial exposure and paleokarst interpretation. The paleorelief features locally developed in the uppermost Pennington Formation at all three outcrop localities are interpreted as paleosinkholes (dolines) and shallow, small-scale karstic solution pits (kamenitzas), as well as small-scale dissolution surfaces (rundkarren). Paleosinkholes are readily identified in the McMinnville outcrop section, where a series of small paleodolines occur which define paleorelief (Figure 3), and at the Monterey section, where two paleodolines are filled with red claystone exhibiting vertic paleosol features, and carbonate breccia (Figure 4). Evidence for collapse of paleocaverns includes sysedimentary deformation in basal Pennsylvanian sandstone strata immediately overlying the paleokarst surface, which occurs at both the McMinnville and the Oneida-Leatherwood localities (Figures 3 and 5B, respectively). Sandstone strata were probably unconsolidated to weakly cemented when paleocavern collapse occurred early in the Pennsylvanian, as indicated by the absence of deformation features in slightly younger Pennsylvanian strata (Figures 3 and 5B). The red claystone that mantles the paleorelief interpreted as paleosinkhole in origin is interpreted as a vertic paleosol resting directly on saprolitized (i.e., weathered, but retaining rock fabric) Pennington limestone at the Oneida-Leatherwood Ford locality (Figure 5C) and at Monterey (Figure 4B). The paleosols contain features indicative of a vertic (Vertisol-like) affinity, including high clay content, pedogenic slickensides, angular blocky peds, and sepic-plasmic (bright-clay) microfabrics; paleosols with similar features are abundant in other parts of the Pennington Formation (Caud-

**Table 1: Summary of paleokarst and other subaerial exposure features in upper Pennington Formation limestone strata (criteria modified after Choquette and James, 1988).**

| Stratigraphic - Geomorphic | Macroscopic - Surface Karst | Macroscopic - Subsurface Karst | Microscopic & Geochemical |
|---|---|---|---|
| Dolines | Rundkarren | Caves & Smaller Non-Selective Dissolution Voids | Illuviated Soil Material in Small Pores |
| Karst "Highs" | Kamenitzas | In-place Brecciated & Fractured Strata | Reddened and Micritized Grains |
| | Reddish Claystone Paleosols Mantling Paleokarst Surface | Collapse Structures That Deform Overlying Pennsylvanian Strata | Extensive Dissolution, or Enlarged, Fabric-Selective Pores |
| | Reddish Clay-Iron Oxide Fracture Fillings and Reddening of Limestone at Exposure Surface | Dissolution-Enlarged Vertical Fractures | More Negative $\delta^{13}C$ & $\delta^{18}O$ Compositions (Whole-Rock and Echinoderm Grains) Towards Paleokarst Surface and Large Dissolution Voids |
| | Mantling Nonsedimentary Breccias | Breccias in Irregular Bodies, Conformable or Not | Stabilization of Metastable Marine Constituents |

ill and others, 1992, 1996; Churnet, 1996; Driese and Harding, in revision) and in lithostratigraphically equivalent rocks in southern West Virginia (Beuthin, 1997). Fine root traces are also present, and the low chroma upper region of the Oneida-Leatherwood Ford paleosol and mottles are redoximorphic features related to soil saturation and water-table perching (Vepraskas, 1992).

## Mesoscale Features

Evidence for subaerial exposure and karst of the upper Pennington Formation limestones include: (1) reddening and micritization of skeletal allochems along the paleokarst surface; 2) calcite spar cement-filled moldic pores formed by dissolution of large allochem grains; and (3) vertically oriented, downward tapering, nonfabric-selective dissolution fissures occurring in limestone beneath carbonate breccia bodies, which are filled with calcite spar cement (Figure 6).

## Microscale Features

The diagenetic history for upper Pennington Formation limestone strata is summarized in Table 2. Meteoric water undersaturated with respect to calcite dissolved upper Pennington Formation limestones during Late Mississippian to Early Pennsylvanian subaerial exposure and karstification, resulting in the formation of abundant moldic pores and non-fabric-selective, vertically oriented dissolution fissures (Figures 6, 7, and 8). These pores were first partially occluded by nonferroan, meteoric calcite cement and then later completely occluded by ferroan, burial calcite cement. The upper Pennington limestone cement phases and their paragenetic sequence greatly resemble that described in the slightly older Newman Limestone of eastern Kentucky and northeastern Tennessee described by Niemann and Read (1988), and are interpreted similarly on the basis of mineralogy and crystal morphology and clarity. Stable isotope data (discussed below) also support our interpretations of early freshwater di-

**Table 2: Paragenetic sequence for diagenetic constituents in limestone strata of the upper Pennington Formation. Criteria for diagenetic environments based on Niemann and Read (1988) and Walker (1989).**

| Timing | Diagenetic Feature/Processes | Interpreted Environment |
|---|---|---|
| (1) | (A) Dissolution of large allochems, solution enhancement of intergranular pores, and formation of vertical solution fissures. (B) Stabilization of echinoderm grains. | *Subaerial exposure environment.* |
| (2) | Precipitation of banded bright/dark luminescent, nonferroan calcite cement on pore walls and calcitized echinoderms. | *Shallow meteoric phreatic environment.* |
| (3) | Precipitation of dull luminescent, ferroan calcite spar pore-filling cement in moldic pores and vertical fissures. | *Burial environment.* |
| (4) | Precipitation of non-luminescent, ferroan calcite spar cement in remaining pore spaces. | *Burial environment.* |
| (5) | Precipitation of zoned ankeritic siderite along paleokarst surface. | *Burial environment.* |
| (6) | Precipitation of very bright luminescent, ferroan calcite cement in horizontal fractures and along along intercrystalline boundaries. | *Burial or near-surface environment.* |

agenesis during subaerial exposure and karstification.

### Stable Isotopes

Stable isotope data (both single-constituent and whole-rock) support a subaerial exposure and meteoric diagenesis interpretation for the upper Pennington Formation limestones. These whole-rock data generally show less variation for carbon and significantly greater variation for oxygen isotopic compositions (Figure 9). This reflects pedogenesis and meteoric diagenesis in a "rock-dominated", as opposed to a "water-dominated" system (Lehmann, 1988; Algeo and others, 1992). Echinoderm grain compositions are considerably depleted in $^{13}C$ and $^{18}O$ (Figure 10) compared to the Mississippian marine calcite compositions ($\delta^{13}C$ = +4.5‰ PDB, $\delta^{18}O$ = -1.5‰ PDB) reported by Meyers and Lohmann (1985) and Popp and others (1986), and strongly suggest stabilization of the echinoderm grains in the presence of meteoric water that was a source of both light oxygen and light carbon, with a calculated composition of -4 ‰ SMOW at 25° C, thereby precipitating calcite with a $\delta^{18}O$ composition of -5 to -6‰ PDB (O'Neill and others, 1969; Hoefs, 1980).

## SUMMARY AND SYNTHESIS

Field, petrographic and geochemical data obtained from the limestone-dominated upper 4-6 m of the Pennington Formation indicate that the top of the Pennington is a surface of subaerial exposure and paleokarst that experienced pedogenesis and meteoric diagenesis. The large-scale dissolution of carbonate components, forming paleodolines, paleocaverns, kamenitzas, rundkarren, carbonate clast breccias and vertical dissolution fissures, suggests alteration of marine limestone by interaction with meteoric water that was undersaturated with respect to metastable carbonate phases; similar features are abundant in association with Mississippian paleokarst reported elsewhere (Walkden, 1974; Wright, 1982; Esteban and Klappa, 1983; Meyers, 1988; Sando, 1988; Palmer and Palmer, 1989; Davies, 1991; Hattin and Dodd, 1992; Demiralin and others, 1993; Webb, 1994).

Occurrences of red, vertic claystone paleosols resting directly on top of the paleokarst surface and filling paleodolines provide additional supporting evidence for subaerial exposure of

the upper Pennington Formation limestones. These paleosols, in particular, provide direct evidence that the Pennington paleokarst represents subaerial karst formed under a thin soil cover (=covered karst), and **not** subjacent (=interstratal) karst formed in the subsurface (Sweeting, 1972; Wright, 1982). Subjacent karst has been proposed for some of the karst present at the contact between the Carboniferous Limestone and the Millstone Grit in the United Kingdom, where the Millstone Grit functioned as a permeable aquifer and the Carboniferous Limestone as a less permeable aquitard; groundwater moving through the upper unit dissolved the top of the carbonate unit, resulting in formation (in the subsurface) of a karstic surface at the stratigraphic contact (cf. Walkden, 1974; Wright, 1983; Walkden and Davies, 1983; Wright, 1991). Field, macro- and microscale features of the clay and iron oxide material filling interstices between carbonate breccia clasts somewhat resemble aluminous lateritic soil material occurring in the Bahamas (Foos, 1991), and the *terra rosa* from the Miami Oolite (Strom and Kim, 1987).

The depth trends of carbon and oxygen isotope compositions in whole-rock and echinoderm grain micro-samples from the upper Pennington Formation limestones reflect two processes consistent with a subaerial exposure interpretation: (1) a significant contribution of isotopically light soil-gas $CO_2$ near the paleoweathering surface, which resulted in more negative $\delta^{13}C$ values of the pedogenically modified carbonate; and (2) enrichment of light oxygen provided by meteoric water, which resulted in more negative $\delta^{18}O$ compositions of carbonate nearer to the exposure surface (Allan and Matthews, 1982; Muchez and others, 1993; Driese and others, 1994c).

The virtual absence of pedogenic carbonate *sensu stricto* (laminar micritic crusts, nodules, or calcified root traces) in the upper Pennington Formation is significant, because these carbonate morphologies are abundant in vertic claystone paleosols occurring in the lower and middle Pennington (Caudill and others, 1992, 1996; Driese and Harding, in revision) and would probably produce a stronger depleted stable isotope "signal" for subaerial exposure than are apparent from the whole-rock data (Goldstein, 1991). Laminar micritic crusts, nodules, pisoids, and calcified root traces are commonly described in many carbonate-parented soils formed in arid to semiarid climates (e.g., James, 1972; Esteban and Klappa, 1983; Wright, 1991). The total absence of laminated micritic crusts, which are very abundant in lower Genevievian carbonate rocks (older than the Pennington) in nearby eastern Kentucky (Walls and others, 1975; Harrison and Steinen, 1978; Ettensohn and others, 1988) and southern Indiana (Hattin and Dodd, 1992; Hunter, 1993), and the abundance of paleokarst features documented here may reflect a change to an overall wetter climate by late Pennington time, in contrast to the semiarid climate hypothesized for middle Pennington time (mean annual precipitation estimated as 648 mm $\pm$ 141), based on depth to pedogenic carbonate horizons in vertic claystone paleosols (Caudill and others, 1996).

## RELEVANCE TO REGIONAL STRATIGRAPHIC PROBLEMS

Correlation of basal Pennsylvanian strata in east-central Tennessee has been problematic, as noted by previous workers; in some localities the Raccoon Mountain Formation (0-90 m) directly overlies the Pennington Formation, whereas at other localities, the Warren Point Sandstone (0-90 m) is the basal deposit (Bergenback, 1994; Churnet, 1996; Hurd and Stapor, 1997). Both Bergenback (1994) and Churnet (1996) postulated that deposition of basal Pennsylvanian strata was localized by extensional "minibasins" or "subbasins". Such extensional basins are difficult to reconcile with the dominantly compressional tectonic processes associated with the Alleghenian orogeny (Quinlan and Beaumont 1984), and as noted by Churnet (1996). Rather than interpreting these as synsedimentary grabens formed by flexural extension (Churnet 1996), we suggest that instead, paleotopographic lows generated by subaerial exposure and paleokarst processes produced variable depositional relief. This paleorelief originated through the formation of pa-

leosinkholes and collapse of paleocaves, some of which we previously demonstrated must have been syndepositional with basal Pennsylvanian strata (Figures 3 and 5B). As basal Pennsylvanian stream systems spread siliciclastic detritus on the weathered Pennington surface, paleolows were initially infilled until the karstic paleotopography was eliminated. Hence lowermost basal Pennsylvanian deposits of the Raccoon Mountain Formation are present in paleotopographic lows, whereas higher stratal units, such as the Warren Point Sandstone, rest on paleotopographic highs. Our hypothesis is much more compatible with recent interpretations of Hurd and Stapor (1997, fig. 2), who also suggested the existence of significant paleorelief on the top of the Pennington Formation.

## CONCLUSIONS

1) Field, petrographic, and stable isotope evidence suggest that limestone deposits of the upper Pennington Formation were subaerially exposed and experienced karst processes during latest Mississippian to earliest Pennsylvanian time.

2) Subaerial exposure of the upper Pennington Formation limestones produced paleotopographic relief by formation of paleosinkholes and paleocave collapse; this paleotopographic relief controlled later deposition of Lower Pennsylvanian strata by localizing initial deposition of fluvial siliciclastic detritus in paleotopgraphic lows.

3) A consistent paragenetic sequence is recognizable in the limestone deposits of the upper Pennington Formation across the entire study area. Meteoric diagenesis began with subaerial exposure, when dissolution and stabilization of metastable allochems, solution enlargement of intergranular and intragranular pores, and formation of both vertical and horizontal dissolution fissures occurred.

4) Stable isotope analysis of single echinoderm grains indicates that they were stabilized and initially cemented during subaerial exposure by meteoric water with a calculated composition of -4 ‰ SMOW at 25 °C, precipitating calcite with a $\delta^{18}O$ composition of -5 to -6‰ PDB.

5) Both echinoderm grains and micrite (whole-rock) samples become depleted in $^{13}C$ and $^{18}O$ approaching the paleokarst surface, recording interaction with isotopically light meteoric water and organic matter associated with surface soil cover.

6) Recognition of paleokarst at the top of the Pennington Formation (Upper Mississippian) is consistent with its interpretation as either a 3rd-order sequence boundary formed during a sea-level lowstand, or with subaerial exposure accompanying Early Pennsylvanian tectonic uplift.

## ACKNOWLEDGMENTS

This research was supported by PRF Grant 25678-AC8-C and by NSF Grants EAR-9206540 and EAR-9418183 to S.G. Driese and C.I. Mora. Srinivasan was partly funded by NSF Grant EAR-9103491 to K.R. Walker. K.Tobin (Princeton), C.I. Mora (Tennessee), R. Goldstein (Kansas), S.J. Mazzulo (Wichita State) and V.P. Wright (Reading, U.K.) reviewed an earlier draft of this manuscript, and their helpful comments are appreciated. We thank *Southeastern Geology* reviewers Frank Stapor (Tennessee Tech) and Frank Ettensohn (Kentucky) for their constructive reviews. The following members of the 1993 University of Tennessee Paleokarst Seminar Class helped with many aspects of this study: S. Dunagan, B. Glumac, P. Milroy, T. Schultz, A. Stefaniak, R. Tolliver, and J. Williams. Ian Richards and Amy Halleran assisted with stable isotope analyses. F.W. Stapor (Tennessee Tech) provided invaluable assistance in locating outcrop sections and in interpreting field relationships. We thank the National Park Service for granting access to outcrop exposures in the Big South Fork National Recreation Area.

## REFERENCES CITED

Algeo, T.J., and Rich, M., 1992, Bangor Limestone: Depositional environments and cyclicity on a late Mississippian carbonate shelf: Southeastern Geology, v. 32, p. 143-162.

Algeo, T.J., Wilkinson, B.H., and Lohmann, K.C., 1992, Meteoric-burial diagenesis of Middle Pennsylvanian limestones in the Orogrande Basin, New Mexico: water-rock interaction and basin geothermics: Journal of Sedimentary Petrology, v. 62, p. 652-670.

Allan, J.R., and Matthews, R.K., 1982, Isotope signatures associated with early meteoric diagenesis: Sedimentology, v. 29, p. 797-817.

Bergenback, R.E., 1994, Sedimentational response to a series of tectonic events, Cumberland Plateau, eastern Tennessee: Southeastern Geology, v. 34, p. 41-55.

Bergenback, R.E., Horne, J.C., and Inden, R.F., 1972, Stops 3 and 4 - Depositional environment of Mississippian rocks at Monteagle, Tennessee: Tennessee Division of Geology, Report of Investigations No. 33, p. 14-18.

Bergenback, R.E., Wilson, R.L., Rich, M., and Hunter, D., 1980, Carboniferous paleodepositional environments in the Chattanooga area, *in* Frey, R.W., ed., Excursions in Southeastern Geology, Volume I, Field Trip Guidebook for Geological Society of America Annual Meeting; Washington, D.C., American Geological Institute, p. 259-279.

Beuthin, J.D., 1994, A sub-Pennsylvanian paleovalley system in the central Appalachians and its implications for tectonic and eustatic controls on the origin of the regional Mississippian-Pennsylvanian unconformity, in Dennison, J.M., and Ettensohn, F.R., eds., Tectonic and eustatic controls on sedimentary cycles: SEPM (Society for Sedimentary Geology) Concepts in Sedimentology and Paleontology, v. 4, p. 107-120.

Beuthin, J.D., 1997, Paleopedological evidence for a eustatic Mississippian-Pennsylvanian (Mid-Carboniferous) unconformity in southern West Virginia: Southeastern Geology, v. 37, p. 25-37.

Caudill, M.R., Mora, C.I., Tobin, K.J., and Driese, S.G., 1992, Preliminary interpretations of paleosols associated with Late Mississippian marginal marine deposits, Pennington Formation, Monterey, Tennessee, *in* Driese, S.G., Mora, C.I., and Walker, K.R., eds., Paleosols, Paleoweathering Surfaces, and Sequence Boundaries: Field Trip Guidebook, Society for Sedimentary Geology Midcontinent Section, Volume 10: University of Tennessee, Department of Geological Sciences, Studies in Geology No. 21, 115 p.

Caudill, M.R., Driese, S.G., and Mora, C.I., 1996, Preservation of a paleo-Vertisol and an estimate of Late Mississippian paleoprecipitation: Journal of Sedimentary Research, v. 66, p. 58-70.

Churnet, H.G., 1996, Depositional environments of Lower Pennsylvanian coal-bearing siliciclastics of southeastern Tennessee, northwestern Georgia, and northeastern Alabama, U.S.A.: International Journal of Coal Geology, v. 31, p. 21-54.

Choquette, P.W., and James, N.P., 1988, Introduction, *in* James, N.P., and Choquette, P.W., eds., 1988, Paleokarst: New York, Springer-Verlag, p. 3-21.

Crawford, T.J., 1985, Upper Mississippian and Lower Pennsylvanian series in the southern Appalachians: United States Geological Survey, Open File Report 85-577, p. 9-10.

Davies, J.R., 1991, Karstification and pedogenesis on a late Dinantian carbonate platform, Anglesey, North Wales: Proceedings of the Yorkshire Geological Society, v. 48, p. 297-321.

Demiralin, A.S., Hurley, N.F., and Oesleby, T.W., 1993, Karst breccias in the Madison Limestone (Mississippian), Garland field, Wyoming, *in* Fritz, R.D., Wilson, J.L., and Yurewicz, eds., Paleokarst related hydrocarbon reservoirs: SEPM (Society for Sedimentary Geology) Core Workshop No. 18, p. 101-118.

Dickson, J.A.D., 1965, Modified staining technique for carbonates in thin section: Nature, v. 205, p. 587.

Dickson, J.A.D., 1966, Carbonate identification and genesis as revealed by staining: Journal of Sedimentary Petrology, v. 36, p. 491-505.

Driese, S.G., Capelle, D.G., Glumac, B., Srinivasan, K., Stefaniak, A., Paleokarst Study Group, and Stapor, F.W., 1994a, Pre-Pennsylvanian paleokarst at the top of the Upper Pennington Formation, central Tennessee: Geological Society of America, Abstracts With Programs, v. 26, no. 4, p. 11.

Driese, S.G., Glumac, B., Srinivasan, K., Stefaniak, A., and Richards, I.J., 1994b, Influence of subaerial exposure and karstification on diagenesis of Mississippian carbonate rocks, Pennington Formation, Tennessee: Geological Society of America, Abstracts With Programs, v. 26, no. 7, p. A-65 to A-66.

Driese, S.G., and Harding, S.D., in revision, The stratigraphy and paleoenvironments of paleosols and associated strata of the lower Pennington Formation (Upper Mississippian) at Sparta, Tennessee: submitted to Southeastern Geology.

Driese, S.G., Srinivasan, K., Mora, C.I., and Stapor, F.W., 1994c, Paleoweathering of Mississippian Monteagle Limestone preceding development of a lower Chesterian transgressive systems tract and sequence boundary, middle Tennessee and northern Alabama: Geological Society of America Bulletin, v. 106, p. 866-878.

England, K.J., Gillespie, W.H., Cecil, W.B., and Windolph, J.F., Jr., 1985, Characteristics of the Mississippian-Pennsylvanian boundary and associated coal-bearing rocks in the southern Appalachians: U.S. Geological Survey Open-File Report 85-577, 84 p.

Esteban, M., and Klappa, C.F., 1983, Subaerial exposure environment, *in* Scholle, P.A., Bebout, D.G., and Moore, C.H., eds., Carbonate Depositional Environments: American Association of Petroleum Geologists Memoir 33, p. 1-54.

Ettensohn, F.R., 1981, Mississippian-Pennsylvanian boundary in northeastern Kentucky, *in* Roberts, T.G., ed., GSA Cincinnati '81 Field Trip Guidebooks, Volume 1: Stratigraphy, sedimentology, p. 195-217.

Ettensohn, F.R., 1985, Depositional environments and stratigraphy of the Pennington Formation (Upper Visean-Namurian A), east-central and eastern Kentucky, U.S.A., *in* Escobedo, J.L, and others, eds., X[e]

Congrès International de Stratigraphie et de Géologie du Carbonifère Madrid 1983, Compte Rendu 3, p. 269-283.

Ettensohn, F.R., 1986, The Mississippian-Pennsylvanian transition along Interstate 64, northeastern Kentucky, *in* Geological Society of America Centennial Field Guide-Southeastern Section, p. 37-41.

Ettensohn, F.R., 1994, Tectonic control on formation and cyclicity of major Appalachian unconformities and associated stratigraphic sequences, in Dennison, J.M., and Ettensohn, F.R., eds., Tectonic and eustatic controls on sedimentary cycles: SEPM (Society for Sedimentary Geology) Concepts in Sedimentology and Paleontology, Volume 4, p. 217-242.

Ettensohn, F.R., and Chestnut, 1989, Nature and probable origin of the Mississippian-Pennsylvanian unconformity in the eastern United States, *in* Yugan, J., and Chun, L., eds., XI$^{e}$ Congrès International de Stratigraphie et de Géologie du Carbonifère Beijing 1987, Compte Rendu 4, p. 145-159.

Ettensohn, F.R., Dever, G.R., Jr., and Grow, J.S., 1988, A paleosol interpretation for profiles exhibiting subaerial exposure "crusts" from the Mississippian of the Appalachian basin, *in* Reinhardt, J., and Sigleo, W.R., eds., Paleosols and Paleoweathering Through Geologic Time: Geological Society of America Special Paper 216, p. 49-79.

Ferm, J.C., 1974, Carboniferous environmental models in the eastern United States and their significance, *in* Briggs, G., ed., Carboniferous of the southeastern United States: Geological Society of America Special Paper 148, p. 45-95.

Ferm, J.C, Milici, R.C., and Eason, J.E., 1972, Carboniferous depositional environments in the Cumberland Plateau of southern Tennessee and northern Alabama: Tennessee Division of Geology, Report of Investigations No. 33, p. 1-22.

Foos, A.M., 1991, Aluminous lateritic soils, Eleuthera, Bahamas: a modern analog to carbonate paleosols: Journal of Sedimentary Petrology, v. 61, p. 340-348.

Goldstein, R.H., 1991, Stable isotope signatures associated with palaeosols, Pennsylvanian Holder Formation, New Mexico: Sedimentology, v. 38, p. 67-77.

Harrison, R.D., and Steinen, R.P., 1977, Subaerial crusts, caliche profiles, and breccia horizons: Comparison of some Holocene and Mississippian exposure surfaces, Barbados and Kentucky: Geological Society of America Bulletin, v. 89, p. 385-396.

Hattin, D.E., and Dodd, J.R, 1992, Mississippian paleosols, paleokarst, and eolian carbonates in Indiana: Ohio Geological Survey, Miscellaneous Report No. 3, 35 p.

Hoefs, J., 1980, Stable Isotope Geochemistry (2nd ed.): New York, Springer-Verlag, 208 p.

Hunter, R.E., 1993, An eolian facies in the Ste. Genevieve Limestone of southern Indiana, *in* Keith, B., and Zuppann, C., eds., Mississippian Oolites and Modern Analogs: American Association of Petroleum Geologists, Studies in Geology No. 35, p. 31-48.

Hurd, S.A., and Stapor, F.W., Jr., 1997, Facies, stratigraphy and provenance of the Warren Point Sandstone (Pennsylvanian), Cumberland Plateau, central Tennessee: Southeastern Geology, v. 36, p. 187-201.

James, N.P., 1972, Holocene and Pleistocene calcareous crust (caliche) profiles: Criteria for subaerial exposure: Journal of Sedimentary Petrology, v. 42, p. 817-836.

Lohmann, K.C., 1988, Geochemical patterns of meteoric diagenetic systems and their application to studies of paleokarst, *in* James, N.P., and Choquette, P.W., eds., Paleokarst: New York, Springer-Verlag, p. 59-80.

McCrea, J.M., 1950, The isotopic chemistry of carbonates and a paleotemperature scale: Journal of Chemistry and Physics, v. 18, p. 849-857.

Meyers, W.J., 1988, Paleokarstic features on Mississippian limestones, New Mexico, *in* James, N.P., and Choquette, P.W., eds., Paleokarst: New York, Springer-Verlag, p. 306-328.

Meyers, W.J., and Lohmann, K.C., 1985, Isotope geochemistry of regionally extensive cement zones and marine components in Mississippian limestones, New Mexico, *in* Schneidermann, N., and Harris, P.M., eds., Carbonate cements: Society of Economic Paleontologists and Mineralogists, Special Publication No. 36, p. 223-239.

Milici, R.C., 1974, Stratigraphy and depositional environments of Upper Mississippian and Lower Pennsylvanian rocks in the southern Cumberland Plataeu of Tennessee, *in* Briggs, G., ed., Carboniferous of the Southeastern United States: Geological Society of America, Special Paper No. 148, p. 115-133.

Milici, R.C., Briggs, G., Knox, L.M., Sitterly, P.D., and Statler, A.T., 1979, The Mississippian and Pennsylvanian (Carboniferous) Systems in the United States-Tennessee: U.S. Geological Survey Professional Paper 1110-G, 38 p.

Muchez, Ph., Peeters, C., Keppens, E., and Viaene, W.A., 1993, Stable isotope composition of paleosols in the Lower Viséan of eastern Belgium: evidence of evaporation and soil-gas $CO_2$: Chemical Geology, v. 106, p. 389-396.

Niemann, J.C., and Read, J.F., 1988, Regional cementation from unconformity-recharged aquifer and basinal fluids, Mississippian Newman Limestone, Kentucky: Journal of Sedimentary Petrology, v. 58, p. 688-705.

O'Neill, J.R., Clayton, R.C., and Mayeda, T.K., 1969, Oxygen isotope fractionation in divalent metal carbonates: Journal of Chemical Physics, v. 51, p. 5547-5558.

Palmer, M.V., and Palmer, A.N., 1989, Paleokarst in the United States, *in* Bosák, P., Ford, D.C., Glazek, J., and Horácek, I., eds., Paleokarst: A Systematic and Regional Review: Developments in Earth Surface Processes 1: New York, Elsevier Pub. Co., 725 p.

Patchen, D.G., Avary, K.L., and Erwin, R.B., 1985, Correlation of stratigraphic units in North America - Southern Appalachian Region Chart #160: American Association of Petroleum Geologists.

Popp, B.N., Takigiku, R., Hayes, J.M., Louda, J.W., and Baker, E.W., 1986, Brachiopods as indicators of origi-

nal isotopic compositions in some Paleozoic limestones: Geological Society of America Bulletin, v. 97, p. 1262-1269.

Sando, W.J., 1988, Madison Limestone (Mississippian) paleokarst: a geologic synthesis, *in* James, N.P., and Choquette, P.W., eds., Paleokarst: New York, Springer-Verlag, p. 256-277.

Saunders, W.B., and Ramsbottom, W.H.C., 1986, The mid-Carboniferous eustatic event: Geology, v. 14, p. 208-212.

Sedimentation Seminar, 1981, Mississippian and Pennsylvanian section at Interstate 75 south of Jellico, Campbell County, Tennessee: Tennessee Division of Geology, Report of Investigations No. 38, 37 p.

Strom, R.N., and Kim, J.J., 1987, Genesis of dioctahedral chlorite-like clays in *terra rosa* soils in South Florida: Florida Science, v. 50, p. 253-263.

Sweeting, M.M., 1972, Karst landforms: New York, MacMillan Pub. Co., 362 p.

Thomas, W.A., 1979, The Mississippian and Pennsylvanian (Carboniferous) systems in the United States - Alabama and Mississippi. Mississippian stratigraphy of Alabama: U.S. Geological Survey, Professional Paper 1110-A-L, p. I1-I22.

Thomas, W.A., and Cramer, H.R., 1979, The Mississippian and Pennsylvanian (Carboniferous) systems in the United States - Georgia: U.S. Geological Survey, Professional Paper 1110-A-L, p. H1-H37.

Vail, P.R., Mitchum, R.M., Jr., Todd, R.G., Widmier, J.M., Thompson, S. III, Sangree, J.B., Bubb, J.N., and Hatelid, W.G., 1977, Seismic stratigraphy and global changes of sea level *in* Payton, C.W., ed., Seismic Stratigraphy - Applications to Hydrocarbon Exploration: American Association of Petroleum Geologists Memoir No. 26, p. 49-212.

Veevers, J.J., and Powell, 1987, Late Paleozoic glacial episodes in Gondwanaland reflected in transgressive-regressive depositional sequences in Euramerica: Geological Society of America Bulletin, v. 98, p. 475-487.

Vepraskas, M.J., 1992, Redoximorphic features for identifying aquatic conditions: North Carolina Agricultural Research Service, Technical Bulletin 301, 33 p.

Walkden, G.M., 1974, Palaeokarstic surfaces in Upper Visean (Carboniferous) limestones of the Derbyshire block, England: Journal of Sedimentary Petrology, v. 44, p. 1232-1247.

Walkden, G. and Davies, J., 1983, Polyphase erosion of subaerial omission surfaces in the Late Dinantian of Anglesey, North Wales: Sedimentology, v. 30, p. 861-878.

Walker, K.R., ed., 1989, The fabric of cements in Paleozoic limestones: Short Course Notes, University of Tennessee, Department of Geological Sciences, Studies in Geology No. 20, 165 p.

Walls, R.A., Harris, W.B., and Nunan, W.E., 1975, Calcareous crust (caliche) profiles and early subaerial exposure of Carboniferous carbonates, northeastern Kentucky: Sedimentology, v. 22, p. 417-440.

Webb, G.E., 1993, A Lower Pennsylvanian encrusting tabulate coral from a rocky shore environment developed on the Mississippian-Pennsylvanian unconformity surface in northwestern Arkansas: Journal of Paleontology, v. 67, p. 1064-1068.

Webb, G.E., 1994, Paleokarst, paleosol, and rocky-shore deposits at the Mississippian-Pennsylvanian unconformity, northwestern Arkansas: Geological Society of America Bulletin, v. 106, p. 634-648.

Wright, V.P., 1982, The recognition and interpretation of paleokarsts: two examples from the Lower Carboniferous of South Wales: Journal of Sedimentary Petrology, v. 52, p. 83-94.

Wright, V.P., 1991, Palaeokarst: types, recognition, controls and associations, in Wright, V.P., Esteban, M., and Smart, P.L., eds., Palaeokarsts and Palaeokarstic Reservoirs: Reading, U.K., Postgraduate Research Institute for Sedimentology, p. 56-88.

SOUTHEASTERN GEOLOGY
V. 37, No. 4, May 1998, p. 205-216

# MIXING OF SANTONIAN AND CAMPANIAN CHONDRICHTHYAN AND AMMONITE MACROFOSSILS ALONG A TRANSGRESSIVE LAG DEPOSIT, GREENE COUNTY, WESTERN ALABAMA

**MARTIN A. BECKER**

*Department of Physics and Geology*
*The College of New Jersey*
*Ewing, NJ 08628-0718*

**WILLIAM SLATTERY**

*Departments of Geological Sciences and Teacher Education*
*Wright State University*
*Dayton, OH 45435*

**JOHN A. CHAMBERLAIN, JR.**

*Department of Geology*
*Brooklyn College and Graduate School of the City University of New York*
*Brooklyn, NY 11210*

## ABSTRACT

**The base of the Tombigbee Sand Member of the Eutaw Formation in Greene County, western Alabama is marked in outcrop by an erosional unconformity and overlying macrofossil lag deposit. Sea level fall eroded, reworked, and hydrodynamically sorted sediments and fossil hard parts which had been previously deposited within the Eutaw Formation. Accumulated hard parts were subsequently reworked and preserved as a transgressive lag deposit directly above the erosional unconformity at the base of the Tombigbee Sand Member.**

**Ammonites and shark teeth with well defined age ranges are common fossil components in this lag. Age range analyses on these fossil organisms indicate mixing of Santonian and Campanian biozones. In the western Alabama study area, ammonite and chondrichthyan biozones indicate the Santonian-Campanian boundary resides within this lag deposit immediately above the base of the Tombigbee Sand Member of the Eutaw Formation.**

## Introduction

Alabama's Cretaceous strata crop out in a belt trending roughly east-west through the center of the state and north-south along the western edge of the state (Fig. 1). This belt is roughly 400 kilometers long and 150-300 kilometers wide. The majority of late Cretaceous strata within this belt were deposited when warm shallow seas invaded the southern and interior parts of the North American continent. Characteristic deposits include nearshore sands, silts and muds in addition to offshore limestones, marls, and chalks (Raymond and others, 1988).

Greene County is located within this Cretaceous belt and contains exposures of the Eutaw Formation and its Tombigbee Sand Member. Stream erosion has exposed the unconsolidated sediments providing cross-sectional exposures of the Eutaw Formation and excellent collecting of *in situ* fossil mollusks, teeth, and vertebrate remains at the base of the Tombigbee Sand Member. These fossils are concentrated in a lag deposit directly above an unconformity at the base of the Tombigbee Sand Member of the upper Eutaw Formation (Becker and others, 1996a).

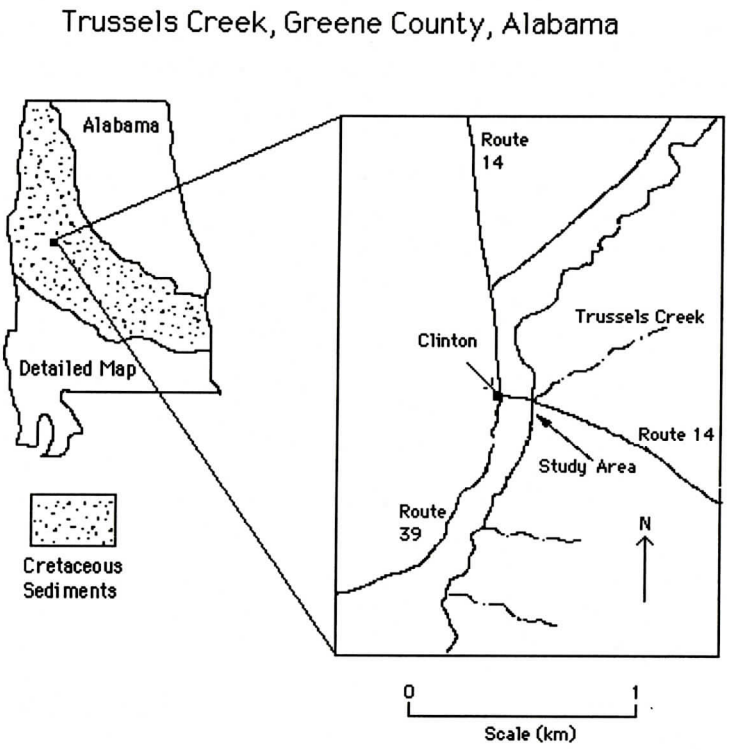


**Figure 1. Location of the study area along Trussels Creek, due south of Clinton, Alabama.**

This study utilizes the paradigm of sequence stratigraphy to analyze the biostratigraphic significance and taphonomic processes associated with the accumulation of macrofossils along the unconformity along the base of the Tombigbee Sand Member of the Eutaw Formation. The role of dynamic forces involved in the erosion and concentration of highstand deposits during sea level fall and subsequent sea level rise allow new insights into the role relative sea level fluctuation plays in the concentration of macrofossil elements by dynamic basin processes; and the biostratigraphical significance of the concentration of fossils within lag deposits, resulting in the placement of the Santonian-Campanian boundary within the Tombigbee Sand Member of the Eutaw Formation in Greene County, western Alabama.

## SEQUENCE STRATIGRAPHY

The sequence stratigraphic framework of the Eastern Gulf Coastal Plain has been studied by several workers, among them King and Skotnicki (1994), and Mancini and others (1995). King and Skotnicki group the sedimentary deposits of the Eutaw Formation in the study area into "genetic packages" (sensu King 1987). In their view, the Eutaw Formation (including the Tombigbee Sand Member) can be subdivided into two genetic packages bounded bottom and top by unconformities. The lower unconformity at the base of genetic package one occurs directly above the non-marine, fluvial sediments of the Tuscaloosa Group. The top of genetic package one is determined by the presence of a low relief erosional surface and facies discontinuity at the base of the Tombigbee Sand Member of the Eutaw Formation. In their view the Tombigbee Sand Member in eastern Alabama was deposited as a result of a progradational shift of depositional environments. The unconformity bounding the top of genetic package two occurs between the Eutaw and the overlying Mooreville-Blufftown Formations. These workers determined that the Eutaw Formation was

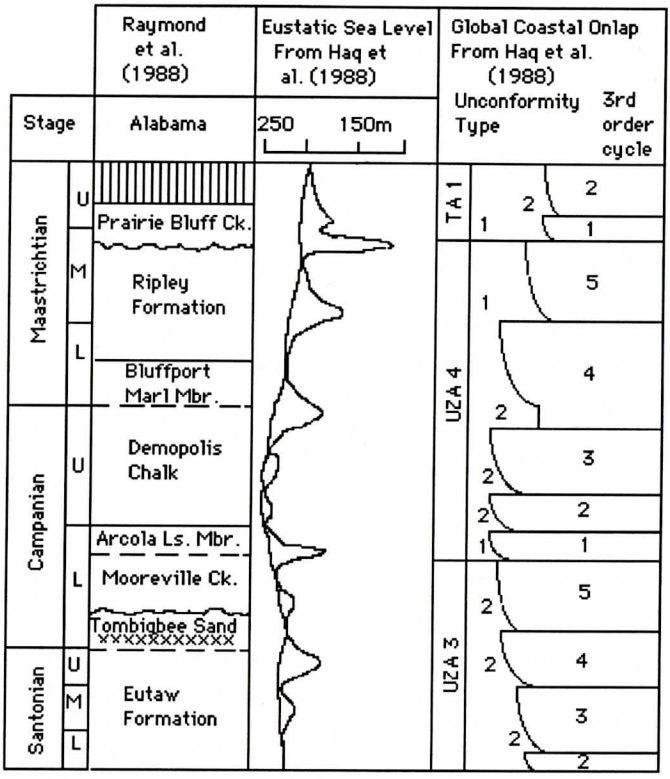


**Figure 2. Approximate stratigraphic position of Alabama lag deposit sampled during this study indicated by xxxxx. The stratigraphic position of this lag deposit corresponds favorably to: 1) facies changes between clay dominated and sand dominated sediments; 2) stage boundaries in the Upper Cretaceous; 3) third order regressive-transgressive events in the eustatic sea level curve of Haq and others (1988); and 4) a parasequence bounday separating genetic packages 1 and 2 of the Eutaw Formation and Tombigbee Sand Member respectively (King and Skotnicki, 1994).**

equivalent to global cycle UZA 3.4 of Haq (1988) (Fig. 2).

Mancini and others (1995) disagree with this interpretation and propose that the Eutaw Formation including the Tombigbee Sand Member is part of an overall coarsening upward, shallowing upward cycle. This cycle subsumes Haq's global cycles UZA 3.4 and UZA 3.5 into one larger cycle, which they term UZAGC 3.0 (Upper Zuni A Gulf Coast 3.0) (Fig. 3). UZAGC 3.0 is interpreted as a Type 1 sequence bounded by an unconformity at the base of the Eutaw Formation. Additional component system tracts include a Eutaw Formation lowstand system tract, a transgressive surface at the Eutaw- Tombigbee Sand contact, and a transgressive system tract including the Tombigbee Sand Member and the lower Mooreville Chalk; a maximum flooding surface within the Mooreville Chalk, and a highstand system tract consisting of deposits of the upper Mooreville Chalk and its Arcola Limestone Member, the basal Demopolis sandy beds, Coffee Sand and the Tupelo tongue of the Coffee Sand. It is beyond the scope of this paper to add further insight into the overall details of Gulf Coast sequence stratigraphy, but both sets of workers referred to above clearly identify the contact between the Eutaw Formation and the Tombigbee Sand Member of the Eutaw Formation as a stratigraphically significant surface of erosion. To use the formal parlance of sequence stratigraphy, the surface is at least a parasequence boundary.

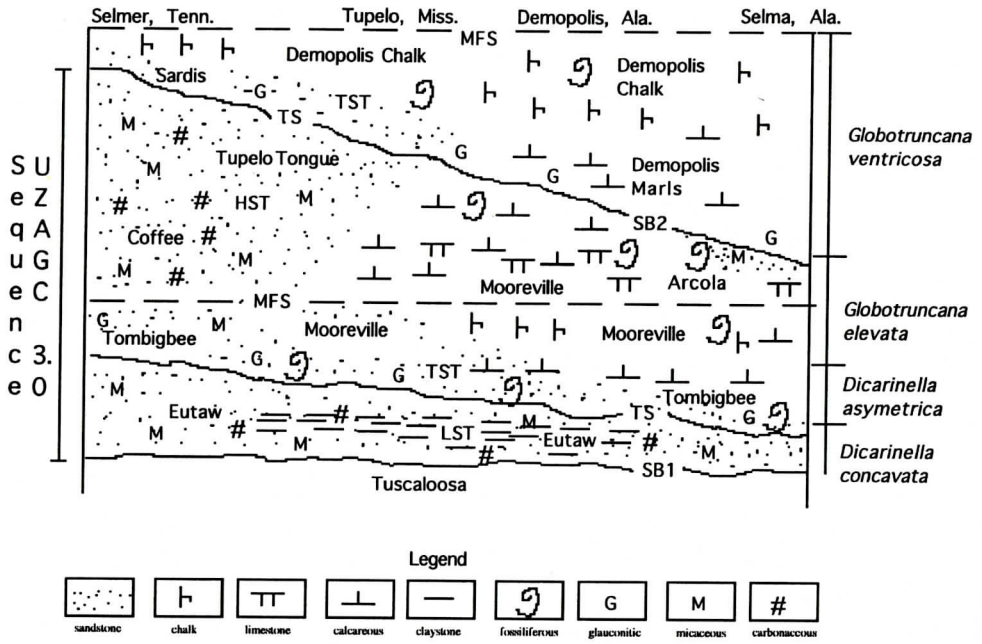


**Figure 3. Cross section of UZAGC-3.0 from Selma, Alabama to Selmer, Tennessee showing lithofacies, planktonic foraminifera biostratigraphy and sequence stratigraphic relationships. SB1=type 1 sequence boundary, SB2=type 2 sequence boundary, TS=transgressive surface, MFS=maximum flooding surface, LST=lowstand systems tract, HST=highstand systems tract. Redrawn from Mancini and others (1995).**

This paper is the result of a study that collected and examined an *in situ* assemblage of marcofossils draped along this surface of erosion at Trussels Creek, western Alabama to determine their biostratigraphical significance.

## SEDIMENTOLOGY OF THE EUTAW FORMATION AND TOMBIGBEE SAND MEMBER

The Eutaw Formation is described in the summary by Raymond, and others (1988) as a light greenish-gray, fine to medium grained, well-sorted, micaceous, cross-bedded sand, silty mud, and carbonaceous mud containing abundant scattered fossils. In western and central Alabama outcrop exposures attain a thickness of 130 meters. Outcrop exposures thin to 30 meters in eastern-most Alabama.

Raymond, and others (1988) describe the Tombigbee Sand Member as a light-gray massive, highly glauconitic sand and mud containing abundant burrows and mollusk shells. These workers state that the discontinuous outcrops of the Tombigbee Sand Member range in thickness from approximately 2 to 7 meters. Russell and Keady (1983) report that the Tombigbee Sand Member reaches a thickness of more than 58 meters near Columbus, Mississippi.

## AGE OF THE EUTAW FORMATION AND TOMBIGBEE SAND MEMBER

Given that the processes of sea-level rise and fall are not instantaneous, and are not synchronous either along depositional strike or perpendicular to it, the following ages have been offered for the Eutaw Formation and its Tombigbee Sand Member. Raymond and others (1988) place the base of the Eutaw Formation at the boundary between the Coniacian and Santonian on top of a regional unconformity. Raymond and others (1988) and King and Skotnicki (1994) place the boundary between the base of

the Tombigbee Sand Member of the upper Eutaw Formation in Alabama near the Santonian-Campanian boundary. King and Stocknicki (1994) support a late Santonian to early Campanian age assignment for this boundary based on: 1) the occurrence of nannoplankton *Calculites obscurus*; from: Sohl and Smith (1980) and Smith and Mancini (1983); 2) palynomorphs from the *Pseudoplicapollis cuneata-Semiocu-lopollis verrucosa* Zone from: Christopher (1979), (1980); and 3) the co-occurrences of various planktonic foraminifera and megafossils compiled by Sohl and Smith (1980) and Smith and Mancini (1983).

Obradovich (1993) indicates an age of 84.09 ± 0.40 Ma for the lower part of the Tombigbee Sand Member from a radiometrically dated bentonite. This estimate is consistent with the Hallam and others (1985) world-wide estimate of 84 Ma for the Santonian-Campanian boundary and was determined using radiometric dating of: 1) a bentonite from the uppermost Santonian *Desmoscaphites bassleri* zone of the Western Interior; 2) basal Campanian lava flows from Texas; and 3) well data from the lower Campanian of Europe.

## FIELD METHODS

Trussels Creek, running roughly northeast-southwest and parallel to Alabama Route 39, was selected for this field study because of: 1) accessibility to exposures of the Eutaw Formation and Eutaw-Tombigbee Sand contact; and 2) excellent *in situ* fossils collecting. At this locality macrofossils blanketing the unconformity at the base of the Tombigbee Sand Member were collected for biostratigraphic interpretation. Vertical thickness of exposed units were measured and described and the horizontal continuity of the erosional disconformity was traced laterally for approximately 1 kilometer along the length of the Creek.

We compiled a detailed measured section of the Tombigbee Sand Member along Trussels Creek in Greene County, Alabama. Careful attention was given to the following parameters: 1) sediment grain size, color and mineralogical make-up; 2) bedding structures and erosion 3) unit and formation contacts; 4) fossil type; and 5) areas of fossil concentration.

Fossils were collected by sieving outcrops with 0.5 centimeter screens. Only *in situ* material was collected and identified. Macrofossils were integrated with the known chondrichthyan and ammonite biostratigraphy for the Cretaceous Atlantic Coastal and Western Interior Seaways from: Cappetta and Case (1975); Case and Schwimmer (1988); Kennedy and Cobban (1991); Welton and Farish (1993); Kennedy and Cobban (1994); Kent (1994); Case (1995); and Kennedy and others (1995). Stage age assignments for the macrofossils collected in this field study were obtained from biostratigraphic zonations of chondrichthyans and ammonites compiled by these authors.

## SEDIMENTOLOGY AND STRATIGRAPHY OF THE TRUSSELS CREEK LAG DEPOSIT

The upper lithofacies of the Eutaw Formation along Trussels Creek consists of light to medium gray muds containing fine sands, glauconite, vertical burrows to 10 centimeters and sparse macrofossils. Bedding is 1-5 centimeters thick and contain *Skolithos* burrows. The lower contact of the Eutaw Formation has not been exposed by stream erosion at the study site along Trussels Creek. The upper contact of the Eutaw Formation is erosional with a maximum of 20 centimeters of relief. Maximum thickness of the upper Eutaw Formation observed along Trussels Creek is approximately 1-2 meters (Fig. 4).

A macrofossil concentration consisting of mollusk steinkerns, arthropod shell material and teeth from reptiles, chondrichthyans and osteichthyans drapes an erosional disconformity at the base of the Tombigbee Sand Member. The basal 25-30 centimeter of the Tombigbee Sand Member consists of light gray muds with tan sands and well rounded quartz pebbles measuring up to 8 centimeters on their longest axis. Additional sedimentological components include clay rip ups, siderite and pyrite nodules, phosphate grains, and fossil wood.

The upper portion of the Tombigbee Sand Member exposed along Trussels Creek contains

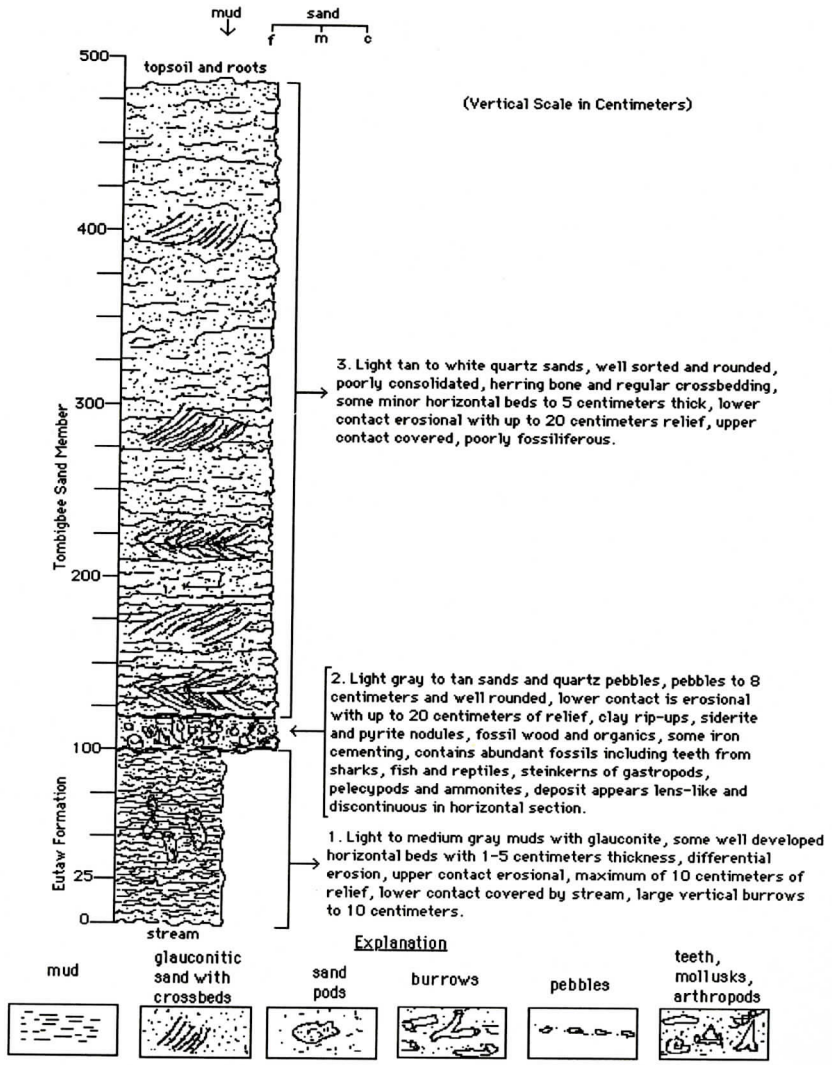


**Figure 4. Measured section of the Eutaw Formation and Tombigbee Sand Member along Trussels Creek, Greene County Alabama.**

light tan to white quartz sands, which are well sorted and rounded. Some minor horizontal beds, approximately 1-5 centimeters thick, with herring bone cross-bedding occur in this lithofacies, perhaps suggesting a tidal influence. Maximum thickness of the upper portion of the Tombigbee Sand Member along Trussels Creek is approximately 4 meters (Fig. 5).

## CHONDRICHTHYAN AND AMMONITE MACROFOSSILS

### Chondrichthyan Teeth

Chondrichthyan teeth collected along the base of the Tombigbee Sand Member from Trussels Creek during this study include the following species: *Squalicorax kaupi* (Agassiz); *Cretolamna appendiculata* (Agassiz); *Ptychodus mortoni* (Mantella); *Scapanorhynchus texanus* (Romer); *Paranomotodon angustidens* (Reuss) and *Brachyrhizodus wichitaensis*


**Figure 5 Excavated outcrop exposure of the Euatw Formation and Tombigbee Sand Member showing stratigraphic position of erosional unconformity and macrofossil lag along Trussels Creek, Greene County Alabama.**

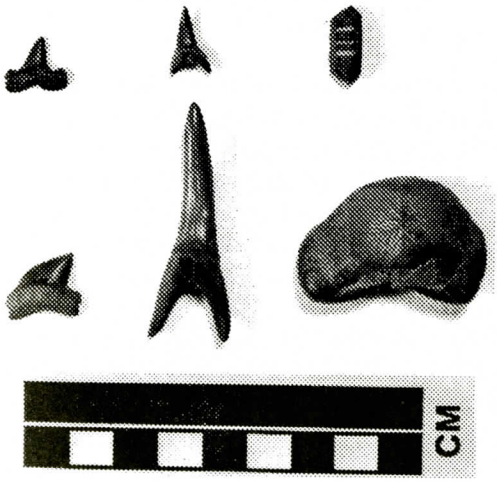


**Figure 6. Chondrichthyan teeth from left to right include: (Top Row): *Cretolamna appendiculata, Paranomotodon angustidens, Brachyrhizodus wichitaensis;* (Bottom Row): *Squalicorax kaupi, Scapanorhynchus texanus* and *Ptychodus mortoni* (Cappetta and Case, 1975; Case and Schwimmer 1988; Welton and Farish, 1993; Kent, 1994; and Case, 1995).**

(Romer). Identifications were compiled from: Cappetta and Case (1975); Case and Schwimmer (1988); Welton and Farish (1993); Kent (1994); and Case (1995); (Fig. 6). The majority of chondrichthyan teeth are fragmentary and show signs of abrasion.

## Ammonites

Ammonites occurring within the lag deposit along the base of the Tombigbee Sand Member along the Trussels Creek field area include *Placenticeras syrtale* (Morton), *Pseudoschloenbachia mexicana* (Renz), *Boehmoceras arculus* (Morton), *Glyptoxoceras* sp. (Spath) and *Baculites capensis* (Woods). Identifications were compiled from: Kennedy and Cobban, 1991; 1994; Kennedy and others, 1995); (Fig. 7). Ammonites are preserved as highly fragmentary siderite steinkerns where dissolution has removed all original shell material.

## AGE INTERPRETATION OF THE MACROFOSSIL LAG

Chondrichthyan and ammonite specimens collected from the lag deposit at the base of the Tombigbee Sand Member of the upper Eutaw Formation exposures in Trussels Creek contain remains from different biozones. The dynamic processes associated with the formation of the unconformity and lag deposit resulted in the mixing of Santonian-Campanian chondrichthyan and ammonite biozones.


**Figure 7. Ammonites from left to right include: *Glyptoxoceras* sp., *Boehmoceras arculus*, *Baculites capensis*, *Placenticeras syrtale* and *Pseudoschloenbachia mexicana* (Kennedy and Cobban, 1991; 1994; Kennedy and others, 1995).**

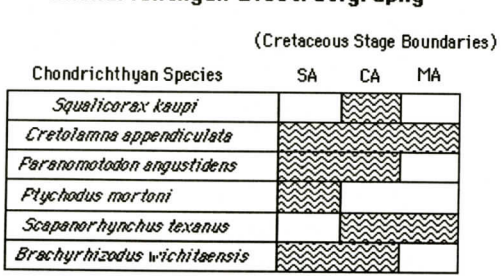


**Figure 8. Age ranges for fossil chondrichthyan teeth collected during this study from Trussels Creek. Age ranges compiled from Cappetta and Case (1975) and Welton and Farish (1993). SA= Santonian, CA= Campanian and MA= Maastrichtian.**

Welton and Farish (1994) indicate a Santonian age for *Ptychodus mortoni*. *Squailcorax kaupi* and *Scapanorhynchus texanus* make their first appearance during the Campanian (Fig. 8). These chondrichthyan teeth can be collected in the same bed of the lag deposit along Trussels Creek.

Kennedy and Cobban (1991) indicate *Placenticeras syrtale* has an upper Santonian to lower Campanian range in northern Mexico, Texas, Alabama and Mississippi. *Boehmoceras arculus*, *Glyptoxoceras* sp. and *Baculites capensis* have a late Santonian age occurring in the *Texanites shiloensis* zone along with the *Boehmoceras* fauna of Mississippi, Alabama and Texas (Kennedy and Cobban, 1991). Kennedy and Cobban (1991) indicate that the biostratigraphy of *Pseudoschloenbachia mexicana* is imprecisely dated. This species occurs in the upper Santonian *Texanites shiloensis* zone fauna of the Dessau Member of the Austin Chalk and the *Boehmoceras* fauna in Texas, Alabama and Mississippi.

The highest occurrence of *Placenticeras syrtale* is in the lower Campanian (Kennedy and Cobban, 1991). This ammonite species occurs with the upper Santonian ammonites: *Boehmoceras arculus*; *Glyptoxoceras* sp. and *Pseudoschloenbachia mexicana* in the lag deposit along the base of the Tombigbee Sand Member along Trussels Creek. This suggests the possibility of lower Campanian *Placenticeras syrtale* ammonites having been mixed with upper Santonian *Boehmoceras arculus*, *Glyptoxoceras* sp. and *Pseudoschloenbachia mexicana* ammonites. Mixing across the upper Santonian and lower Campanian is further supported by the fact that these four ammonite species co-occur

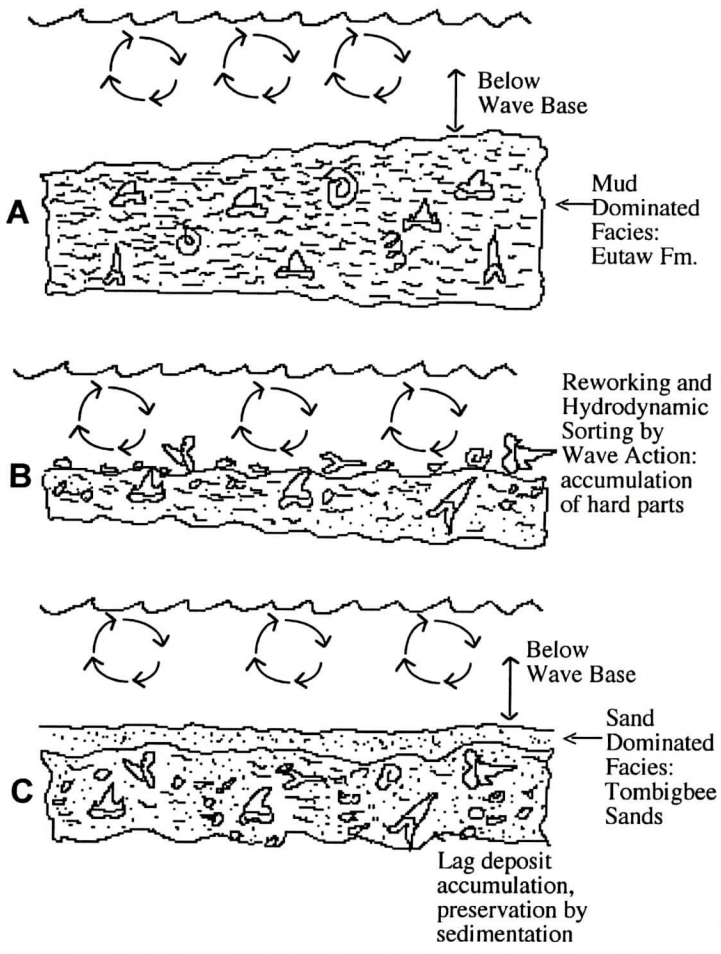


**Figure 9. Taphonomic Model for Chondrichthyan Teeth Mixing: a. Initial sea level fall: middle to late highstand systems tract; b. Sea level fall: late highstand systems tract; c. Sea level rise: early transgressive systems tract.**

in the lag deposit with *Squailcorax kaupi*, and *Scapanorhynchus texanus* which make their first appearance during the Campanian.

## MODEL FOR LAG DEPOSIT FORMATION

The dynamic processes of sea level fall and subsequent sea level rise formed the lag deposit along the study area in Trussels Creek. Sea level fall reworked biological material and depositional environments previously undisturbed by wave activity. In this higher energy environment, hydrodynamically stable material remains essentially in place, while unstable materials are remobilized and redeposited. Previously buried biological hard parts are exhumed, reworked, and incorporated with younger biological material in longshore troughs proximal to the shoreline. Subsequent transgression continues to rework the accumulating lag and distribute the contents as thin, discontinuous lenses. Continued transgression and sedimentation eventually preserved the lag as an historical layer below the reworking effects of wave base. Lag deposits created by sea level fluctuation characteristically occur in shoreface to shelf environments at the interface between facies changes and/or formation contacts (Becker and others, 1996b). These processes

are diagrammed in figure 9.

## DISCUSSION

The erosional unconformity at the base of the Tombigbee Sand Member of the Eutaw Formation at Trussels Creek marks a major sedimentary facies change from clay dominated to sand dominated conditions. The erosional surface is diachronous both parallel and perpendicular to depositional strike. Evidence for the diachronous nature of the surface includes: 1. an abundance of chondrichthyan and ammonite fossils from different biozones occurring in lag deposits along the base of Tombigbee Sand Member, and 2. the fragmentary nature of some fossils along an undulating erosional surface reflecting active transport and reworking.

Sparse fossil evidence for ammonites and chondrichthyan teeth exists *above* and *below* the lag deposit along Trussels Creek. Chondrichthyans are nektonic organisms and their teeth can be found in back barrier, shelf, and even deep marine environments. In the Trussels Creek lag deposit, chondrichthyan teeth have been mixed with molluscan assemblages representing mobile benthic, pelagic, and nektonic life modes characteristic of shoreface to outer shelf paleobathymetries. These fossils are concentrated with clay rip ups, siderite and pyrite nodules, phosphate grains, and fossil wood along an unconformity representing a major facies change from clay dominated to sand dominated conditions.

Storm or deep sea condensed lags do not show the prominent facies changes observed in the Alabama lag deposit. In our view, such a concentration of fossils and sedimentological components must be the product of a relative sea level regressive-transgressive event.

Lamb and others (1991) identified what appears to be a continuation of this lag deposit along Catoma Creek in Montgomery, Alabama in an intergradational zone of the Tombigbee Sand Member. Chondrichthyan teeth *Cretoxyrhina mantelli, Cretolamna appendiculata, Ptychodus mortoni, Scapanorhynchus texanus* and *Squalicorax kaupi* as well as osteichthyan and reptile teeth were also collected from this lag. Lamb and others (1991) further state that ammonites included with this lag deposit are latest Santonian and early Campanian forms.

Puckett (1994) and Puckett (personal communication) places the Santonian-Campanian boundary in nearby eastern Mississippi close to the Tombigbee-Mooreville contact based on the highest occurrence surface, (HOS), of planktonic foraminifera *Dicarinella asymetrica*. Considering the diachroneity of the transgressive surface between the Eutaw Formation and its Tombigbee Sand Member and the fact that the Tombigbee Sand is only 3 meters thick in the Trussels Creek field area, our placement of the Santonian-Campanian boundary in western Alabama along Trussels Creek appears to be quite consistent with the (HOS) of *D. asymetrica*.

In the Trussels Creek lag, at the base of the Tombigbee Sand Member, Campanian chondrichthyan teeth *Squailcorax kaupi* and *Scapanorhynchus texanus* can be collected directly adjacent to Santonian ammonites: *Boehmoceras arculus*, *Glyptoxoceras* sp. *Baculites capensis* and *Pseudoschloenbachia mexicana*. The biostratigraphy of chondrichthyan teeth and ammonites presented in our paper, has been cross-checked in sections ranging across New Jersey, Mississippi, Alabama, Texas and Mexico (Cappetta and Case, 1975; Kennedy and Cobban, 1991; Welton and Farish, 1993; and Case, 1995). Based on chondrichthyan and ammonite biostratigraphy, we interpret the Santonian-Campanian boundary in the Trussels Creek field area to reside within the eroded and redeposited lag at the base of the Tombigbee Sand Member of the Eutaw Formation.

The pattern and processes that formed the erosion and lag deposit at the base of the Tombigbee Sand may have counterparts in basins that were not tectonically linked to the Gulf Coastal Plain during the late Cretaceous. In the Santonian-Campanian Lagerdorf section in Northern Germany, for example, sedimentary facies changes indicate a regression and period of non-deposition across the Santonian-Campanian boundary (Birkelund and others 1984). This situation is similar to what we have observed at the base of the Tombigbee Sand Mem-

ber along Trussels Creek and suggests that eustasy, rather than tectonics may be the primary process driving the formation of the lag deposit at Trussels Creek.

The mechanism of chondrichthyan lag deposit formation described here appears to occur at other times in the geologic record. Haq and others (1988) identified fossil shark teeth concentrated by third order sea level processes in the lower Lutetian stage at St. Leu d'Esserent in the Paris Basin. At St. Leu d'Esserent, the lowest sequence boundary of 49.5 Ma is placed along an unconformity which separates micaceous sands of the Cuisian stage and coarse glauconitic sands of the lower Lutetian stage. The transgressive surface of the onlapping coarse glauconitic sands contains bryozoans and chondrichthyan teeth (Haq and others, 1988).

Becker and others (1996) identified a fossil chondrichthyan lag deposit along the Campanian-Maastrichtian boundary in New Jersey separating the Marshalltown and Navesink Depositional Sequences. The stratigraphic position of this lag deposit corresponds to a regressive-transgressive event across third order eustatic cycles 3 and 4 of UZA 4 of Haq and others (1988).

Case and Schwimmer (1988) identified a chondrichthyan lag deposit in Georgia near the boundary between the Blufftown Formation and Cusseta Sand Member of the Ripley Formation at the lower-upper Campanian boundary. This chondrichthyan lag occurs near the boundary between the clay dominated, Blufftown Formation and the sand dominated, Cusseta Sands Member, again suggesting sea level cyclicity as a first order variable in chondrichthyan lag deposit formation.

## CONCLUSIONS

The research has shown that third order sea level cyclicity plays an important role in the concentration of fossils along unconformities. As evidenced by the Trussels Creek lag deposit, chondrichthyans and other co-occurring fossils are: 1) artifacts of physical sorting processes associated with sea level cyclicity; and 2) within the hydrodynamically sorted lag deposit fossils more than likely lived in oceans separated in time by millions of years.The concept of remobilization of macrofossils and subsequent deposition above unconformities during the formation of transgressive lags, which are developed in this study, can be applied to a variety of geologic issues: 1) differing biostratigraphic zonations for both macrofossil and microfossils; 2) the identification and placement of sequence boundaries; and 3) the selection of appropriate field areas for paleontological, biostratigraphic and chronostratigraphic studies.

## ACKNOWLEDGMENTS

The authors would like to thank Dr. William Cobban for his assistance in the identification of the ammonite specimens and review of our manuscript. We also thank Dr. T. Markham Puckett for his suggestions and review of our manuscript. Finally, we thank Dr. Robert Wellner and Mr. John Petruccione for their assistance in field work and fossil collection during this project.

## REFERENCES CITED

Becker, M., Slattery, W., and Chamberlain, J., 1996a, Sr87/Sr86 Isotopic ages of Upper Cretaceous chondrichthyan teeth of the Atlantic and Eastern Gulf Coastal Plains: Implications for sea level cyclicity and macrofossil time averaging: Geologic Society of America, Abstracts with Programs, A-186.

Becker, M., Slattery, W. and Chamberlain, J., 1996b, Reworked Campanian and Maastrichtian macrofossils in a sequence bounding, transgressive lag deposit, Monmouth County, New Jersey, Northeast Geology and Environmental Science, Vol. 18, p. 234-252.

Birkelund, T., Hancock, J.M., Hart, M.B., Rawson, P.F., Remane, J., Robaszynski, F., Schmid, F., and Surlyk, F, 1984, Cretaceous stage boundaries symposium: Bulletin of the Geological Society of Denmark. Vol. 33, 1-2, p.3-20

Cappetta, H., and Case, G., 1975, Contributions a l' etude des selaciens du groupe Monmouth (Campanian-Maastrichtian) du New Jersey: Paleontographica, Abt. 15, p. 1-46.

Case, G., 1995, Fossil shark remains from the Early and Middle Maastrichtian of the Upper Cretaceous of Monmouth County, New Jersey, *in* Baker, J., ed., Contributions to the Paleontology of New Jersey, The Geological Society of New Jersey, Vol. XII, p. 72-80.

Case, G., and Schwimmer, D., 1988, Late Cretaceous fish

from the Blufftown Formation (Campanian) in Western Georgia: Journal of Paleontology, Vol. 62, p. 290-301.

Hallam, A., Hancock, J., La Brecque, J., Lowrie, W., and Channell, J., 1985, Jurassic to Paleogene, Part 1, Jurassic and Cretaceous geochronology and Jurassic to Paleogene magnetostratigraphy, *in* Snelling, N., ed., The chronology of the geologic record, The Geologic Society of America Memoir, No. 10, p. 118-140.

Haq, B., Hardenbol, J., and Vail, P., 1988, Mesozoic and Cenozoic chronostratigraphy and eustatic cycles, *in* Wilgus, C., Posamentier, H., Ross, C., and Kendall, C., eds. Sea level changes: An integrated approach: Tulsa Oklahoma, Society of Economic Paleontologists and Mineralogists Special Publication 42, p. 71-104.

Kennedy, W. and Cobban W., 1991, Upper Cretaceous (upper Santonian) boehmoceras fauna from the Gulf Coast region of the United States: Geology, Vol. 128, p. 167-189.

Kennedy, W. and Cobban W., 1994, Ammonite fauna from the Wenonah Formation (Upper Cretaceous) of New Jersey: Journal of Paleontology, Vol. 68, p. 95-110.

Kennedy, W., Johnson, R., and W., Cobban, 1995, Upper Cretaceous ammonite faunas of New Jersey, *in* Baker, J., ed., Contributions to the Paleontology of New Jersey, The Geological Society of New Jersey, Vol. XII, p. 24-55.

Kent, B., 1994, Fossil sharks of the Chesapeake Bay region: Egan Rees and Boyer Publishers, 146 p.

King, D.T., Jr., 1987, Sedimentary facies, depositional environments, and sea-level history — Mooreville Chalk, lower Campanian of east-central Alabama: Southeastern Geology v.27 p.141-154

King, D., and Skotnicki, M., 1994, Upper Cretaceous stratigraphy and sea level history, Gulf Coast Plain of Central and Eastern Alabama: Geological Society of America Special Paper, 287, p. 27-41.

Lamb, J., Bell, G., Rinsburg, A., 1991, The Catoma Creek scrap fauna (Late Cretaceous) from Montgomery, Alabama: Journal of Vertebrate Paleontology, Abstracts with Programs, Vol. 11, A-121.

Mancini, E., Puckett, T., Tew, B., and Smith, C., 1995, Upper Cretaceous sequence stratigraphy of the Mississippi-Alabama area: Gulf Coast Association of Geological Societies Transactions, Vol. 45, p. 377-384.

Obradovich, J., 1988, A different perspective on glauconite as a chronometer for geologic time scale studies: Paleoceanography, Vol. 3, p. 757-770.

Owens, J. and Gohn, G., 1985, Depositional history of the Cretaceous series in the U.S. Atlantic Coastal Plain: Stratigraphy, Paleoenvironments, and Tectonic Controls of Sedimentation, *in* Poag, C. ed., Geologic Evolution of the United States Atlantic Margin: New York, Van Nostrand Reinhold, p. 25-86.

Puckett, T., 1994, Planktonic foraminifera and ostracode biostratigraphy of Upper Santonian through Lower Maastrichtian strata in central Alabama: Gulf Coast Association of Geologic Societies Transactions, Vol. 44, p. 585-595.

Raymond, D., Osborne, W., Copeland, C., and Neathery, T., 1988, Alabama stratigraphy: Geologic Survey of Alabama, Circular 140 Tuscaloosa, Alabama, p. 42, 83-84.

Russell, E.E. and Keady, D.M., 1983, Notes on the Upper Cretaceous lithostratigraphy of the eastern Mississippi Embayment: Society of Economic Paleontologists and Mineralogists. Gulf Coast Section. Guidebook for Spring Fieldtrip, p.1-15

Smith. C., and Mancini, E., 1983, Calcareous nannofossils and planktonic foraminifera biostratigraphy: Society of Economic Paleontologists and Mineralogists Gulf Coast Section, Guidebook for Spring Fieldtrips p. 16-28.

Sohl, N., and Smith, C., 1980, Notes on Cretaceous biostratigraphy, *in* Frey, R., ed., Excursions in Southeastern Geology, Vol. 2, American Geological Institute, p. 392-402.

Sugarman, P., Miller, K., Bukry, D., and Feigenson, M., 1995, Uppermost Campanian-Maestrichtian strontium isotopic biostratigraphic and sequence stratigraphic framework of the New Jersey Coastal Plain: Geologic Society of America Bulletin, Vol. 107, p. 19-37.

Welton, B. and Farish, R., 1993, The collector's guide to fossil sharks and rays from the Cretaceous of Texas: Before Time Publishers, p. 1-204.

## ERRATUM FOR VOLUME 37, NO. 3, FEBRUARY 1998

### TABLE OF CONTENTS

The Table of Contents for Volume 37, Number 3 listed the volume number as 38. Please change the 38 to 37.